

COMPRESSIBLE FLOW RELATED TERMS

**Based on Information in Wikipedia,
the free encyclopedia**

Prepared by Patrick H. Oosthuizen

**Department of Mechanical and Materials Engineering
Queen's University
Kingston, Ontario, Canada**

August, 2009

CONTENTS

1. Area Rule
2. Atmospheric Reentry
3. Ballistic Reentry
4. Blast Wave
5. Choked Flow
6. Compressible Flow
7. Compressibility
8. Compressibility Factor
9. Critical Mach Number
10. DeLaval Nozzle
11. Drag Divergence Mach Number
12. Hypersonic
13. Interferometer
14. Jet Engine
15. Mach Wave
16. Moving Shock Wave
17. Oblique Shock Wave
18. Prandtl-Meyer Function
19. Prandtl-Meyer Wave

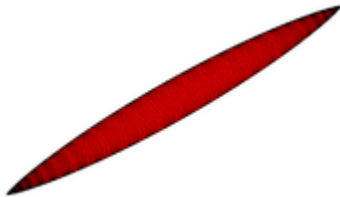
20. Real Gas
21. Rocket Engine Nozzle
22. Schlieren Photography
23. Shadowgraph
24. Shock Tube
25. Shock Wave
26. Sonic Boom
27. Sound Barrier
28. Speed of Sound
29. Subsonic and Transonic Wind-tunnels
30. Supercritical Airfoil
31. Supersonic
32. Supersonic Transport Aircraft
33. Supersonic Wind-tunnel
34. Transonic
35. Wave Drag

Area rule

From Wikipedia, the free encyclopedia

The **Whitcomb area rule**, also called the **transonic area rule**, is a design technique used to reduce an aircraft's drag at transonic and supersonic speeds, particularly between Mach 0.8 and 1.2. This is the operating speed range of the majority of commercial and military fixed-wing aircraft today.

Description



The Sears-Haack body shape

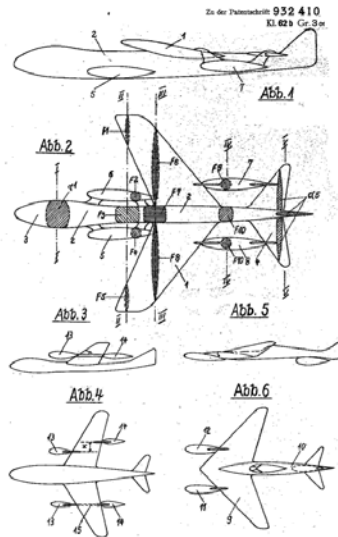
At high-subsonic flight speeds, supersonic airflow can develop in areas where the flow accelerates around the aircraft body and wings. The speed at which this occurs varies from aircraft to aircraft, and is known as the critical Mach number. The resulting shock waves formed at these points of supersonic flow can bleed away a considerable amount of power, which is experienced by the aircraft as a sudden and very powerful form of drag, called wave drag. To reduce the number and power of these shock waves, an aerodynamic shape should change in cross-sectional area as smoothly as possible. This leads to a "perfect" aerodynamic shape known as the **Sears-Haack body**, roughly shaped like a cigar but pointed at both ends.

The area rule says that an airplane designed with the same cross-sectional area as the Sears-Haack body generates the same wave drag as this body, largely independent of the actual shape. As a result, aircraft have to be carefully arranged so that large volumes like wings are positioned at the widest area of the Sears-Haack body, and that the cockpit, tailplane, intakes and other "bumps" are spread out along the fuselage.

The area rule also holds true at speeds higher than the speed of sound, but in this case the body arrangement is in respect to the Mach line for the design speed. For instance, at Mach 1.3 the angle of the Mach cone formed off the body of the aircraft will be at about $\mu = \arcsin(1/M) = 50,3^\circ$ (μ is the sweep angle of the Mach cone). In this case the "perfect shape" is biased rearward, which is why aircraft designed for high speed cruise tend to be arranged with the wings at the rear.^[1] A classic example of such a design is Concorde.

History

Germany



Junkers patent drawing from March 1944.

The area rule was discovered by Otto Frenzl when comparing a swept wing with a w-wing with extreme high wave drag^[2] working on a transonic wind tunnel at Junkers works in Germany between 1943 and 1945. He wrote a description on 17 December 1943, with the title “Arrangement of Displacement Bodies in High-Speed Flight”; this was used in a patent filed in 1944.^[3] The results of this research were presented to a wide circle in March 1944 by Theodor Zobel at the “Deutsche Akademie der Luftfahrtforschung” (German Academy of aeronautics research) in the lecture “Fundamentally new ways to increase performance of high speed aircraft.”^[4] The design concept was applied to German wartime aircraft, including a rather odd Messerschmitt project, but their complex double-boom design was never built even to the extent of a model. Several other researchers came close to developing a similar theory, notably Dietrich Küchemann who designed a tapered fighter that was dubbed the “Küchemann Coke Bottle” when it was discovered by U.S. forces in 1946. In this case Küchemann arrived at the solution by studying airflow, notably spanwise flow, over a swept wing. The swept wing is already an application of the area rule.

United States

Wallace D. Hayes, a pioneer of supersonic flight, developed the supersonic area rule in publications beginning in 1947 with his Ph.D. thesis at the California Institute of Technology.

Richard T. Whitcomb, after whom the rule is named, independently discovered this rule in 1952, while working at the NACA. While using the new Eight-Foot High-Speed Tunnel, a wind tunnel with performance up to Mach 0.95 at NACA's Langley Research Center, he was surprised by the increase in drag due to shock wave formation. The shocks could be seen using Schlieren photography, but the reason they were being created at speeds far below the speed of sound, sometimes as low as Mach 0.70, remained a mystery.

In late 1951, the lab hosted a talk by Adolf Busemann, a famous German aerodynamicist who had moved to Langley after World War II. He talked about the difference in the behavior of airflow at speeds approaching the supersonic, where it no longer behaved as an incompressible fluid. Whereas engineers were used to thinking of air flowing smoothly around the body of the aircraft, at high speeds it simply did not have time to "get out of the way", and instead started to flow as if it were rigid pipes of flow, a concept Busemann referred to as "streampipes", as opposed to streamlines, and jokingly suggested that engineers had to consider themselves "pipefitters".

Several days later Whitcomb had a "Eureka" moment. The reason for the high drag was that the "pipes" of air were interfering with each other in three dimensions. One could not simply consider the air flowing over a 2D cross-section of the aircraft as others could in the past; now they also had to consider the air to the "sides" of the aircraft which would also interact with these streampipes. Whitcomb realized that the Sears-Haack shaping had to apply to the aircraft *as a whole*, rather than just to the fuselage. That meant that the extra cross-sectional area of the wings and tail had to be accounted for in the overall shaping, and that the fuselage should actually be narrowed where they meet to more closely match the ideal.

Applications



Underside of an A-380. Several area rule-dictated features are visible - see text

The area rule was immediately applied to a number of development efforts. One of the most famous was Whitcomb's personal work on the re-design of the Convair F-102 Delta Dagger, a U.S. Air Force jet fighter that was demonstrating performance considerably worse than expected. By indenting the fuselage beside the wings, and (paradoxically) adding more volume to the rear of the plane, transonic drag was considerably reduced and the original Mach 1.2 design speeds were reached. The culminating design of this research was the Convair F-106 Delta Dart, an aircraft which for many years was the USAF's primary all-weather interceptor.

Numerous designs of the era were likewise modified in this fashion, either by adding new fuel tanks or tail extensions to smooth out the profile. The Tupolev Tu-95 'Bear', a Soviet-era bomber, was modified by adding large bulged nacelles behind the two inner engines, instead of decreasing the cross section of the fuselage next to the wing root. It remains the highest speed propeller aircraft in the world. The Convair 990 used a similar solution, adding bumps called antishock bodies to the trailing edge of the upper wing. The 990 remains the fastest U.S. airliner in history, cruising at up to Mach 0.89. Designers at Armstrong-Whitworth took the concept a step further in their proposed M-Wing, in which the wing was first swept forward and then to the rear. This allowed the fuselage to be narrowed on either side of the root instead of just behind it, leading to a smoother fuselage that remained wider on average than one using a classic swept wing.

One interesting outcome of the area rule is the shaping of the Boeing 747's upper deck. The aircraft was designed to carry standard cargo containers in a two-wide, two-high stack on the main deck, which was considered a serious accident risk for the pilots if they were located in a cockpit at the front of the aircraft. They were instead moved above the deck in a small "hump", which was designed to be as small as possible given normal streamlining principles. It was later realized that the drag could be reduced much more by lengthening the hump, using it to reduce wave drag offsetting the tail surface's contribution. The new design was introduced on the 747-300, improving its cruise speed and lowering drag.

Aircraft designed according to Whitcomb's area rule looked odd at the time they were first tested, (eg. the Blackburn Buccaneer), and were dubbed "flying Coke bottles," but the area rule is effective and came to be an expected part of the appearance of any transonic aircraft. Later designs started with the area rule in mind, and came to look much more pleasing. Although the rule still applies, the visible fuselage "waisting" can only be seen on the B-1B Lancer, Learjet 60, and the Tupolev Tu-160 'Blackjack' — the same effect is now achieved by careful positioning of aircraft components, like the boosters and cargo bay on rockets; the jet engines in front of (and not directly below) the wings of the Airbus A380; the jet engines behind (and not purely at the side of) the fuselage of a Cessna Citation X; the shape and location of canopy on the F-22 Raptor; and the image of the Airbus A380 above showing obvious area rule shaping at the wing root, but these modifications are practically invisible from any other angle. Aftershock bodies are likewise "invisible" today, serving double-duty as flap actuators, which are also visible in the A380.

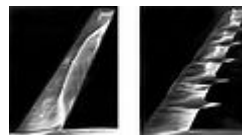
Images



The F-106 Delta Dart, a development of the F-102 Delta Dagger, shows the "wasp-waisted" shaping due to area rule considerations



NASA Convair 990 with antishock bodies on the rear of the wings



Oilflow visualization of flow separation without and with antishock bodies



Two large bulged nacelles can be seen behind the engines of this Tu-95

Notes

1. ^ Super sonic area rule by Robert T. Jones NACA Report 1284
2. ^ *Werner Heinzerling, Deutsches Museum München, Flügelpfeilung und Flächenregel, zwei grundlegende deutsche Patente der Flugzeugaerodynamik. PDF
3. ^ Patentschrift zur Flächenregel, 21. März 1944
4. ^ Hans-Ulrich Meier Die Pfeilflügelentwicklung in Deutschland bis 1945 ISBN 3763761306 page 166-199

Atmospheric reentry

From Wikipedia, the free encyclopedia

Atmospheric reentry refers to the movement of human-made or natural objects as they enter the atmosphere of a planet from outer space, in the case of Earth from an altitude above the "edge of space." This article primarily addresses the process of controlled reentry of vehicles which are intended to reach the planetary surface intact, but the topic also includes uncontrolled (or minimally controlled) cases, such as the intentionally or circumstantially occurring, destructive deorbiting of satellites and the falling back to the planet of "space junk" due to orbital decay.

Vehicles that typically undergo this process include ones returning from orbit (spacecraft) and ones on exo-orbital (suborbital) trajectories (ICBM reentry vehicles, some spacecraft.) Typically this process requires special methods to protect against aerodynamic heating. Various advanced technologies have been developed to enable atmospheric reentry and flight at extreme velocities.



Mars Exploration Rover (MER) aeroshell, artistic rendition.



Apollo Command Module flying at a high angle of attack for lifting entry, artistic rendition.



Apollo 13 service module and lunar lander reentering and breaking up

History

The technology of atmospheric reentry was a consequence of the Cold War. Ballistic missiles and nuclear weapons were legacies of World War II left to both the Soviet Union and the United States. Both nations initiated massive research and development programs to further the military capability of those technologies. However before a missile-delivered nuclear weapon could be practical they lacked an essential ingredient: an *atmospheric reentry technology*. In theory, the nation first developing reentry technology had a decisive military advantage, yet it was unclear whether the technology was physically possible. Basic calculations showed the kinetic energy of a nuclear warhead returning from orbit was sufficient to completely vaporize the warhead. Despite these calculations, the military stakes were so high that simply assuming atmospheric reentry's impossibility was unacceptable, and it was known that meteorites were able to successfully reach ground level. Consequently a high-priority program was initiated to develop reentry technology. Atmospheric reentry was successfully developed, which made possible nuclear-armed intercontinental ballistic missiles.

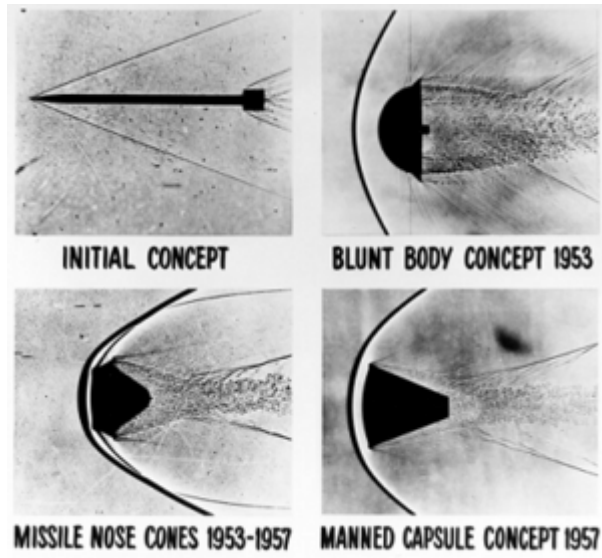
The technology was further pushed forward for human use by another consequence of the Cold War. The Soviet Union saw a propaganda and military advantage in pursuing space exploration. To the embarrassment of the United States, the Soviet Union orbited an artificial satellite, followed by a series of other technological firsts that culminated with a Soviet cosmonaut orbiting the Earth and returning safely to Earth. Many of these achievements were enabled through atmospheric reentry technology. The United States saw the Soviet Union's achievements as a challenge to its national pride as well as a threat to national security. Consequently, the United States followed the Soviet Union's initiative and increased its nascent space program, thus beginning the Space Race.

The concept of the ablative heat shield was described as early as 1920 by Robert Goddard, "In the case of meteors, which enter the atmosphere with speeds as high as 30 miles per second, the interior of the meteors remains cold, and the erosion is due, to a large extent, to chipping or cracking of the suddenly heated surface. For this reason, if the outer surface of the apparatus were to consist of layers of a very infusible hard substance with layers of a poor heat conductor between, the surface would not be eroded to any considerable extent, especially as the velocity of the apparatus would not be nearly so great as that of the average meteor." ^[1]

Terminology, definitions and jargon

Over the decades since the 1950s, a rich technical jargon has grown around the engineering of vehicles designed to enter planetary atmospheres. It is recommended that the reader review the jargon glossary before continuing with this article on atmospheric reentry.

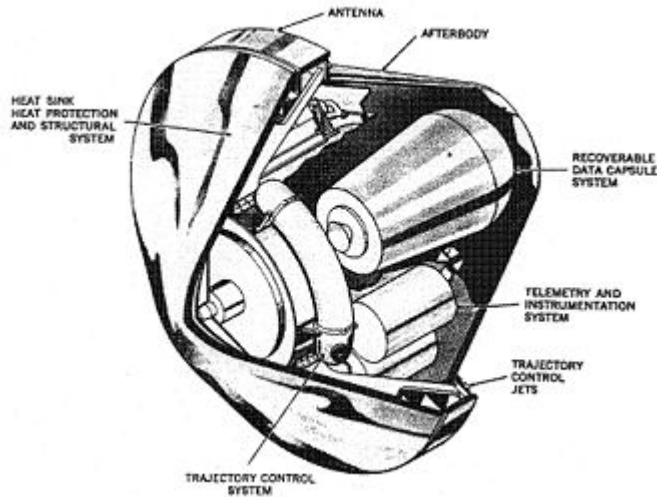
Blunt body entry vehicles



Various reentry shapes (NASA)

These four shadowgraph images represent early reentry-vehicle concepts. A shadowgraph is a process that makes visible the disturbances that occur in a fluid flow at high velocity, in which light passing through a flowing fluid is refracted by the density gradients in the fluid resulting in bright and dark areas on a screen placed behind the fluid.

In the United States, H. Julian Allen and A. J. Eggers, Jr. of the National Advisory Committee for Aeronautics (NACA) made the counterintuitive discovery in 1951^[2] that a blunt shape (high drag) made the most effective heat shield. From simple engineering principles, Allen and Eggers showed that the heat load experienced by an entry vehicle was inversely proportional to the drag coefficient, i.e. the greater the drag, the less the heat load. Through making the reentry vehicle blunt, air can't "get out of the way" quickly enough, and acts as an air cushion to push the shock wave and heated shock layer forward (away from the vehicle). Since most of the hot gases are no longer in direct contact with the vehicle, the heat energy would stay in the shocked gas and simply move around the vehicle to later dissipate into the atmosphere.



Prototype Version of the Mk-2 Reentry Vehicle (RV) was derived from Blunt Body Theory

The Allen and Eggers discovery, though initially treated as a military secret, was eventually published in 1958.^[3] The Blunt Body Theory made possible the heat shield designs that were embodied in the Mercury, Gemini and Apollo space capsules, enabling astronauts to survive the fiery reentry into Earth's atmosphere.

In the Soviet Union the R-7 ICBM was first successfully tested in 1957 with a sharp-nosed conical warhead. This burned up at an altitude of 10 km over the target area, and was replaced with a blunt-nosed conical design. Soviet heat shields consisted of layers of fiberglass together with asbestos textolite.

Entry vehicle shapes

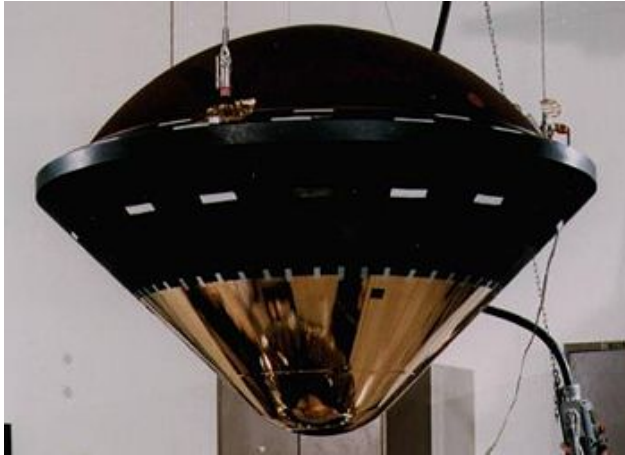
There are several basic shapes used in designing entry vehicles:

Sphere or spherical section

The simplest axisymmetric shape is the sphere or spherical section. This can either be a complete sphere or a spherical section forebody with a converging conical afterbody. The sphere or spherical section's aerodynamics are easy to model analytically using Newtonian impact theory. Likewise, the spherical section's heat flux can be accurately modeled with the Fay-Riddell equation.^[4] The static stability of a spherical section is assured if the vehicle's center of mass is upstream from the center of curvature (dynamic stability is more problematic). Pure spheres have no lift. However by flying at an angle of attack, a spherical section has modest aerodynamic lift thus providing some cross-range capability and widening its entry corridor. In the late 1950s and early 1960s, high-speed computers were not yet available and CFD was still embryonic. Because the spherical section was amenable to closed-form analysis, that geometry became the default for conservative design. Consequently, manned capsules of that era were based upon the spherical section. Pure spherical entry vehicles were used in the early Soviet Vostok and in Soviet Mars and Venera descent vehicles. The Apollo Command/Service Module used a spherical section forebody heatshield with a converging conical afterbody. It flew a lifting entry with a hypersonic trim angle of attack of -27°

(0° is blunt-end first) to yield an average L/D of 0.368.^[5] This angle of attack was achieved by precisely offsetting the vehicle's center of mass from its axis of symmetry. Other examples of the spherical section geometry in manned capsules are Soyuz/Zond, Gemini and Mercury.

Sphere-cone



Galileo Probe during final assembly

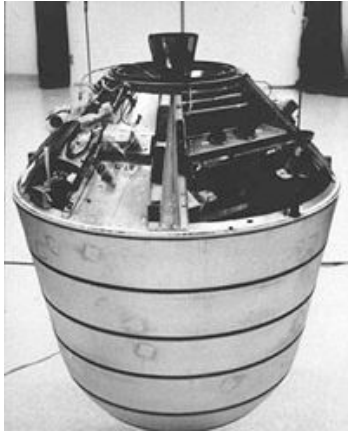
The sphere-cone is a spherical section with a frustum or blunted cone attached. The sphere-cone's dynamic stability is typically better than that of a spherical section. With a sufficiently small half-angle and properly placed center of mass, a sphere-cone can provide aerodynamic stability from Keplerian entry to surface impact. (The "half-angle" is the angle between the cone's axis of rotational symmetry and its outer surface, and thus half the angle made by the cone's surface edges.)

The original American sphere-cone aeroshell was the Mk-2 RV which was developed in 1955 by the General Electric Corp. The Mk-2's design was derived from blunt-body theory and used a radiatively cooled thermal protection system (TPS) based upon a metallic heat shield (the different TPS types are later described in this article). The Mk-2 had significant defects as a weapon delivery system, i.e., it loitered too long in the upper atmosphere due to its lower ballistic coefficient and also trailed a stream of vaporized metal making it very visible to radar. These defects made the Mk-2 overly susceptible to anti-ballistic missile (ABM) systems. Consequently an alternative sphere-cone RV to the Mk-2 was developed by General Electric.



Mk-6 RV, Cold War weapon and ancestor to most of NASA's entry vehicles

This new RV was the Mk-6 which used a non-metallic ablative TPS (nylon phenolic). This new TPS was so effective as a reentry heat shield that significantly reduced bluntness was possible. However the Mk-6 was a huge RV with an entry mass of 3360 kg, a length of 3.1 meters and a half-angle of 12.5° . Subsequent advances in nuclear weapon and ablative TPS design allowed RVs to become significantly smaller with a further reduced bluntness ratio compared to the Mk-6. Since the 1960s, the sphere-cone has become the preferred geometry for modern ICBM RVs with typical half-angles being between 10° to 11° .



"Discoverer" type reconnaissance satellite film Recovery Vehicle (RV)



Opportunity rover's heat shield lying inverted on the surface of Mars.

Reconnaissance satellite RVs (recovery vehicles) also used a sphere-cone shape and were the first American example of a non-munition entry vehicle (Discoverer-I, launched on 28 February 1959). The sphere-cone was later used for space exploration missions to other celestial bodies or for return from open space, e.g., Stardust probe. Unlike with military RVs, the advantage of the blunt body's lower TPS mass remained with space exploration entry vehicles like the Galileo Probe with a half angle of 45° or the Viking aeroshell with a half angle of 70° . Space exploration sphere-cone entry vehicles have landed on the surface or entered the atmospheres of Mars, Venus, Jupiter and Titan.

Biconic

The biconic is a sphere-cone with an additional frustum attached. The biconic offers a significantly improved L/D ratio. A biconic designed for Mars aerocapture typically has an L/D of approximately 1.0 compared to an L/D of 0.368 for the Apollo-CM. The higher L/D makes a biconic shape better suited for transporting people to Mars due to the lower peak deceleration. Arguably, the most significant biconic ever flown was the *Advanced Maneuverable Reentry Vehicle* (AMaRV). Four AMaRVs were made by the McDonnell-Douglas Corp. and represented a significant leap in RV sophistication. Three of the AMaRVs were launched by Minuteman-1 ICBMs on 20 December 1979, 8 October 1980 and 4 October 1981. AMaRV had an entry mass of approximately 470 kg, a

nose radius of 2.34 cm, a forward frustum half-angle of 10.4° , an inter-frustum radius of 14.6 cm, aft frustum half angle of 6° , and an axial length of 2.079 meters. No accurate diagram or picture of AMaRV has ever appeared in the open literature. However a schematic sketch of an AMaRV-like vehicle along with trajectory plots showing hairpin turns has been published.^[6]

AMaRV's attitude was controlled through a split body flap (also called a "split-windward flap") along with two yaw flaps mounted on the vehicle's sides. Hydraulic actuation was used for controlling the flaps. AMaRV was guided by a fully autonomous navigation system designed for evading anti-ballistic missile (ABM) interception. The McDonnell Douglas DC-X (also a biconic) was essentially a scaled up version of AMaRV. AMaRV and the DC-X also served as the basis for an unsuccessful proposal for what eventually became the Lockheed Martin X-33. Amongst aerospace engineers, AMaRV has achieved legendary status alongside such marvels as the SR-71 Blackbird and the Saturn V Rocket.

Non-axisymmetric shapes

Non-axisymmetric shapes have been used for manned entry vehicles. One example is the winged orbit vehicle that uses a delta wing for maneuvering during descent much like a conventional glider. This approach has been used by the American Space Shuttle and the Soviet Buran. The lifting body is another entry vehicle geometry and was used with the X-23 PRIME (Precision Recovery Including Maneuvering Entry) vehicle.

The FIRST (Fabrication of Inflatable Re-entry Structures for Test) system was an Aerojet proposal for an inflated-spar Rogallo wing made up from Inconel wire cloth impregnated with silicone rubber and Silicon Carbide dust. FIRST was proposed in both one-man and six man versions, used for emergency escape and reentry of stranded space station crews, and was based on an earlier unmanned test program that resulted in a partially successful reentry flight from space (the launcher nose cone fairing hung up on the material, dragging it too low and fast for the TPS, but otherwise it appears the concept would have worked, even with the fairing dragging it, the test article flew stably on reentry until burn-through).

The proposed MOOSE system would have used a one-man inflatable ballistic capsule as an emergency astronaut entry vehicle. This concept was carried further by the Douglas Paracone project. While these concepts were unusual, the inflated shape on reentry was in fact axisymmetric.

Shock layer gas physics

An approximate rule-of-thumb used by heat shield designers for estimating peak shock layer temperature is to assume the air temperature in kelvins to be equal to the entry speed in meters per second - a mathematical coincidence. For example, a spacecraft entering the atmosphere at 7.8 km/s would experience a peak shock layer temperature of 7800 K. This is unexpected, since the kinetic energy increases with the square of the velocity, and can only occur because the specific heat of the gas increases greatly with temperature (unlike the nearly constant specific heat assumed for solids under ordinary conditions).

At typical reentry temperatures, the air in the shock layer is both ionized and dissociated. This chemical dissociation necessitates various physical models to describe the shock layer's thermal and

chemical properties. There are four basic physical models of a gas that are important to aeronautical engineers who design heat shields:

Perfect gas model

Almost all aeronautical engineers are taught the perfect (ideal) gas model during their undergraduate education. Most of the important perfect gas equations along with their corresponding tables and graphs are shown in NACA Report 1135.^[7] Excerpts from NACA Report 1135 often appear in the appendices of thermodynamics textbooks and are familiar to most aeronautical engineers who design supersonic aircraft.

Perfect gas theory is elegant and extremely useful for designing aircraft but assumes the gas is chemically inert. From the standpoint of aircraft design, air can be assumed to be inert for temperatures less than 550 K at one atmosphere pressure. Perfect gas theory begins to break down at 550 K and is not usable at temperatures greater than 2000 K. For temperatures greater than 2000 K, a heat shield designer must use a *real gas model*.

Real (equilibrium) gas model

The real gas equilibrium model is normally taught to aeronautical engineers studying towards a master's degree. Not surprisingly, it is a common error for a bachelor's-level engineer to incorrectly use perfect-gas theory on a hypersonic design. An entry vehicle's pitching moment can be significantly influenced by real-gas effects. Both the Apollo-CM and the Space Shuttle were designed using incorrect pitching moments determined through inaccurate real-gas modeling. The Apollo-CM's trim-angle angle of attack was higher than originally estimated, resulting in a narrower lunar return entry corridor. The actual aerodynamic center of the *Columbia* was upstream from the calculated value due to real-gas effects. On *Columbia*'s maiden flight (STS-1), astronauts John W. Young and Robert Crippen had some anxious moments during reentry when there was concern about losing control of the vehicle.^[8]

An equilibrium real-gas model assumes that a gas is chemically reactive but also assumes all chemical reactions have had time to complete and all components of the gas have the same temperature (this is called *thermodynamic equilibrium*). When air is processed by a shock wave, it is superheated by compression and chemically dissociates through many different reactions (DIRECT friction upon the reentry object is not the main cause of shock-layer heating. It is caused mainly from isentropic heating of the air molecules within the compression wave. Friction based entropy increases of the molecules within the wave also account for some heating.). The distance from the shock wave to the stagnation point on the entry vehicle's leading edge is called *shock wave stand off*. An approximate rule of thumb for shock wave standoff distance is 0.14 times the nose radius. One can estimate the time of travel for a gas molecule from the shock wave to the stagnation point by assuming a free stream velocity of 7.8 km/s and a nose radius of 1 meter, i.e., time of travel is about 18 microseconds. This is roughly the time required for shock-wave-initiated chemical dissociation to approach chemical equilibrium in a shock layer for a 7.8 km/s entry into air during peak heat flux. Consequently, as air approaches the entry vehicle's stagnation point, the air effectively reaches chemical equilibrium thus enabling an equilibrium model to be usable. For this case, most of the shock layer between the shock wave and leading edge of an entry vehicle is chemically reacting and *not* in a state of equilibrium. The Fay-Riddell equation, which is of extreme

importance towards modeling heat flux, owes its validity to the stagnation point being in chemical equilibrium. It should be emphasized that the time required for the shock layer gas to reach equilibrium is strongly dependent upon the shock layer's pressure. For example, in the case of the Galileo Probe's entry into Jupiter's atmosphere, the shock layer was mostly in equilibrium during peak heat flux due to the very high pressures experienced (this is counterintuitive given the free stream velocity was 39 km/s during peak heat flux).

Determining the thermodynamic state of the stagnation point is more difficult under an equilibrium gas model than a perfect gas model. Under a perfect gas model, the *ratio of specific heats* (also called "isentropic exponent", adiabatic index, "gamma" or "kappa") is assumed to be constant along with the gas constant. For a real gas, the ratio of specific heats can wildly oscillate as a function of temperature. Under a perfect gas model there is an elegant set of equations for determining thermodynamic state along a constant entropy stream line called the *isentropic chain*. For a real gas, the isentropic chain is unusable and a *Mollier diagram* would be used instead for manual calculation. However graphical solution with a Mollier diagram is now considered obsolete with modern heat shield designers using computer programs based upon a digital lookup table (another form of Mollier diagram) or a chemistry based thermodynamics program. The chemical composition of a gas in equilibrium with fixed pressure and temperature can be determined through the *Gibbs free energy method*. Gibbs free energy is simply the total enthalpy of the gas minus its total entropy times temperature. A chemical equilibrium program normally does not require chemical formulas or reaction-rate equations. The program works by preserving the original elemental abundances specified for the gas and varying the different molecular combinations of the elements through numerical iteration until the lowest possible Gibbs free energy is calculated (a Newton-Raphson method is the usual numerical scheme). The data base for a Gibbs free energy program comes from spectroscopic data used in defining partition functions. Among the best equilibrium codes in existence is the program *Chemical Equilibrium with Applications* (CEA) which was written by Bonnie J. McBride and Sanford Gordon at NASA Lewis (now renamed "NASA Glenn Research Center"). Other names for CEA are the "Gordon and McBride Code" and the "Lewis Code". CEA is quite accurate up to 10,000 K for planetary atmospheric gases but unusable beyond 20,000 K (double ionization is not modeled). CEA can be downloaded from the Internet along with full documentation and will compile on Linux under the G77 Fortran compiler.

Real (non-equilibrium) gas model

A non-equilibrium real gas model is the most accurate model of a shock layer's gas physics but is more difficult to solve than an equilibrium model. The simplest non-equilibrium model is the *Lighthill-Freeman model*.^{[9][10]} The Lighthill-Freeman model initially assumes a gas made up of a single diatomic species susceptible to only one chemical formula and its reverse, e.g. $N_2 \rightarrow N + N$ and $N + N \rightarrow N_2$ (dissociation and recombination). Because of its simplicity, the Lighthill-Freeman model is a useful pedagogical tool but is unfortunately too simple for modeling non-equilibrium air. Air is typically assumed to have a mole fraction composition of 0.7812 molecular nitrogen, 0.2095 molecular oxygen and 0.0093 argon. The simplest real gas model for air is the *five species model* which is based upon N_2 , O_2 , NO , N and O . The five species model assumes no ionization and ignores trace species like carbon dioxide.

When running a Gibbs free energy equilibrium program, the iterative process from the originally specified molecular composition to the final calculated equilibrium composition is essentially

random and not time accurate. With a non-equilibrium program, the computation process is time accurate and follows a solution path dictated by chemical and reaction rate formulas. The five species model has 17 chemical formulas (34 when counting reverse formulas). The Lighthill-Freeman model is based upon a single ordinary differential equation and one algebraic equation. The five species model is based upon 5 ordinary differential equations and 17 algebraic equations. Because the 5 ordinary differential equations are loosely coupled, the system is numerically "stiff" and difficult to solve. The five species model is only usable for entry from low Earth orbit where entry velocity is approximately 7.8 km/s. For lunar return entry of 11 km/s, the shock layer contains a significant amount of ionized nitrogen and oxygen. The five species model is no longer accurate and a twelve species model must be used instead. High speed Mars entry which involves a carbon dioxide, nitrogen and argon atmosphere is even more complex requiring a 19 species model.

An important aspect of modeling non-equilibrium real gas effects is radiative heat flux. If a vehicle is entering an atmosphere at very high speed (hyperbolic trajectory, lunar return) and has a large nose radius then radiative heat flux can dominate TPS heating. Radiative heat flux during entry into an air or carbon dioxide atmosphere typically comes from unsymmetric diatomic molecules, e.g. cyanogen (CN), carbon monoxide, nitric oxide (NO), single ionized molecular nitrogen, et cetera. These molecules are formed by the shock wave dissociating ambient atmospheric gas followed by recombination within the shock layer into new molecular species. The newly formed diatomic molecules initially have a very high vibrational temperature that efficiently transforms the vibrational energy into radiant energy, i.e. radiative heat flux. The whole process takes place in less than a millisecond which makes modeling a challenge. The experimental measurement of radiative heat flux (typically done with shock tubes) along with theoretical calculation through the unsteady Schrödinger equation are among the more esoteric aspects of aerospace engineering. Most of the aerospace research work related to understanding radiative heat flux was done in the 1960s but largely discontinued after conclusion of the Apollo Program. Radiative heat flux in air was just sufficiently understood to insure Apollo's success. However radiative heat flux in carbon dioxide (Mars entry) is still barely understood and will require major research.

Frozen gas model

The frozen gas model describes a special case of a gas that is not in equilibrium. The name "frozen gas" can be misleading. A frozen gas is not "frozen" like ice is frozen water. Rather a frozen gas is "frozen" in time (all chemical reactions are assumed to have stopped). Chemical reactions are normally driven by collisions between molecules. If gas pressure is slowly reduced such that chemical reactions can continue then the gas can remain in equilibrium. However it is possible for gas pressure to be so suddenly reduced that almost all chemical reactions stop. For that situation the gas is considered frozen.

The distinction between equilibrium and frozen is important because it is possible for a gas such as air to have significantly different properties (speed-of-sound, viscosity, et cetera) for the same thermodynamic state, e.g. pressure and temperature. Frozen gas can be a significant issue in the wake behind an entry vehicle. During reentry, free stream air is compressed to high temperature and pressure by the entry vehicle's shock wave. Non-equilibrium air in the shock layer is then transported past the entry vehicle's leading side into a region of rapidly expanding flow that causes freezing. The frozen air can then be entrained into a trailing vortex behind the entry vehicle. Correctly modeling the flow in the wake of an entry vehicle is very difficult. TPS heating in the

vehicle's afterbody is usually not very high but the geometry and unsteadiness of the vehicle's wake can significantly influence aerodynamics (pitching moment) and particularly dynamic stability.

Thermal protection systems

Ablative

The type of heat shield that best protects against high heat flux is the *ablative heat shield*. The ablative heat shield functions by lifting the hot shock layer gas away from the heat shield's outer wall (creating a cooler boundary layer) through *blowing*. The overall process of reducing the heat flux experienced by the heat shield's outer wall is called *blockage*. Ablation causes the TPS layer to char, melt, and sublime through the process of pyrolysis. The gas produced by pyrolysis is what drives blowing and causes blockage of convective and catalytic heat flux. Pyrolysis can be measured in real time using thermogravimetric analysis, so that the ablative performance can be evaluated.^[11] Ablation can also provide blockage against radiative heat flux by introducing carbon into the shock layer thus making it optically opaque. Radiative heat flux blockage was the primary thermal protection mechanism of the Galileo Probe TPS material (carbon phenolic). Carbon phenolic was originally developed as a rocket nozzle throat material (used in the Space Shuttle Solid Rocket Booster) and for RV nose tips. Thermal protection can also be enhanced in some TPS materials through coking. Coking is the process of forming solid carbon on the outer char layer of the TPS. TPS coking was discovered accidentally during development of the Apollo-CM TPS material (Avcoat 5026-39).



Mars Pathfinder during final assembly showing the aeroshell, cruise ring and solid rocket motor

The thermal conductivity of a TPS material is proportional to the material's density. Carbon phenolic is a very effective ablative material but also has high density which is undesirable. If the heat flux experienced by an entry vehicle is insufficient to cause pyrolysis then the TPS material's conductivity could allow heat flux conduction into the TPS bondline material thus leading to TPS failure. Consequently for entry trajectories causing lower heat flux, carbon phenolic is sometimes inappropriate and lower density TPS materials such as the following examples can be better design choices:

SLA-561V

"SLA" in *SLA-561V* stands for "Super Light weight Ablator". SLA-561V is a proprietary ablative made by Lockheed Martin that has been used as the primary TPS material on all of the 70 degree

sphere-cone entry vehicles sent by NASA to Mars. SLA-561V begins significant ablation at a heat flux of approximately 110 W/cm^2 but will fail for heat fluxes greater than 300 W/cm^2 . The Mars Science Laboratory (MSL) aeroshell TPS is currently designed to withstand a peak heat flux of 234 W/cm^2 . The peak heat flux experienced by the Viking-1 aeroshell which landed on Mars was 21 W/cm^2 . For Viking-1, the TPS acted as a charred thermal insulator and never experienced significant ablation. Viking-1 was the first Mars lander and based upon a very conservative design. The Viking aeroshell had a base diameter of 3.54 meters (the largest yet used on Mars). SLA-561V is applied by packing the ablative material into a honeycomb core that is pre-bonded to the aeroshell's structure thus enabling construction of a large heat shield.



NASA's Stardust sample return capsule successfully landed at the USAF Utah Range.

PICA

Phenolic Impregnated Carbon Ablator (PICA) was developed by NASA Ames Research Center and was the primary TPS material for the Stardust aeroshell.^[12] Because the Stardust sample-return capsule was the fastest man-made object to reenter Earth's atmosphere (12.4 km/s or $28,000 \text{ mph}$ relative velocity at 135 km altitude), PICA was an enabling technology for the Stardust mission. (For reference, the Stardust reentry was faster than the Apollo Mission capsules and 70% faster than the reentry velocity of the Shuttle.) PICA is a modern TPS material and has the advantages of low density (much lighter than carbon phenolic) coupled with efficient ablative capability at high heat flux. Stardust's heat shield (0.81 m base diameter) was manufactured from a single monolithic piece sized to withstand a nominal peak heating rate of 1200 W/cm^2 . PICA is a good choice for ablative applications such as high-peak-heating conditions found on sample-return missions or lunar-return missions. PICA's thermal conductivity is lower than other high-heat-flux ablative materials, such as conventional carbon phenolics.

SIRCA



Deep Space 2 impactor aeroshell, a classic 45° sphere-cone with spherical section afterbody enabling aerodynamic stability from atmospheric entry to surface impact

Silicone Impregnated Reuseable Ceramic Ablator (SIRCA) was also developed at NASA Ames Research Center and was used on the Backshell Interface Plate (BIP) of the Mars Pathfinder and

Mars Exploration Rover (MER) aeroshells. The BIP was at the attachment points between the aeroshell's backshell (also called the "afterbody" or "aft cover") and the *cruise ring* (also called the "cruise stage"). SIRCA was also the primary TPS material for the unsuccessful Deep Space 2 (DS/2) Mars impactor probes with their 0.35 m base diameter aeroshells. SIRCA is a monolithic, insulative material that can provide thermal protection through ablation. It is the only TPS material that can be machined to custom shapes and then applied directly to the spacecraft. There is no post-processing, heat treating, or additional coatings required (unlike current Space Shuttle tiles). Since SIRCA can be machined to precise shapes, it can be applied as tiles, leading edge sections, full nose caps, or in any number of custom shapes or sizes. SIRCA has been demonstrated in BIP applications but not yet as a forebody TPS material.^[13]

Early research on ablation technology in the USA was centered at NASA's Ames Research Center located at Moffett Field, California. Ames Research Center was ideal, since it had numerous wind tunnels capable of generating varying wind velocities. Initial experiments typically mounted a mock-up of the ablative material to be analyzed within a hypersonic wind tunnel.^[14]

Thermal soak



Astronaut Andrew S. W. Thomas takes a close look at TPS tiles underneath Space Shuttle Atlantis.

Thermal soak is a part of almost all TPS schemes. For example, an ablative heat shield loses most of its thermal protection effectiveness when the outer wall temperature drops below the minimum necessary for pyrolysis. From that time to the end of the heat pulse, heat from the shock layer soaks into the heat shield's outer wall and would eventually convect to the payload. This outcome is prevented by ejecting the heat shield (with its heat soak) prior to the heat convecting to the inner wall.



Excellent thermal insulator: white hot 1260 °C silica tile material is safely hand held 10 seconds after removal from high temperature oven

Thermal soak TPS is intended to shield mainly against heat load and not against a high peak heat flux (a long duration heat pulse of low intensity is assumed for the TPS design). The Space Shuttle orbit vehicle was designed with a reusable heat shield based upon a thermal soak TPS. It should be emphasized that the tradeoff for TPS reusability is an inability to withstand a high heat flux, e.g. a Space Shuttle TPS would not be practical as a primary thermal protection for lunar return. A Space Shuttle's underside is coated with thousands of tiles made of silica foam, which are intended to survive multiple reentries with only minor repairs between missions. Fabric sheets known as gap fillers are inserted between the tiles where necessary. These gap fillers provide for a snug fit between separate tiles while allowing for thermal expansion. When a Space Shuttle lands, a significant amount of heat is stored in the TPS. Shortly after landing, a ground-support cooling unit connects to the Space Shuttle's internal Freon coolant loop to remove heat soaked in the TPS and orbiter structure.



Rigid black LI-900 tiles are used on the Space Shuttle. (Shuttle shown is *Atlantis*.)

Typical Space Shuttle's TPS tiles (LI-900) have remarkable thermal protection properties but are relatively brittle and break easily, and cannot survive in-flight rain. An LI-900 tile exposed to a temperature of 1000 K on one side will remain merely warm to the touch on the other side. An impressive stunt that can be performed with a cube of LI-900 is to remove it glowing white hot from a furnace and then hold it with one's bare fingers without discomfort along the cube's edges.

Passively cooled

In some early ballistic missile RVs, e.g. the Mk-2 and the sub-orbital Mercury spacecraft, *radiatively cooled TPS* were used to initially absorb heat flux during the heat pulse and then after the heat pulse, radiate and convect the stored heat back into the atmosphere. However, the earlier version of this technique required a considerable quantity of metal TPS (e.g. titanium, beryllium, copper, et cetera). Modern designers prefer to avoid this added mass by using ablative and thermal soak TPS instead.



The Mercury Capsule design (shown with escape tower) originally used a radiatively cooled TPS but was later converted to an ablative TPS

Radiatively cooled TPS can still be found on modern entry vehicles but Reinforced Carbon-Carbon (also called *RCC* or *carbon-carbon*) is normally used instead of metal. RCC is the TPS material on the nose cone and leading edges of the Space Shuttle's wings. RCC was also proposed as the leading edge material for the X-33. Carbon is the most refractory material known with a one atmosphere sublimation temperature of 3825 °C for graphite. This high temperature made carbon an obvious choice as a radiatively cooled TPS material. Disadvantages of RCC are that it is currently very expensive to manufacture and lacks impact resistance.^[15]

Some high-velocity aircraft, such as the SR-71 Blackbird and Concorde, had to deal with heating similar to that experienced by spacecraft at much lower intensity, but for hours at a time. Studies of the SR-71's titanium skin revealed the metal structure was restored to its original strength through annealing due to aerodynamic heating. In the case of Concorde the aluminium nose was permitted to reach a maximum operating temperature of 127 °C (typically 180 °C warmer than the sub-zero ambient air); the metallurgical implications (loss of temper) that would be associated with a higher peak temperature was the most significant factor determining the top speed of the aircraft.

A radiatively cooled TPS for an entry vehicle is often called a "hot metal TPS". Early TPS designs for the Space Shuttle called for a hot metal TPS based upon titanium shingles. Unfortunately the earlier Shuttle TPS concept was rejected because it was incorrectly believed a silica tile based TPS offered less expensive development and manufacturing costs. A titanium shingle TPS was again proposed for the unsuccessful X-33 Single-Stage to Orbit (SSTO) prototype.

Recently, newer radiatively cooled TPS materials have been developed that could be superior to RCC. Referred to by their prototype vehicle "SHARP" (Slender Hypervelocity Aerothermodynamic Research Probe), these TPS materials have been based upon substances such as zirconium diboride and hafnium diboride. SHARP TPS have suggested performance improvements allowing for sustained Mach 7 flight at sea level, Mach 11 flight at 100,000 ft altitudes and significant improvements for vehicles designed for continuous hypersonic flight. SHARP TPS materials enable sharp leading edges and nose cones to greatly reduce drag for air breathing combined cycle propelled space planes and lifting bodies. SHARP materials have exhibited effective TPS characteristics from zero to more than 2000 °C, with melting points over 3500 °C . They are

structurally stronger than RCC thus not requiring structural reinforcement with materials such as Inconel. SHARP materials are extremely efficient at re-radiating absorbed heat thus eliminating the need for additional TPS behind and between SHARP materials and conventional vehicle structure. NASA initially funded (and discontinued) a multi-phase R&D program through the University of Montana in 2001 to test SHARP materials on test vehicles.^{[16][17]}

Actively cooled

Various advanced reusable spacecraft and hypersonic aircraft designs have been proposed to employ heat shields made from temperature-resistant metal alloys that incorporated a refrigerant or cryogenic fuel circulating through them. Such a TPS concept was proposed for the X-30 National Aerospace Plane (NASP). The NASP was supposed to have been a scramjet powered hypersonic aircraft but failed in development.

In the early 1960s various TPS systems were proposed to use water or other cooling liquid sprayed into the shock layer, or passed through channels in the heat shield. Advantages included the possibility of more all-metal designs which would be cheaper to develop, more rugged, and eliminating the need for classified technology. The disadvantage is increased weight and complexity, and lower reliability. The concept has never been flown, but a similar technology (the plug nozzle^[18]) did undergo extensive ground testing.

Feathered reentry



SpaceShipOne in flight

In 2004, aircraft designer Burt Rutan demonstrated the feasibility of a shape changing airfoil for reentry with the suborbital SpaceShipOne. The wings on this craft rotate to provide a shuttlecock effect. Notably, SpaceShipOne does not experience significant thermal loads on reentry.

This increases drag, as the craft is now less streamlined. This results in more atmospheric gas particles hitting the spacecraft at higher altitudes than otherwise. The aircraft thus slows down more in higher atmospheric layers (which is the very key to efficient reentry, see above). It should also be noted that SpaceShipOne, in its "wings flipped" configuration, will *automatically* orient itself to a high drag attitude. Rutan has compared this to a falling shuttlecock. However, it is important to realize that the velocity attained by SpaceShipOne prior to reentry is much lower than that of an orbital spacecraft, and most engineers (including Rutan) do not consider the shuttlecock reentry technique viable for return from orbit.

The feathered or *shuttlecock reentry* was first described by Dean Chapman of NACA in 1958.^[19] In the section of his report on *Composite Entry*, Chapman described a solution to the problem using a high-drag device:

"It may be desirable to combine lifting and nonlifting entry in order to achieve some advantages... For landing maneuverability it obviously is advantageous to employ a lifting vehicle. The total heat absorbed by a lifting vehicle, however, is much higher than for a nonlifting vehicle... Nonlifting vehicles can more easily be constructed... by employing, for example, a large, light drag device... The larger the device, the smaller is the heating rate"

Chapman noted that:

"Nonlifting vehicles with shuttlecock stability are advantageous also from the viewpoint of minimum control requirements during entry."

Finally, Chapman said:

"an evident composite type of entry, which combines some of the desirable features of lifting and nonlifting trajectories, would be to enter first without lift but with a... drag device; then, when the velocity is reduced to a certain value... the device is jettisoned or retracted, leaving a lifting vehicle... for the remainder of the descent"

Entry vehicle design considerations

There are four critical parameters considered when designing a vehicle for atmospheric entry:

1. Peak heat flux
2. Heat load
3. Peak deceleration
4. Peak dynamic pressure

Peak heat flux and dynamic pressure selects the TPS material. Heat load selects the thickness of the TPS material stack. Peak deceleration is of major importance for manned missions. The upper limit for manned return to Earth from Low Earth Orbit (LEO) or lunar return is 10 Gs^[20]. For Martian atmospheric entry after long exposure to zero gravity, the upper limit is 4 Gs^[20]. Peak dynamic pressure can also influence the selection of the outermost TPS material if spallation is an issue.

Starting from the principle of *conservative design*, the engineer typically considers two worst case trajectories, the undershoot and overshoot trajectories. The undershoot trajectory is typically defined as the shallowest allowable entry velocity angle prior to atmospheric skip-off. The overshoot trajectory has the highest heat load and sets the TPS thickness. The undershoot trajectory is defined by the steepest allowable trajectory. For manned missions the steepest entry angle is limited by the peak deceleration. The undershoot trajectory also has the highest peak heat flux and dynamic pressure. Consequently the undershoot trajectory is the basis for selecting the TPS material. There is no "one size fits all" TPS material. A TPS material that is ideal for high heat flux may be too conductive (too dense) for a long duration heat load. A low density TPS material might lack the tensile strength to resist spallation if the dynamic pressure is too high. A TPS material can perform

well for a specific peak heat flux but fail catastrophically for the same peak heat flux if the wall pressure is significantly increased (this happened with NASA's R-4 test spacecraft).^[20] Older TPS materials tend to be more labor intensive and expensive to manufacture compared to modern materials. However modern TPS materials often lack the flight history of the older materials (an important consideration for a risk adverse designer).

Based upon Allen and Eggers discovery, maximum aeroshell bluntness (maximum drag) yields minimum TPS mass. Maximum bluntness (minimum ballistic coefficient) also yields a minimal terminal velocity at maximum altitude (very important for Mars EDL but detrimental for military RVs). However there is an upper limit to bluntness imposed by aerodynamic stability considerations based upon *shock wave detachment*. A shock wave will remain attached to the tip of a sharp cone if the cone's half-angle is below a critical value. This critical half-angle can be estimated using perfect gas theory (this specific aerodynamic instability occurs below hypersonic speeds). For a nitrogen atmosphere (Earth or Titan), the maximum allowed half-angle is approximately 60°. For a carbon dioxide atmosphere (Mars or Venus), the maximum allowed half-angle is approximately 70°. After shock wave detachment, an entry vehicle must carry significantly more shocklayer gas around the leading edge stagnation point (the subsonic cap). Consequently, the aerodynamic center moves upstream thus causing aerodynamic instability. It is incorrect to reapply an aeroshell design intended for Titan entry (Huygens probe in a nitrogen atmosphere) for Mars entry (Beagle-2 in a carbon dioxide atmosphere). After being abandoned, the Soviet Mars lander program achieved no successful landings (no useful data returned) after multiple attempts. The Soviet Mars landers were based upon a 60° half-angle aeroshell design. In the early 1960s, it was incorrectly believed the Martian atmosphere was mostly nitrogen, (actual Martian atmospheric mole fractions are carbon dioxide 0.9550, nitrogen 0.0270 and argon 0.0160). The Soviet aeroshells were probably(?) based upon an incorrect Martian atmospheric model and then not revised when new data became available.

A 45 degree half-angle sphere-cone is typically used for atmospheric probes (surface landing not intended) even though TPS mass is not minimized. The rationale for a 45° half-angle is either aerodynamic stability from entry-to-impact (the heat shield is not jettisoned) or a short-and-sharp heat pulse followed by prompt heat shield jettison. A 45° sphere-cone design was used with the DS/2 Mars impactor and Pioneer Venus Probes.

History's most difficult atmospheric entry

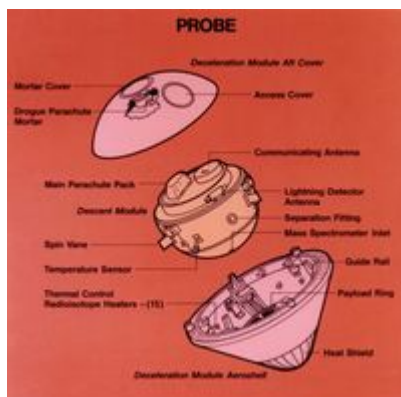
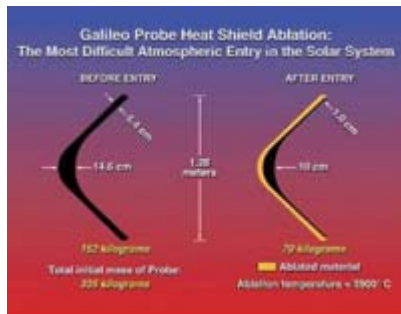


Diagram of Galileo atmospheric entry probe instruments and subsystems.

The highest speed controlled entry so far achieved was by the Galileo Probe. The Galileo Probe was a 45° sphere-cone that entered Jupiter's atmosphere at 47.4 km/s (atmosphere relative speed at 450 km above the 1 bar reference altitude). The peak deceleration experienced was 230 g (2.3 km/s²). Peak stagnation point pressure before aeroshell jettison was 9 bars (900 kPa). The peak shock layer temperature was approximately 16000 K (the solar photosphere is merely 5800 K). Approximately 26% of the Galileo Probe's original entry mass of 338.93 kg was vaporized during the 70 second heat pulse. Total blocked heat flux peaked at approximately 15000 W/cm². By way of comparison, the peak total heat flux experienced by the Mars Pathfinder aeroshell, the highest experienced by a successful Mars lander, was 106 W/cm², and the Apollo-4 (AS-501) command module, re-entering at 10.77 km/s (atmosphere relative speed at 121.9 km altitude) experienced a peak total heat flux of 497 W/cm².



Galileo probe heat shield profile before and after entry.

Conservative design was used in creating the Galileo Probe. Due to the extreme state of the Galileo Probe's entry conditions, the radiative heat flux and turbulence of the shock layer along with the TPS material response were barely understood. Carbon Phenolic was used for the Galileo Probe TPS. Carbon phenolic was earlier used for the Pioneer Venus Probes which were the design ancestors to the Galileo Probe. The Galileo Probe experienced far greater TPS recession near the base of its frustum than expected. Despite a safety-factor of two in TPS thickness, the Galileo Probe's heatshield almost failed. The precise mechanism for this higher TPS recession is still unknown and currently beyond definitive theoretical analysis.

After successfully completing its mission, the Galileo Probe continued descending into Jupiter's atmosphere where the ambient temperature grew with greater depth due to isentropic compression. In the depths of Jupiter's atmosphere, the ambient atmospheric gas temperature became so hot that the entire probe, including its jettisoned heat shield, were vaporized into monatomic gas.

Notable atmospheric entry mishaps



Genesis entry vehicle after crash

Not all atmospheric re-entries have been successful and some have led to significant disasters.

- Mercury 6 — Instrument readings show that the heat shield and landing bag were not locked. The decision was made to leave the retrorocket pack in position during reentry. Lone astronaut John Glenn survived. The instrument readings were later found to be erroneous.
- Voskhod 2 — The service module failed to detach for some time, but the crew survived.
- Soyuz 1 — Different accounts exist. Either the attitude control system failed while still in orbit and/or parachutes got entangled during the landing sequence (entry, descent and landing (EDL) failure). Lone cosmonaut Vladimir Mikhailovich Komarov died.
- Soyuz 5 — The service module failed to detach, but the crew survived.
- Soyuz 11 — Early depressurization led to the death of all three crew.
- Mars Polar Lander — Failed during EDL. The failure was believed to be the consequence of a software error. The precise cause is unknown due to lack of real time telemetry.



The CNN report of the *Columbia* disaster.

- Space Shuttle Columbia disaster — The failure of an RCC panel on a wing leading edge led to breakup of the orbiter at hypersonic speed resulting in the loss of all seven crew members.
- Genesis — The parachute failed to deploy due to a G-switch being installed backwards (a similar error delayed parachute deployment for the Galileo Probe). Consequently, the Genesis entry vehicle crashed into the desert floor. The payload was damaged but it was later claimed that some scientific data was recoverable.

Uncontrolled and unprotected reentries

More than 100 tonnes (110 short tons) of man-made objects reenter in an uncontrolled fashion each year. Of satellites that reenter, approximately 10-40% of the mass of the object is likely to reach the surface of the Earth.^[21] On average, about one catalogued object reenters per day. Approximately a quarter of all objects are of U.S. origin.

Due to the Earth's surface being primarily water, most objects that survive reentry land in one of the world's oceans. The estimated chances that a given person will get hit and injured during his/her lifetime is around 1 in a trillion.^[22]

In 1978, Cosmos 954 reentered uncontrolled and crashed near Great Slave Lake in the Northwest Territories of Canada. Cosmos 954 was nuclear powered and left radioactive debris near its impact site.

In 1979, Skylab reentered uncontrolled and parts of it crashed into Esperance, Western Australia, damaging several buildings. Local authorities issued a fine for littering to the United States, but the fine was never settled.^[23]

Deorbit disposal

On June 4, 2000 the Gamma Ray Observatory was deliberately de-orbited after one of its gyroscopes failed. The debris that did not burn up fell harmlessly into the Pacific Ocean. At the time, the observatory was still operational, however the failure of another gyroscope would have made de-orbiting much more difficult and dangerous. With some controversy, NASA decided in the interest of public safety that a controlled crash was preferable to letting the craft come down on its own at random.

In 2001, the Russian Mir space station was deliberately de-orbited, and broke apart during atmospheric re-entry. Mir entered the Earth's atmosphere on March 23, 2001, near Nadi, Fiji, and fell into the South Pacific Ocean. Previously, its two predecessors, Salyut 6 and Salyut 7, were deorbited in a controlled manner as well.


On February 21, 2008, a disabled U.S. spy satellite, USA 193, was successfully intercepted and destroyed, at an altitude of approximately 246 kilometres (153 mi) above the Earth, by a U.S. Navy cruiser off the coast of Hawaii, which fired an SM-3 missile. The satellite had been inoperative upon its launch in 2006, and had never reached its designated orbit, but was in a rapidly deteriorating Low Earth orbit, and destined for an uncontrolled reentry within a month. United States Department of Defense expressed concern that the debris, including a 1,000-pound (450 kg) highly toxic hydrazine fuel tank, might reach the Earth's surface. Several governments including those of Russia, China, and Belarus protested the US action.^[24]

Countries having performed successful re-entries

Manned Orbital Re-entry

-  United States
-  Russia
-  China

Unmanned Orbital Reentry

- | | |
|---|---|
| ▪  United States | ▪  India |
| ▪  Russia | ▪  Japan |
| ▪  China | ▪  European Union |

Research into atmospheric entry



Mk-12A RV retrofitted with hafnium diboride strakes for a NASA research project (Sharp-B2)

Aerospace technologies can be used for civilian or military purposes (known as dual use). Atmospheric entry technology owes its origins to the development of ballistic missiles during the Cold War. Given the enormous expense required in developing this technology, it is doubtful it could have appeared as quickly as it did without the military incentive. Mankind's survival beyond its planet of origin could be dependent upon atmospheric entry technology. It is ironic that the same technology enabling destructive nuclear-tipped missiles also enables the exploration and development of outer space. Aerospace technology is needed for civilian space exploration, yet certain aspects are and will remain restricted to impede military proliferation of the technology. This basic dilemma is present throughout the literature on atmospheric entry. There is a *glass wall* between pedagogical and practical information. For example, in the text books referenced in this article, a topic thread will proceed as long as the information is nonspecific but almost always stops at the point of practical application. To go beyond pedagogical information, one must search the technical literature (NACA/NASA Technical Reports, declassified technical reports and peer reviewed archive literature). Declassified technical reports are a frustrating information source since many of the reports were destroyed prior to going through the legally required declassification process. It is almost always true that significant documents referred to in declassified technical reports no longer exist (technical information costing many millions of dollars has simply vanished).

Further reading

- Martin, John J. (1966). *Atmospheric Entry - An Introduction to Its Science and Engineering*. Old Tappan, NJ: Prentice-Hall.^[25]
- Regan, Frank J. (1984). *Re-Entry Vehicle Dynamics (AIAA Education Series)*. New York: American Institute of Aeronautics and Astronautics, Inc.. ISBN 0-915928-78-7.^[26]
- Etkin, Bernard (1972). *Dynamics of Atmospheric Flight*. New York: John Wiley & Sons, Inc.. ISBN 0-471-24620-4.^[27]

- Vincenti, Walter G.; Kruger, Jr., Charles H. (1986). *Introduction to Physical Gas Dynamics*. Malabar, Florida: Robert E. Krieger Publishing Co.. ISBN 0-88275-309-6.^[28]
- Hansen, C. Frederick (1976). *Molecular Physics of Equilibrium Gases, A Handbook for Engineers*. NASA. NASA SP-3096.^[29]
- Hayes, Wallace D.; Probstein, Ronald F. (1959). *Hypersonic Flow Theory*. New York and London: Academic Press. A revised version of this classic text has been reissued as an inexpensive paperback: Hayes, Wallace D. (1966, reissued in 2004). *Hypersonic Inviscid Flow*. Mineola, New York: Dover Publications. ISBN 0-486-43281-5.
- Anderson, Jr., John D. (1989). *Hypersonic and High Temperature Gas Dynamics*. New York: McGraw-Hill, Inc.. ISBN 0-07-001671-2.

Notes and references

1. ^ Goddard, R.H., "Report Concerning Further Developments", March 1920, The Smithsonian Institution Archives
2. ^ Hansen, James R. (1987) "Engineer in Charge: A History of the Langley Aeronautical Laboratory, 1917-1958." The NASA History Series, sp-4305. Chapter 12.
3. ^ Allen, H. Julian and Eggers, Jr., A. J., "A Study of the Motion and Aerodynamic Heating of Ballistic Missiles Entering the Earth's Atmosphere at High Supersonic Speeds," NACA Report 1381, (1958).
4. ^ Fay, J. A. and Riddell, F. R., "Theory of Stagnation Point Heat Transfer in Dissociated Air," *Journal of the Aeronautical Sciences*, Vol. 25, No. 2, page 73, February 1958.
5. ^ Hillje, Ernest R., "Entry Aerodynamics at Lunar Return Conditions Obtained from the Flight of Apollo 4 (AS-501)," NASA TN D-5399, (1969).
6. ^ Regan, Frank J. and Anadakrishnan, Satya M., "Dynamics of Atmospheric Re-Entry," AIAA Education Series, American Institute of Aeronautics and Astronautics, Inc., New York, ISBN 1-56347-048-9, (1993).
7. ^ [1] Ames Research Staff, "Equations, Tables, and Charts for Compressible Flow," NACA Report 1135, (1953).]
8. ^ Kenneth Iliff and Mary Shafer, *Space Shuttle Hypersonic Aerodynamic and Aerothermodynamic Flight Research and the Comparison to Ground Test Results*, Page 5-6
9. ^ Lighthill, M.J., "Dynamics of a Dissociating Gas. Part I. Equilibrium Flow," *Journal of Fluid Mechanics*, vol. 2, pt. 1. p. 1 (1957).
10. ^ Freeman, N.C., "Non-equilibrium Flow of an Ideal Dissociating Gas." *Journal of Fluid Mechanics*, vol. 4, pt. 4, p. 407 (1958).
11. ^ Parker, John and C. Michael Hogan, "Techniques for Wind Tunnel assessment of Ablative Materials," NASA Ames Research Center, Technical Publication, August, 1965.
12. ^ Tran, Huy K, et al., "Qualification of the forebody heatshield of the Stardust's Sample Return Capsule," AIAA, Thermophysics Conference, 32nd, Atlanta, GA; 23-25 June 1997.
13. ^ Tran, Huy K., et al., "Silicone impregnated reusable ceramic ablators for Mars follow-on missions," AIAA-1996-1819, Thermophysics Conference, 31st, New Orleans, LA, June 17-20, 1996.
14. ^ Hogan, C. Michael, Parker, John and Winkler, Ernest, of NASA Ames Research Center, "An Analytical Method for Obtaining the Thermogravimetric Kinetics of Char-forming Ablative Materials from Thermogravimetric Measurements", AIAA/ASME Seventh Structures and Materials Conference, April, 1966
15. ^ [2] Columbia Accident Investigation Board report.
16. ^ http://hubbard.engr.scu.edu/docs/thesis/2003/SHARP_Thesis.pdf
17. ^ sharp structure homepage w left
18. ^ <http://www.astronautix.com/engines/j2.htm> - J2T-200K & J2T-250K

19. ^ Chapman, Dean R., "An approximate analytical method for studying reentry into planetary atmospheres," NACA Technical Note 4276, May 1958.
20. ^ ^{a b c} Pavlosky, James E., St. Leger, Leslie G., "Apollo Experience Report - Thermal Protection Subsystem," NASA TN D-7564, (1974).
21. ^ Spacecraft Reentry FAQ: How much material from a satellite will survive reentry?
22. ^ Center for Orbital and Reentry Debris Studies- Spacecraft Reentry
23. ^ Australians Take Mir Deorbit Risks in Stride, Space.com
24. ^ Gray, Andrew (2008-02-21). "U.S. has high confidence it hit satellite fuel tank". Reuters. <http://www.reuters.com/article/scienceNews/idUSN1930844420080222>. Retrieved on 2008-02-23.
25. ^ John J. Martin's book was the first and arguably the best in the open literature about designing reentry vehicles. In his book, Martin showed an incredible depth and breadth of knowledge. Unfortunately, this book has been out-of-print for decades but is sometimes available second hand through the Internet.
26. ^ "Dynamics of Atmospheric Re-Entry" by Frank J. Regan and Satya M. Anandakrishnan is a revision of Regan's earlier book, "Re-Entry Vehicle Dynamics". Unfortunately Chapter 10 of "Re-Entry Vehicle Dynamics" was deleted when the book was revised into the newer version. Chapter 10, titled "Moment Equations in Constant Density Atmosphere" concerned the subjects of entry vehicle roll resonance and tricyclic theory. "Re-Entry Vehicle Dynamics" has been out-of-print for years and currently no used copies are listed on the Internet. If you find a second-hand copy of "Re-Entry Vehicle Dynamics", *buy it* (it's a very rare book). Should you find "Re-Entry Vehicle Dynamics" in a library, photocopy Chapter 10. Despite the omissions from the earlier version, "Dynamics of Atmospheric Re-Entry" is a very useful book and still in print, though very expensive (current list price of \$105.95).
27. ^ Classical 6-DoF theory for aircraft assumes a flat Earth with constant atmospheric density in an inertial frame. Consequently classical 6-DoF theory should not be used for simulating hypersonic atmospheric flight that lasts for several minutes. Classical 6-DoF for hypersonic flight is approximately correct only for a few seconds, e.g. stability analysis for a time discrete event. Etkin's treatment of 6-DoF theory in "Dynamics of Atmospheric Flight" was unusual in being sufficiently general that it touched upon hypersonic flight.
28. ^ "Introduction to Physical Gas Dynamics" by Vincenti and Kruger is widely used for graduate course work in real gas physics. The book provides an excellent introduction into non-equilibrium gas physics and describes the Lighthill-Freeman model in detail. Most university bookstores offer Vincenti and Kruger for sale (it's a very common book).
29. ^ Frederick Hansen's NASA SP-3096 is arguably one of the best introductory texts on equilibrium thermodynamics and was written specifically for aeronautical engineers doing entry vehicle work. The partition functions listed in NASA SP-3096 are inaccurate (use the polynomial fits from the Gordon and McBride code, CEA). NASA SP-3096 can sometimes be found used and is in US government document libraries. NASA SP-3096 is worth the trouble of photocopying (it's in the public domain).

Ballistic reentry

From Wikipedia, the free encyclopedia

A **ballistic reentry** is a type of atmospheric reentry of an atmosphere that relies solely on drag within the atmosphere to slow the vehicle. By contrast, the U.S. space shuttle relies heavily on aerodynamic lift for its reentry, both vertically, to prolong the reentry process, and horizontally, to dissipate energy into a series of S-turns. The U.S. Mercury and Soviet Vostok spacecraft used a ballistic reentry. The U.S. Gemini and Apollo spacecraft and Russian Soyuz spacecraft use a lifting reentry, where aerodynamic lift makes for a gentler and aim able reentry, but have a backup ballistic reentry mode. Lately ballistic re-entries have accidentally occurred on the Soyuz TMA-10 and Soyuz TMA-11 missions.

Blast wave

From Wikipedia, the free encyclopedia

A **blast wave** in fluid dynamics is the pressure and flow resulting from the deposition of a large amount of energy in a small very localised volume. The flow field can be approximated as a lead shock wave, followed by a 'self-similar' subsonic flow field.

History

The classic flow solution — the so-called "similarity solution" — was independently devised by Geoffrey Ingram Taylor^[1] and John von Neumann^[2] during World War II. After the war, the similarity solution was published by three other authors — L. I. Sedov^[3], R. Latter^[4], and J. Lockwood-Taylor^[5] — who had discovered it independently^[6].

Applications

Bombs

In response to an inquiry from the British MAUD Committee, G. I. Taylor estimated the amount of energy that would be released by the explosion of an atomic bomb in air. He postulated that for an idealized point source of energy, the spatial distributions of the flow variables would have the same form during a given time interval, the variables differing only in scale. (Thus the name of the "similarity solution.") This hypothesis allowed the partial differential equations in terms of r (the radius of the blast wave) and t (time) to be transformed into an ordinary differential equation in

terms of the similarity variable $\frac{r^5 \rho_o}{t^2 E}$,

where ρ_o is the density of the air and E is the energy that's released by the explosion^{[7][8][9]}. This result allowed G. I. Taylor to estimate the yield of the first atomic explosion in New Mexico in 1945 using only photographs of the blast, which had been published in newspapers and magazines^[6]. The yield of the explosion was determined by using the equation:

$$E = \left(\frac{\rho_o}{t^2} \right) \left(\frac{r}{C} \right)^5,$$

where C is a dimensionless constant that is a function of the ratio of the specific heat of air at constant pressure to the specific heat of air at constant volume. In 1950, G. I. Taylor published two articles in which he revealed the yield E of the first atomic explosion^[10], which had previously been classified and whose publication therefore caused a great to-do.

Astronomy

This so called **Sedov-Taylor** solution has become useful in astrophysics, i.e. for quantitative estimation of the outcome from supernova-explosions. The Sedov-Taylor expansion is also known as 'Blast Wave' phase, which is an adiabatic expansion phase in the life cycle of supernova. The temperature of the material in supernova shell decreases with time, but the internal energy of the

material is always 72% of E_0 , the initial energy released. This is helpful for Astrophysicists in predicting the behavior of supernova remnants.

The radius R of the blast wave is given as,

$$R = 14 (E_0/n)^{1/5} t^{2/5} \text{ pc}$$

where,

E is the initial energy,
 t is the age
 n is the surrounding medium density

The shock temperature is also given as,

$$T = 1.0 \times 10^{10} (E_0/n) R^{-3} \text{ K}^{[11]}$$

Further reading

- Cathy J. Clarke & Bob Carswell; *Principles of Astrophysical Fluid Dynamics*, Cambridge University Press (2007), Chapter 8. ISBN 978-0521853316

References

1. ^ Taylor, Sir Geoffrey Ingram, "The formation of a blast wave by a very intense explosion. I. Theoretical discussion," *Proceedings of the Royal Society of London. Series A, Mathematical and Physical Sciences*, Vol. 201, No. 1065, pages 159 - 174 (22 March 1950).
2. ^ Neumann, John von, "The point source solution," *John von Neumann. Collected Works*, edited by A. J. Taub, Vol. 6 [Elmsford, N.Y.: Pergamon Press, 1963], pages 219 - 237.
3. ^ Sedov, L. I., "Propagation of strong shock waves," *Journal of Applied Mathematics and Mechanics*, Vol. 10, pages 241 - 250 (1946).
4. ^ Latter, R., "Similarity solution for a spherical shock wave," *Journal of Applied Physics*, Vol. 26, pages 954 - 960 (1955).
5. ^ Lockwood-Taylor, J., "An exact solution of the spherical blast wave problem," *Philosophical Magazine*, Vol. 46, pages 317 - 320 (1955).
6. ^ ^a ^b Batchelor, George, *The Life and Legacy of G. I. Taylor*, [Cambridge, England: Cambridge University Press, 1996], pages 202 - 207.
7. ^ Discussion of similarity solutions, including G. I. Taylor's:
http://en.wikipedia.org/wiki/Buckingham_Pi_theorem
8. ^ Derivation of G. I. Taylor's similarity solution:
<http://www.atmosp.physics.utoronto.ca/people/codoban/PHY138/Mechanics/dimensional.pdf>
9. ^ Discussion of G. I. Taylor's research, including his similarity solution:
http://www.deas.harvard.edu/brenner/taylor/physic_today/taylor.htm
10. ^ Taylor, Sir Geoffrey Ingram, "The formation of a blast wave by a very intense explosion. II. The atomic explosion of 1945," *Proceedings of the Royal Society of London. Series A, Mathematical and Physical Sciences*, Vol. 201, No. 1065, pages 175 - 186 (22 March 1950).
11. ^ Exploring the X-ray Universe, Philip A. Charles, Frederick D. Seward

Choked flow

From Wikipedia, the free encyclopedia

Choked flow of a fluid is a fluid dynamic condition caused by the Venturi effect. When a flowing fluid at a certain pressure and temperature flows through a restriction (such as the hole in an orifice plate or a valve in a pipe) into a lower pressure environment, under the conservation of mass the fluid velocity must increase for initially subsonic upstream conditions as it flows through the smaller cross-sectional area of the restriction. At the same time, the Venturi effect causes the static pressure to decrease. **Choked flow** is a limiting condition which occurs when the mass flow rate will not increase with a further decrease in the downstream pressure environment while upstream pressure is fixed.

For homogeneous fluids, the physical point at which the choking occurs for adiabatic conditions is when the exit plane velocity is at sonic conditions or at a Mach number of 1.^{[1][2][3]} It is most important to note that the mass flow rate can still be increased by increasing the upstream stagnation pressure, or by decreasing the upstream stagnation temperature.

The choked flow of gases is useful in many engineering applications because the mass flow rate is independent of the downstream pressure, depending only on the temperature and pressure on the upstream side of the restriction. Under choked conditions, valves and calibrated orifice plates can be used to produce a particular mass flow rate.

If the fluid is a liquid, a different type of limiting condition (also known as choked flow) occurs when the Venturi effect acting on the liquid flow through the restriction decreases the liquid pressure to below that of the liquid vapor pressure at the prevailing liquid temperature. At that point, the liquid will partially flash into bubbles of vapor and the subsequent collapse of the bubbles causes cavitation. Cavitation is quite noisy and can be sufficiently violent to physically damage valves, pipes and associated equipment. In effect, the vapor bubble formation in the restriction limits the flow from increasing any further.^{[4][5]}

Mass flow rate of a gas at choked conditions

All gases flow from upstream higher stagnation pressure sources to downstream lower pressure sources. There are several situations in which choked flow occurs, such as: change of cross section (as in a convergent-divergent nozzle or flow through an orifice plate), Fanno flow, isothermal flow and Rayleigh flow.

Choking in change of cross section flow

Assuming ideal gas behavior, steady state choked flow occurs when the ratio of the absolute upstream pressure to the absolute downstream pressure is equal to or greater than $\left[\frac{k+1}{2} \right]^{k/(k-1)}$, where k is the specific heat ratio of the gas (sometimes called the isentropic expansion factor and sometimes denoted as γ).

For many gases, k ranges from about 1.09 to about 1.41, and therefore $[(k + 1) / 2]^{k / (k - 1)}$ ranges from 1.7 to about 1.9 ... which means that choked flow usually occurs when the absolute source vessel pressure is at least 1.7 to 1.9 times as high as the absolute downstream pressure.

When the gas velocity is choked, the equation for the mass flow rate in SI metric units is: ^{[1][2][3][6]}

$$\dot{m} = C A \sqrt{k \rho P \left(\frac{2}{k + 1} \right)^{(k+1)/(k-1)}}$$

where the terms are defined in the table below. If the density ρ is not known directly, then it is useful to eliminate it using the Ideal gas law corrected for the real gas compressibility:

$$\dot{m} = C A P \sqrt{\left(\frac{k M}{Z R T} \right) \left(\frac{2}{k + 1} \right)^{(k+1)/(k-1)}}$$

so that the mass flow rate is primarily dependent on the cross-sectional area A of the hole and the upstream pressure P , and only weakly dependent on the temperature T . The rate does not depend on the downstream pressure at all. All other terms are constants that depend only on the composition of the material in the flow. Although the gas velocity reaches a maximum and becomes choked, the mass flow rate is not choked. The mass flow rate can still be increased if the upstream pressure is increased.

where:

\dot{m} = mass flow rate, kg/s

C = discharge coefficient, dimensionless (usually about 0.72)

A = discharge hole cross-sectional area, m²

k = c_p/c_v of the gas

c_p = specific heat of the gas at constant pressure

c_v = specific heat of the gas at constant volume

ρ = real gas density at P and T , kg/m³

P = absolute upstream stagnation pressure, Pa

M = the gas molecular mass, kg/mole (also known as the molecular weight)

R = Universal gas law constant = 8314.5 (N·m) / (kmole·K)

T = absolute gas temperature, K

Z = the gas compressibility factor at P and T , dimensionless

The above equations calculate the steady state mass flow rate for the stagnation pressure and temperature existing in the upstream pressure source.

If the gas is being released from a closed high-pressure vessel, the above steady state equations may be used to approximate the **initial** mass flow rate. Subsequently, the mass flow rate will decrease during the discharge as the source vessel empties and the pressure in the vessel decreases. Calculating the flow rate versus time since the initiation of the discharge is much more complicated,

but more accurate. Two equivalent methods for performing such calculations are explained and compared online.^[7]

The technical literature can be very confusing because many authors fail to explain whether they are using the universal gas law constant R which applies to any ideal gas or whether they are using the gas law constant R_s which only applies to a specific individual gas. The relationship between the two constants is $R_s = R / M$.

Notes:

- For a monatomic ideal gas, $Z = 1$ and ρ is the ideal gas density.
- kmole = 1000 moles

Thin-plate orifices

The flow of real gases through thin-plate orifices never becomes fully choked. The mass flow rate through the orifice continues to increase as the downstream pressure is lowered to a perfect vacuum, though the mass flow rate increases slowly as the downstream pressure is reduced below the critical pressure.^[8] Cunningham (1951) first drew attention to the fact that choked flow will not occur across a standard, thin, square-edged orifice.^{[9] [10]}

Minimum pressure ratio required for choked flow to occur

The minimum pressure ratios required for choked conditions to occur (when some typical industrial gases are flowing) are presented in Table 1. The ratios were obtained using the criteria that choked flow occurs when the ratio of the absolute upstream pressure to the absolute downstream pressure is equal to or greater than $[(k + 1) / 2]^{k/(k-1)}$, where k is the specific heat ratio of the gas. The minimum pressure ratio may be understood as the ratio between the upstream pressure and the pressure at the nozzle throat when the gas is traveling at Mach 1; if the upstream pressure is too low compared to the downstream pressure, sonic flow cannot occur at the throat.

Table 1

Gas	$k = c_p/c_v$	Minimum P_u/P_d required for choked flow
Hydrogen	1.410	1.899
Methane	1.307	1.837
Propane	1.131	1.729
Butane	1.096	1.708
Ammonia	1.310	1.838
Chlorine	1.355	1.866
Sulfur dioxide	1.290	1.826
Carbon monoxide	1.404	1.895

Notes:

- P_u = absolute upstream gas pressure
- P_d = absolute downstream gas pressure
- k values obtained from:
 1. Perry, Robert H. and Green, Don W. (1984). *Perry's Chemical Engineers' Handbook* (6th Edition ed.). McGraw-Hill Company. ISBN 0-07-049479-7.
 2. Phillips Petroleum Company (1962). *Reference Data For Hydrocarbons And Petro-Sulfur Compounds* (Second Printing ed.). Phillips Petroleum Company.

References

1. ^ a b *Perry's Chemical Engineers' Handbook*, Sixth Edition, McGraw-Hill Co., 1984.
2. ^ a b *Handbook of Chemical Hazard Analysis Procedures*, Appendix B, Federal Emergency Management Agency, U.S. Dept. of Transportation, and U.S. Environmental Protection Agency, 1989. *Handbook of Chemical Hazard Analysis*, Appendix B Click on PDF icon, wait and then scroll down to page 391 of 520 PDF pages.
3. ^ a b *Methods For The Calculation Of Physical Effects Due To Releases Of Hazardous Substances (Liquids and Gases)*, PGS2 CPR 14E, Chapter 2, The Netherlands Organization Of Applied Scientific Research, The Hague, 2005. PGS2 CPR 14E
4. ^ Valve Sizing Calculations Scroll to discussion of liquid flashing and cavitation.
5. ^ Control Valve Handbook Search document for "Choked".
6. ^ *Risk Management Program Guidance For Offsite Consequence Analysis*, U.S. EPA publication EPA-550-B-99-009, April 1999. Guidance for Offsite Consequence Analysis
7. ^ Calculating Accidental Release Rates From Pressurized Gas Systems
8. ^ Section 3 -- Choked Flow
9. ^ Forum post on 1 Apr 03 19:37
10. ^ Richard W. Miller (1996). *Flow Measurement Engineering Handbook* (Third Edition ed.). McGraw Hill. ISBN 0-07-042366-0.

Compressibility

From Wikipedia, the free encyclopedia

In thermodynamics and fluid mechanics, **compressibility** is a measure of the relative volume change of a fluid or solid as a response to a pressure (or mean stress) change.

$$\beta = -\frac{1}{V} \frac{\partial V}{\partial p}$$

where V is volume and p is pressure. The above statement is incomplete, because for any object or system the magnitude of the compressibility depends strongly on whether the process is adiabatic or isothermal.

Accordingly we define the isothermal compressibility as:

$$\beta_T = -\frac{1}{V} \left(\frac{\partial V}{\partial p} \right)_T$$

where the subscript T indicates that the partial differential is to be taken at constant temperature.

The adiabatic compressibility as:

$$\beta_S = -\frac{1}{V} \left(\frac{\partial V}{\partial p} \right)_S$$

where S is entropy. For a solid, the distinction between the two is usually negligible.

The inverse of the compressibility is called the bulk modulus, often denoted K (sometimes B). That page also contains some examples for different materials.

Thermodynamics

The term "compressibility" is also used in thermodynamics to describe the deviance in the thermodynamic properties of a real gas from those expected from an ideal gas. The **compressibility factor** is defined as

$$Z = \frac{pV}{RT}$$

where p is the pressure of the gas, T is its temperature, and V is its molar volume. In the case of an ideal gas, the compressibility factor Z is equal to unity, and the familiar ideal gas law is recovered:

$$p = \frac{RT}{V}$$

Z can, in general, be either greater or less than unity for a real gas.

Material Properties	
Specific heat	$c = \frac{T}{N} \left(\frac{\partial S}{\partial T} \right)$
Compressibility	$\beta = -\frac{1}{V} \left(\frac{\partial V}{\partial p} \right)$
Thermal expansion	$\alpha = \frac{1}{V} \left(\frac{\partial V}{\partial T} \right)$

The deviation from ideal gas behavior tends to become particularly significant (or, equivalently, the compressibility factor strays far from unity) near the critical point, or in the case of high pressure or low temperature. In these cases, a generalized compressibility chart or an alternative equation of state better suited to the problem must be utilized to produce accurate results.

A related situation occurs in hypersonic aerodynamics, where dissociation causes an increase in the “notational” molar volume, because a mole of oxygen, as O_2 , becomes 2 moles of monatomic oxygen and N_2 similarly dissociates to $2N$. Since this occurs dynamically as air flows over the aerospace object, it is convenient to alter Z , defined for an initial 30 gram mole of air, rather than track the varying mean molecular weight, millisecond by millisecond. This pressure dependent transition occurs for atmospheric oxygen in the 2500 K to 4000 K temperature range, and in the 5000 K to 10,000 K range for nitrogen.^[1]

In transition regions, where this pressure dependent dissociation is incomplete, both beta (the volume/pressure differential ratio) and the differential, constant pressure heat capacity will greatly increase.

For moderate pressures, above 10,000 K the gas further dissociates into free electrons and ions. Z for the resulting plasma can similarly be computed for a mole of initial air, producing values between 2 and 4 for partially or singly ionized gas. Each dissociation absorbs a great deal of energy in a reversible process and this greatly reduces the thermodynamic temperature of hypersonic gas decelerated near the aerospace object. Ions or free radicals transported to the object surface by diffusion may release this extra (non-thermal) energy if the surface catalyzes the slower recombination process.

The isothermal compressibility is related to the isentropic (or adiabatic) compressibility by the relation,

$$\beta_S = \beta_T - \frac{\alpha^2 T}{\rho c_p}$$

via Maxwell's relations. More simply stated,

$$\frac{\beta_T}{\beta_S} = \gamma$$

where, γ is the heat capacity ratio.

Aerodynamics

Compressibility is an important factor in aerodynamics. At low speeds, the compressibility of air is not significant in relation to aircraft design, but as the airflow nears and exceeds the speed of sound, a host of new aerodynamic effects become important in the design of aircraft. These effects, often several of them at a time, made it very difficult for World War II era aircraft to reach speeds much beyond 800 km/h (500 mph).

Some of the minor effects include changes to the airflow that lead to problems in control. For instance, the P-38 Lightning with its thick high-lift wing had a particular problem in high-speed dives that led to a nose-down condition. Pilots would enter dives, and then find that they could no longer control the plane, which continued to nose over until it crashed. Adding a "dive flap" beneath

the wing altered the center of pressure distribution so that the wing would not lose its lift. This fixed the problem.

A similar problem affected some models of the Supermarine Spitfire. At high speeds the ailerons could apply more torque than the Spitfire's thin wings could handle, and the entire wing would twist in the opposite direction. This meant that the plane would roll in the direction opposite to that which the pilot intended, and led to a number of accidents. Earlier models weren't fast enough for this to be a problem, and so it wasn't noticed until later model Spitfires like the Mk.IX started to appear. This was mitigated by adding considerable torsional rigidity to the wings, and was wholly cured when the Mk.XIV was introduced.

The Messerschmitt Bf 109 and Mitsubishi Zero had the exact opposite problem in which the controls became ineffective. At higher speeds the pilot simply couldn't move the controls because there was too much airflow over the control surfaces. The planes would become difficult to maneuver, and at high enough speeds aircraft without this problem could out-turn them.

Finally, another common problem that fits into this category is flutter. At some speeds the airflow over the control surfaces will become turbulent, and the controls will start to flutter. If the speed of the fluttering is close to a harmonic of the control's movement, the resonance could break the control off completely. This was a serious problem on the Zero. When problems with poor control at high speed were first encountered, they were addressed by designing a new style of control surface with more power. However this introduced a new resonant mode, and a number of planes were lost before this was discovered.

All of these effects are often mentioned in conjunction with the term "compressibility", but in a manner of speaking, they are incorrectly used. From a strictly aerodynamic point of view, the term should refer only to those side-effects arising as a result of the changes in airflow from an incompressible fluid (similar in effect to water) to a compressible fluid (acting as a gas) as the speed of sound is approached. There are two effects in particular, wave drag and critical mach.

Wave drag is a sudden rise in drag on the aircraft, caused by air building up in front of it. At lower speeds this air has time to "get out of the way", guided by the air in front of it that is in contact with the aircraft. But at the speed of sound this can no longer happen, and the air which was previously following the streamline around the aircraft now hits it directly. The amount of power needed to overcome this effect is considerable. The critical mach is the speed at which some of the air passing over the aircraft's wing becomes supersonic.

At the speed of sound the way that lift is generated changes dramatically, from being dominated by Bernoulli's principle to forces generated by shock waves. Since the air on the top of the wing is traveling faster than on the bottom, due to Bernoulli effect, at speeds close to the speed of sound the air on the top of the wing will be accelerated to supersonic. When this happens the distribution of lift changes dramatically, typically causing a powerful nose-down trim. Since the aircraft normally approached these speeds only in a dive, pilots would report the aircraft attempting to nose over into the ground.

Dissociation absorbs a great deal of energy in a reversible process. This greatly reduces the thermodynamic temperature of hypersonic gas decelerated near an aerospace vehicle. In transition regions, where this pressure dependent dissociation is incomplete, both the differential, constant pressure heat capacity and beta (the volume/pressure differential ratio) will greatly increase. The latter has a pronounced effect on vehicle aerodynamics including stability.

Compressibility factor

From Wikipedia, the free encyclopedia

The **compressibility factor** (**Z**) is a useful thermodynamic property for modifying the ideal gas law to account for the real gas behaviour.^[1] In general, deviations from ideal behavior become more significant the closer a gas is to a phase change, the lower the temperature or the larger the pressure. Compressibility factor values are usually obtained by calculation from equations of state (EOS), such as the virial equation which take compound specific empirical constants as input. Alternatively, the compressibility factor for specific gases can be read from generalized compressibility charts.^[1] that plot *Z* as a function of pressure at constant temperature.

Definition and physical significance

The compressibility factor is defined as:

$$Z = \frac{p\tilde{V}}{RT}$$

where, *p* is the pressure, \tilde{V} is the molar volume of the gas, *T* is the temperature, and *R* is the gas constant.

For an ideal gas the compressibility factor is *Z* = 1 per definition. In many real world applications requirements for accuracy demand that deviations from ideal gas behaviour, i.e. real gas behaviour, is taken into account. The value of *Z* generally increases with pressure and decreases with temperature. At high pressures molecules are colliding more often, and at low temperatures they are moving less rapidly. This allows attractive forces between molecules to have a noticeable effect, making the volume of the real gas (*V_{real}*) less than the volume of an ideal gas (*V_{ideal}*) which causes *Z* to drop below one.^[2] When pressures are lower or temperatures higher, the molecules are more free to move. In this case repulsive forces dominate, making *Z* > 1. The closer the gas is to its critical point or its boiling point, the more *Z* deviates from the ideal case.

Example experimental values

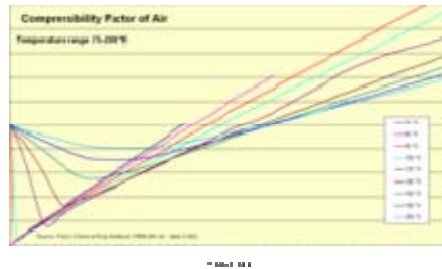
It is extremely difficult to generalize at what pressures or temperatures the deviation from the ideal gas becomes important. As a rule of thumb, the ideal gas law is reasonably accurate up to a pressure of about 2 atm, and even higher for small non-associating molecules. For example methyl chloride, a highly polar molecule and therefore with significant intermolecular forces, the experimental value for the compressibility factor is *Z*=0.9152 at a pressure of 10 atm and temperature of 100 °C^[3]. For air (small non-polar molecules) at approximately the same conditions, the compressibility factor is only *Z*=1.0025 (see table below for 10 bars, 400 K).

Compressibility of air

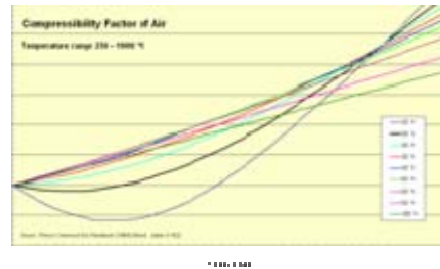
Normal air comprises in crude numbers 80 percent nitrogen N₂ and 20 percent oxygen O₂. Both molecules are small and non-polar (and therefore non-associating). We can therefore expect that the

behaviour of air within broad temperature and pressure ranges can be approximated as an ideal gas with reasonable accuracy. Experimental values for the compressibility factor confirm this.

Z for air as function of pressure 1-500 bars



75-200 K isotherms



250-1000 K isotherms

Compressibility factor for air (experimental values)

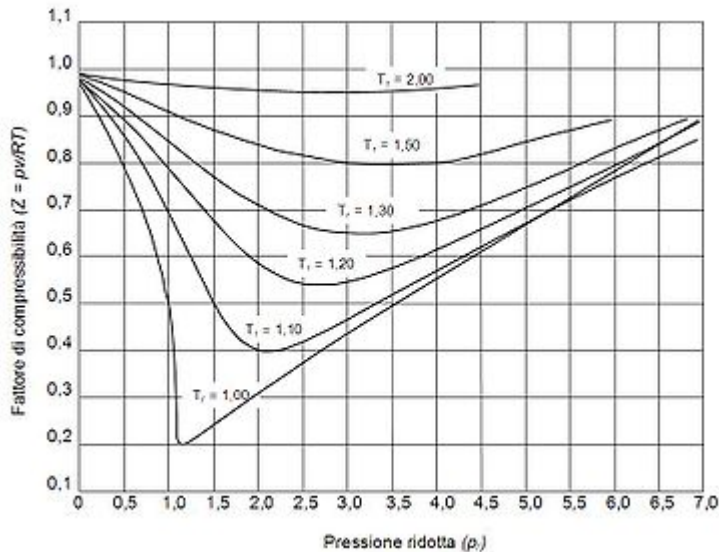
Temp, K	Pressure, bars (absolute)													
	1	5	10	20	40	60	80	100	150	200	250	300	400	500
75	0.0052	0.0260	0.0519	0.1036	0.2063	0.3082	0.4094	0.5099	0.7581	1.0125				
80		0.0250	0.0499	0.0995	0.1981	0.2958	0.3927	0.4887	0.7258	0.9588	1.1931	1.4139		
90	0.9764	0.0236	0.0453	0.0940	0.1866	0.2781	0.3686	0.4681	0.6779	0.8929	1.1098	1.3110	1.7161	2.1105
100	0.9797	0.8872	0.0453	0.0900	0.1782	0.2635	0.3498	0.4337	0.6386	0.8377	1.0395	1.2227	1.5937	1.9536
120	0.9880	0.9373	0.8860	0.6730	0.1778	0.2557	0.3371	0.4132	0.5964	0.7720	0.9530	1.1076	1.5091	1.7366
140	0.9927	0.9614	0.9205	0.8297	0.5856	0.3313	0.3737	0.4340	0.5909	0.7699	0.9114	1.0393	1.3202	1.5903
160	0.9951	0.9748	0.9489	0.8954	0.7803	0.6603	0.5696	0.5489	0.6340	0.7564	0.8840	1.0105	1.2585	1.4970
180	0.9967	0.9832	0.9660	0.9314	0.8625	0.7977	0.7432	0.7084	0.7180	0.7986	0.9000	1.0068	1.2232	1.4361
200	0.9978	0.9886	0.9767	0.9539	0.9100	0.8701	0.8374	0.8142	0.8061	0.8549	0.9311	1.0185	1.2054	1.3944
250	0.9992	0.9957	0.9911	0.9822	0.9671	0.9549	0.9463	0.9411	0.9450	0.9713	1.0152	1.0702	1.1990	1.3392
300	0.9999	0.9987	0.9974	0.9950	0.9917	0.9901	0.9903	0.9930	1.0074	1.0326	1.0669	1.1089	1.2073	1.3163
350	1.0000	1.0002	1.0004	1.0014	1.0038	1.0075	1.0121	1.0183	1.0377	1.0635	1.0947	1.1303	1.2116	1.3015
400	1.0002	1.0012	1.0025	1.0046	1.0100	1.0159	1.0229	1.0312	1.0533	1.0795	1.1087	1.1411	1.2117	1.2890
450	1.0003	1.0016	1.0034	1.0063	1.0133	1.0210	1.0287	1.0374	1.0614	1.0913	1.1183	1.1463	1.2090	1.2778
500	1.0003	1.0020	1.0034	1.0074	1.0151	1.0234	1.0323	1.0410	1.0650	1.0913	1.1183	1.1463	1.2051	1.2667
600	1.0004	1.0022	1.0039	1.0081	1.0164	1.0253	1.0340	1.0434	1.0678	1.0920	1.1172	1.1427	1.1947	1.2475
800	1.0004	1.0020	1.0038	1.0077	1.0157	1.0240	1.0321	1.0408	1.0621	1.0844	1.1061	1.1283	1.1720	1.2150
1000	1.0004	1.0018	1.0037	1.0068	1.0142	1.0215	1.0290	1.0365	1.0556	1.0744	1.0948	1.1131	1.1515	1.1889

Source: *Perry's chemical engineers' handbook* (6ed ed.). McGraw-Hill. 1984. ISBN 0-07-049479-7. (table 3-162). Z-value are calculated from values of pressure, volume (or density), and temperature in Vassernan, Kazavchinskii, and Rabinovich, "Thermophysical Properties of Air and Air Components," Moscow, Nauka, 1966, and NBS-NSF Trans. TT 70-50095, 1971: and Vassernan and Rabinovich, "Thermophysical Properties of Liquid Air and Its Component," Moscow, 1968, and NBS-NSF Trans. 69-55092, 1970.

Compressibility of ammonia gas

Ammonia is small but highly polar molecule with significant interactions. Values can be obtained from Perry 4th ed (awaits future library visit)

Generalized compressibility factor graphs for pure gases



Generalized compressibility factor diagram.

The unique relationship between the compressibility factor and the so-called reduced temperature, T_r , and the so-called reduced pressure, P_r , was first recognized by Johannes Diderik van der Waals in 1873 and is known as the two-parameter principle of corresponding states. The principle of corresponding states expresses the generalization that the properties of a gas which are dependent on intermolecular forces are related to the critical properties of the gas in a universal way. That provides a most important basis for developing correlations of molecular properties.

As for the compressibility of gases, the principle of corresponding states indicates that any pure gas at the same reduced temperature, T_r , and reduced pressure, P_r , should have the same compressibility factor.

The reduced temperature and pressure are defined as:

$$T_r = \frac{T}{T_c} \quad \text{and} \quad P_r = \frac{P}{P_c}$$

T_c and P_c are known as the critical temperature and critical pressure of a gas. They are characteristics of each specific gas with T_c being the temperature above which it is not possible to liquify a given gas and P_c is the minimum pressure required to liquefy a given gas at its critical temperature. Together they define the critical point of a fluid above which distinct liquid and gas phases of a given fluid do not exist. The pressure-volume-temperature (PVT) data for real gases varies from one pure gas to another. However, when the compressibility factors of various single-

component gases are graphed versus pressure along with temperature isotherms many of the graphs exhibit similar isotherm shapes. In order to obtain a generalized graph that can be used for many different gases, the reduced pressure and temperature, P_r and T_r , are used to normalize the compressibility factor data. Figure 2 is an example of a generalized compressibility factor graph derived from hundreds of experimental P-V-T data points of 10 pure gases, namely methane, ethane, ethylene, propane, n-butane, i-pentane, n-hexane, nitrogen, carbon dioxide and steam. There are more detailed generalized compressibility factor graphs based on as many as 25 or more different pure gases, such as the Nelson-Obert graphs. Such graphs are said to have an accuracy within 1-2 percent for Z values greater than 0.6 and within 4-6 percent for Z values of 0.3-0.6. The generalized compressibility factor graphs may be considerably in error for strongly polar gases which are gases for which the centers of positive and negative charge do not coincide. In such cases the estimate for Z may be in error by as much as 15-20 percent. The quantum gases hydrogen, helium, and neon do not conform to the corresponding-states behavior and the reduced pressure and temperature for those three gases should be redefined in the following manner to improve the accuracy of predicting their compressibility factors when using the generalized graphs:

$$T_r = \frac{T}{T_c + 8} \quad \text{and} \quad P_r = \frac{P}{P_c + 8}$$

Theoretical models

The virial equation is especially useful to describe the causes of non-ideality at a molecular level (very few gases are mono-atomic) as it is derived directly from statistical mechanics:

$$\frac{P\tilde{V}}{RT} = 1 + \frac{B}{\tilde{V}} + \frac{C}{\tilde{V}^2} + \frac{D}{\tilde{V}^3} + \dots$$

Where the coefficients in the numerator are known as virial coefficients and are functions of temperature.

The virial coefficients account for interactions between successively larger groups of molecules. For example, B accounts for interactions between pairs, C for interactions between three gas molecules, and so on. Because interactions between large numbers of molecules are rare, the virial equation is usually truncated after the third term.^[4]

References

1. ^ a b Properties of Natural Gases. Includes a chart of compressibility factors versus reduced pressure and reduced temperature (on last page of the PDF document)
2. ^ McQuarrie, Donald A. and Simon, John D. (1999). *Molecular Thermodynamics*. University Science Books. ISBN 1-891389-05-X. page 55
3. ^ *Perry's chemical engineers' handbook* (6ed ed.). McGraw-Hill. 1984. ISBN 0-07-049479-7. page 3-268
4. ^ Smith, J.M. et al. (2005). *Introduction to Chemical Engineering Thermodynamics* (Seventh Edition ed.). McGraw Hill. ISBN 0-07-310445-0. page73

Compressible Flow

From Wikipedia, the free encyclopedia

In fluid dynamics, a flow is considered to be a **compressible flow** if the density of the fluid changes with respect to pressure. In general, this is the case where the Mach number (defined as the ratio of the flow speed to the local speed of sound) of the flow exceeds 0.3. The Mach 0.3 value is rather arbitrary, but it is used because gas flows with a Mach number below that value introduce less than 5% change in density. Furthermore, the maximum density change occurs at the stagnation points and the density change in the rest of the flow field will be significantly lower.

The factor that distinguishes a flow from being compressible or incompressible is the fact that in compressible flow the changes in the velocity of the flow can lead to changes in the temperature which are not negligible. On the other hand in case of incompressible flow, the changes in the internal energy (i.e. temperature) are negligible even if the entire kinetic energy of the flow is converted to internal energy (i.e. the flow is brought to rest).

These definitions, though they seem to be inconsistent, are all saying one and the same thing: the Mach number of the flow is high enough so that the effects of compressibility can no longer be neglected.

For subsonic compressible flows, it is sometimes possible to model the flow by applying a correction factor to the answers derived from incompressible calculations or modelling - for example, the Prandtl-Glauert rule:

$$\frac{a_c}{a_i} \sim \frac{1}{\sqrt{1 - M^2}}$$

(a_c is compressible lift curve slope, a_i is the incompressible lift curve slope, and M is the Mach number). Note that this correction only yields acceptable results over a range of approximately $0.3 < M < 0.7$.

For many other flows, their nature is qualitatively different to subsonic flows. A flow where the local Mach number reaches or exceeds 1 will usually contain shock waves. A shock is an abrupt change in the velocity, pressure and temperature in a flow; the thickness of a shock scales with the molecular mean free path in the fluid (typically a few micrometers).

Shocks form because information about conditions downstream of a point of sonic or supersonic flow cannot propagate back upstream past the sonic point.

The behaviour of a fluid changes radically as it starts to move above the speed of sound (in that fluid), ie. when the Mach number is greater than 1. For example, in subsonic flow, a stream tube in an accelerating flow contracts. But in a supersonic flow, a stream tube in an accelerating flow expands. To interpret this in another way, consider steady flow in a tube that has a sudden expansion: the tube's cross section suddenly widens, so the cross-sectional area increases.

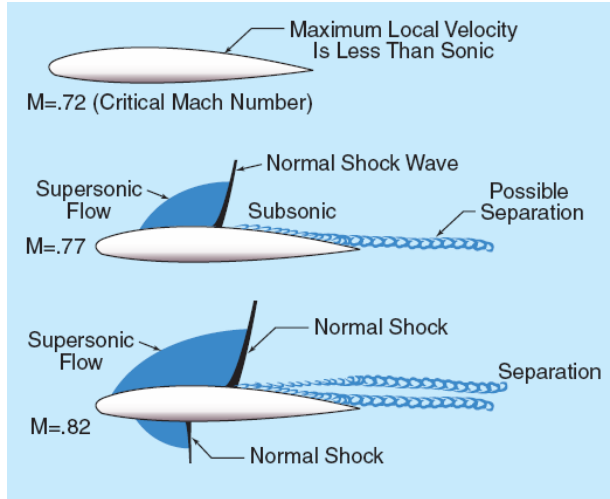
In subsonic flow, the fluid speed drops after the expansion (as expected). In supersonic flow, the fluid speed increases. This sounds like a contradiction, but it isn't: the mass flux is conserved but because supersonic flow allows the density to change, the volume flux is not constant. This effect is utilized in De Laval nozzles.

References

- Shapiro, Ascher H.. *The Dynamics and Thermodynamics of Compressible Fluid Flow, Volume 1*. Ronald Press. ISBN 978-0-471-06691-0.
- Anderson, John D.. *Modern Compressible Flow*. McGraw-Hill. ISBN 0071241361.
- Liepmann, H. W.; Roshko A.. *Elements of Gasdynamics*. Dover Publications. ISBN 0486419630.
- von Mises, Richard. *Mathematical Theory of Compressible Fluid Flow*. Dover Publications. ISBN 0486439410.
- Saad, Michael A. *Compressible Fluid Flow*. Prentice Hall. ISBN 0-13-163486-0.
- Hodge, B. K.; Koenig K.. *Compressible Fluid Dynamics with Personal Computer Applications*. Prentice Hall. ISBN 013308552X.

Critical Mach number

From Wikipedia, the free encyclopedia



Transonic flow patterns on an aircraft wing showing the effects at critical mach.

In aerodynamics, the **critical Mach number (M_{cr})** of an aircraft is the lowest Mach number at which the airflow over a small region of the wing reaches the speed of sound.^[1]

For all aircraft in flight, the airflow around the aircraft is not exactly the same as the airspeed of the aircraft due to the airflow speeding up and slowing down to travel around the aircraft structure. At the Critical Mach number, local airflow in some areas near the airframe reaches the speed of sound, even though the aircraft itself has an airspeed lower than Mach 1.0. This creates a weak shock wave. At speeds faster than the Critical Mach number:

- drag coefficient increases suddenly, causing dramatically increased drag^[2]
- in aircraft not designed for transonic or supersonic speeds, changes to the airflow over the flight control surfaces lead to deterioration in control of the aircraft.^[2]

In aircraft not designed to fly at the Critical Mach number, shock waves in the flow over the wing and tailplane were sufficient to stall the wing, make control surfaces ineffective or lead to loss of control such as Mach tuck. The phenomena associated with problems at the Critical Mach number became known as compressibility. Compressibility led to a number of accidents involving high-speed military and experimental aircraft in the 1930s and 1940s.

Although unknown at the time, compressibility was the cause of the phenomenon known as the sound barrier. Subsonic aircraft such as the Supermarine Spitfire, BF 109, P-51 Mustang, Gloster Meteor, Me 262, P-80 have relatively thick, unswept wings and are incapable of reaching Mach 1.0. In 1947, Chuck Yeager flew the Bell X-1 to Mach 1.0 and beyond, and the sound barrier was finally broken.

Early transonic military aircraft such as the Hawker Hunter and F-86 Sabre were designed to fly satisfactorily faster than their Critical Mach number. They did not possess sufficient engine thrust to reach Mach 1.0 in level flight but could be dived to Mach 1.0 and beyond, and remain controllable.

Modern passenger-carrying jet aircraft such as Airbus and Boeing aircraft have Maximum Operating Mach numbers slower than Mach 1.0 but they are routinely operated faster than their Critical Mach numbers.

Supersonic aircraft, such as Concorde, the English Electric Lightning, Lockheed F-104, Dassault Mirage III, and MiG 21 are designed to exceed Mach 1.0 in level flight. They have very thin wings. Their Critical Mach numbers are faster than those of subsonic and transonic aircraft but less than Mach 1.0.

The actual Critical Mach number varies from wing to wing. In general a thicker wing will have a lower Critical Mach number, because a thicker wing accelerates the airflow to a faster speed than a thinner one. For instance, the fairly thick wing on the P-38 Lightning led to a Critical Mach number of about .69 Mach, a speed it could reach with some ease in dives, which led to a number of crashes. The much thinner wing on the Supermarine Spitfire caused this aircraft to have a Critical Mach number of about 0.89 Mach.

References

- Clancy, L.J. (1975) *Aerodynamics*, Pitman Publishing Limited, London ISBN 0 273 01120 0

Notes

1. ^ Clancy, L.J. *Aerodynamics*, Section 11.6
2. ^ ^{a b} Clancy, L.J., *Aerodynamics*, Chapter 11

De Laval Nozzle

From Wikipedia, the free encyclopedia

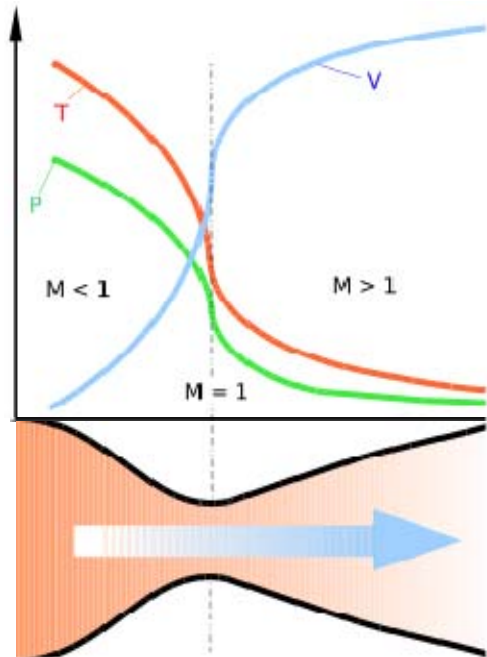


Diagram of a de Laval nozzle, showing approximate flow velocity (v), together with the effect on temperature (t) and pressure (p)

A **de Laval nozzle** (or **convergent-divergent nozzle**, **CD nozzle** or **con-di nozzle**) is a tube that is pinched in the middle, making an hourglass-shape. It is used as a means of accelerating the flow of a gas passing through it to a supersonic speed. It is widely used in some types of steam turbine and is an essential part of the modern rocket engine and supersonic jet engines.

Similar flow properties have been applied to jet streams within astrophysics. ^[1]

History

The nozzle was developed by Swedish inventor Gustaf de Laval in 1897 for use on an impulse steam turbine. ^[1]

This principle was used in a rocket engine by Robert Goddard, and very nearly all modern rocket engines that employ hot gas combustion use de Laval nozzles.

Operation

Its operation relies on the different properties of gases flowing at subsonic and supersonic speeds. The speed of a subsonic flow of gas will increase if the pipe carrying it narrows because the mass

flow rate is constant. The gas flow through a de Laval nozzle is isentropic (gas entropy is nearly constant). At subsonic flow the gas is compressible; sound, a small pressure wave, will propagate through it. At the "throat", where the cross sectional area is a minimum, the gas velocity locally becomes sonic (Mach number = 1.0), a condition called choked flow. As the nozzle cross sectional area increases the gas begins to expand and the gas flow increases to supersonic velocities where a sound wave will not propagate backwards through the gas as viewed in the frame of reference of the nozzle (Mach number > 1.0).

Conditions for operation

A de Laval nozzle will only choke at the throat if the pressure and mass flow through the nozzle is sufficient to reach sonic speeds, otherwise no supersonic flow is achieved and it will act as a Venturi tube.

In addition, the pressure of the gas at the exit of the expansion portion of the exhaust of a nozzle must not be too low. Because pressure cannot travel upstream through the supersonic flow, the exit pressure can be significantly below ambient pressure it exhausts into, but if it is too far below ambient, then the flow will cease to be supersonic, or the flow will separate within the expansion portion of the nozzle, forming an unstable jet that may 'flop' around within the nozzle, possibly damaging it.

In practice ambient pressure must be no higher than roughly 2-3 times the pressure in the supersonic gas at the exit for supersonic flow to leave the nozzle.

Analysis of gas flow in de Laval nozzles

The analysis of gas flow through de Laval nozzles involves a number of concepts and assumptions:

- For simplicity, the gas is assumed to be an ideal gas.
- The gas flow is isentropic (i.e., at constant entropy). As a result the flow is reversible (frictionless and no dissipative losses), and adiabatic (i.e., there is no heat gained or lost).
- The gas flow is constant (i.e., steady) during the period of the propellant burn.
- The gas flow is along a straight line from gas inlet to exhaust gas exit (i.e., along the nozzle's axis of symmetry)
- The gas flow behavior is compressible since the flow is at very high velocities.

Exhaust gas velocity

As the gas enters a nozzle, it is traveling at subsonic velocities. As the throat contracts down the gas is forced to accelerate until at the nozzle throat, where the cross-sectional area is the smallest, the linear velocity becomes sonic. From the throat the cross-sectional area then increases, the gas expands and the linear velocity becomes progressively more supersonic.

The linear velocity of the exiting exhaust gases can be calculated using the following equation:^{[1] [2]}
^[3]

$$V_e = \sqrt{\frac{T}{M} \cdot \frac{R}{k-1} \cdot \frac{2k}{k-1} \cdot \left[1 - (P_e/P)^{(k-1)/k}\right]}$$

where:

V_e = Exhaust velocity at nozzle exit, m/s

T = absolute temperature of inlet gas, K

R = Universal gas law constant = 8314.5 J/(kmol·K)

M = the gas molecular mass, kg/kmol (also known as the molecular weight)

$k = c_p/c_v$ = isentropic expansion factor

c_p = specific heat of the gas at constant pressure

c_v = specific heat of the gas at constant volume

P_e = absolute pressure of exhaust gas at nozzle exit, Pa

P = absolute pressure of inlet gas, Pa

Some typical values of the exhaust gas velocity V_e for rocket engines burning various propellants are:

- 1.7 to 2.9 km/s (3,800 to 6,500 mph) for liquid monopropellants
- 2.9 to 4.5 km/s (6,500 to 10,100 mph) for liquid bipropellants
- 2.1 to 3.2 km/s (4,700 to 7,200 mph) for solid propellants

As a note of interest, V_e is sometimes referred to as the *ideal exhaust gas velocity* because it is based on the assumption that the exhaust gas behaves as an ideal gas.

As an example calculation using the above equation, assume that the propellant combustion gases are: at an absolute pressure entering the nozzle of $P = 7.0$ MPa and exit the rocket exhaust at an absolute pressure of $P_e = 0.1$ MPa; at an absolute temperature of $T = 3500$ K; with an isentropic expansion factor of $k = 1.22$ and a molar mass of $M = 22$ kg/kmol. Using those values in the above equation yields an exhaust velocity $V_e = 2802$ m/s or 2.80 km/s which is consistent with above typical values.

The technical literature can be very confusing because many authors fail to explain whether they are using the universal gas law constant R which applies to any ideal gas or whether they are using the gas law constant R_s which only applies to a specific individual gas. The relationship between the two constants is $R_s = R/M$.

Examples

For example a de Laval nozzle using hot air at a pressure of 1,000 psi (6.9 MPa or 68 atm), temperature of 1470 K, would have a pressure of 540 psi (3.7 MPa or 37 atm), temperature of 1269 K at the throat, and 15 psi (0.1 MPa or 1 atm), temperature of 502 K at the nozzle exit. The expansion ratio, nozzle cross sectional area at exit divided by area at throat, would be 6.8. The specific impulse would be 151 s (1480 N·s/kg).

Application to celestial objects

Theoretical astrophysicists have found that pipes with the flow pattern of a De Laval nozzle have analogous phenomena in the interstellar medium. The interior of an accretion disk has a similar function as the pipe, save it is not a solid wall, but itself a fluid that can contain a relativistic jet by a pressure balanced boundary.

References

1. ^ Flack, Ronald D. (June 2005). *Fundamentals of Jet Propulsion with Applications*. Cambridge University Press. doi:10.2277/0521819830. ISBN 978-0521819831.
<http://www.cambridge.org/uk/catalogue/catalogue.asp?isbn=9780521819831&ss=exc>.
1. ^ Clarke, C. J. & Carswell B. (2007). *Principles of Astrophysical Fluid Dynamics, chpt 9.2* (1st Edition ed.). Cambridge University Press. pp. 226. ISBN 978-0521853316.
2. ^ Richard Nakka's Equation 12
3. ^ Robert Braeuning's Equation 2.22
4. ^ Sutton, George P. (1992). *Rocket Propulsion Elements: An Introduction to the Engineering of Rockets* (6th Edition ed.). Wiley-Interscience. pp. 636. ISBN 0471529389.

Drag Divergence Mach Number

From Wikipedia, the free encyclopedia

The **drag divergence Mach number** is the Mach number at which the aerodynamic drag on an airfoil or airframe begins to increase rapidly as the Mach number continues to increase^[1]. This increase can cause the drag coefficient to rise to more than ten times its low speed value.

The value of the drag divergence Mach number is typically greater than 0.6; therefore it is a transonic effect. The drag divergence Mach number is usually close to, and always greater than, the critical Mach number. Generally, the drag coefficient peaks at Mach 1.0 and begins to decrease again after the transition into the supersonic regime above approximately Mach 1.2.

The large increase in drag is caused by the formation of a shock wave on the upper surface of the airfoil, which can induce flow separation and adverse pressure gradients on the aft portion of the wing. This effect requires that aircraft intended to fly at supersonic speeds have a large amount of thrust. In early development of transonic and supersonic aircraft, a steep dive was often used to provide extra acceleration through the high drag region around Mach 1.0. In the early days of aviation, this steep increase in drag gave rise to the popular false notion of an unbreakable sound barrier, because it seemed that no aircraft technology in the foreseeable future would have enough propulsive force or control authority to overcome it. Indeed, one of the popular analytical methods for calculating drag at high speeds, the Prandtl-Glauert rule, predicts an infinite amount of drag at Mach 1.0.

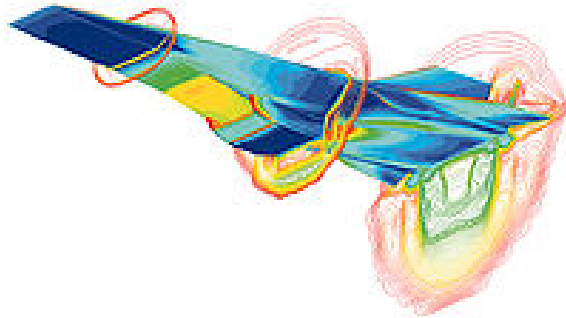
Two of the important technological advancements that arose out of attempts to conquer the sound barrier were the Whitcomb area rule and the supercritical airfoil. A supercritical airfoil is shaped specifically to make the drag divergence Mach number as high as possible, allowing aircraft to fly with relatively lower drag at high subsonic and low transonic speeds. These, along with other advancements including computational fluid dynamics, have been able to reduce the factor of increase in drag to two or three for modern aircraft designs^[2].

Notes

- [^] Anderson, John D. (2001). *Fundamentals of Aerodynamics*. McGraw-Hill. pp. 613.
- [^] Anderson, John D. (2001). *Fundamentals of Aerodynamics*. McGraw-Hill. pp. 615.

Hypersonic

From Wikipedia, the free encyclopedia



Boeing X-43 at Mach 7

In aerodynamics, **hypersonic** speeds are speeds that are highly supersonic. Since the 1970s, the term has generally been assumed to refer to speeds of Mach 5 (5 times the speed of sound) and above. The hypersonic regime is a subset of the supersonic regime.

Supersonic airflow is very different from subsonic flow. Nearly everything about the way an aircraft flies changes dramatically as it accelerates to supersonic speed. Even with this strong demarcation, there is still some debate as to the definition of "supersonic". One definition is that the aircraft, as a whole, is traveling at Mach 1 or greater. More technical definitions state that it is only supersonic if the airflow over the entire aircraft is supersonic, which occurs around Mach 1.2 on typical designs. The range Mach 0.75 to 1.2 is therefore considered transonic.

Considering the problems with this simple definition, the precise Mach number at which a craft can be said to be fully hypersonic is even more elusive, especially since physical changes in the airflow (molecular dissociation, ionization) occur at quite different speeds. Generally, a combination of effects become important "as a whole" around Mach 5. The hypersonic regime is often defined as speeds where ramjets do not produce net thrust. This is a nebulous definition in itself, as there exists a proposed change to allow them to operate in the hypersonic regime (the Scramjet).

Characteristics of flow

While the definition of hypersonic flow can be quite vague and is generally debatable (especially due to the lack of discontinuity between supersonic and hypersonic flows), a hypersonic flow may be characterized by certain physical phenomena that can no longer be analytically discounted as in supersonic flow. These phenomena include:

Thin shock layer

As Mach numbers increase, the density behind the shock also increases, which corresponds to a decrease in volume behind the shock wave due to conservation of mass. Consequently, the shock layer, that volume between the body and the shock wave, is thin at high Mach numbers.

Entropy layer

As Mach numbers increase, the entropy change across the shock also increases, which results in a strong entropy gradient and highly vortical flow that mixes with the boundary layer.

Viscous interaction

A portion of the large kinetic energy associated with flow at high Mach numbers transforms into internal energy in the fluid due to viscous effects. The increase in internal energy is realized as an increase in temperature. Since the pressure gradient normal to the flow within a boundary layer is approximately zero for low to moderate hypersonic Mach numbers, the increase of temperature through the boundary layer coincides with a decrease in density. Thus, the boundary layer over the body grows and can often merge with the thin shock layer.

High temperature flow

High temperatures discussed previously as a manifestation of viscous dissipation cause non-equilibrium chemical flow properties such as dissociation and ionization of molecules resulting in convective and radiative heating.

Effects

The hypersonic flow regime is characterized by a number of effects which are not found in typical aircraft operating at low subsonic Mach numbers. The effects depend strongly on the speed and type of vehicle under investigation.

Classification

Generally, NASA defines "high" hypersonic as any mach number from 10 to 25 and Re-entry speeds as anything greater. Aircraft operating in this regime are the Space Shuttle and various space planes in future development.

Comparison of regimes					
Regime	Mach	Mph	km/h	m/s	General Plane Characteristics
Subsonic	<1.0	<764	<1,230	<340	Most often propeller-driven and commercial turbofan aircraft with straight wings
Transonic	0.8-1.2	610-915	980-1,475	270-410	Sharp intakes; compressibility becomes noticeable; slightly swept wings
Supersonic	1.0-5.0	764-3,820	1,230-6,150	340-1,710	Sharper edges; tailplane is a stabilator
Hypersonic	5.0-10.0	3,820-7,640	6,150-12,300	1,710-3,415	Cooled nickel-titanium skin; highly integrated, small wings
High-hypersonic	10.0-25.0	7,640-19,100	12,300-30,740	3,415-8,465	Silicon thermal tiles, blunt wings
Re-entry speeds	>25.0	>19,100	>30,740	>8,465	Ablative heat shield; no wings; blunt capsule shape

Similarity parameters

The categorization of airflow relies on a number of similarity parameters, which allow the simplification of a nearly infinite number of test cases into groups of similarity. For transonic and compressible flow, the Mach and Reynolds numbers alone allow good categorization of many flow cases.

Hypersonic flows, however, require other similarity parameters. Firstly, the analytic equations for the Oblique shock angle become nearly independent of Mach number at high ($\sim > 10$) Mach numbers. Secondly, the formation of strong shocks around aerodynamic bodies mean that the freestream Reynolds number is less useful as an estimate of the behavior of the boundary layer over a body (although it is still important). Finally, the increased temperature of hypersonic flows mean that real gas effects become important. For this reason, research in hypersonics is often referred to as aerothermodynamics, rather than aerodynamics.

The introduction of real gas effects mean that more variables are required to describe the full state of a gas. Whereas a stationary gas can be described by three variables (pressure, temperature, adiabatic index), and a moving gas by four (velocity), a hot gas in chemical equilibrium also requires state equations for the chemical components of the gas, and a gas in nonequilibrium solves those state equations using time as an extra variable. This means that for a nonequilibrium flow, something between 10 and 100 variables may be required to describe the state of the gas at any given time. Additionally, rarefied hypersonic flows (usually defined as those with a Knudsen number above one) do not follow the Navier-Stokes equations.

Hypersonic flows are typically categorized by their total energy, expressed as total enthalpy (MJ/kg), total pressure (kPa-MPa), stagnation pressure (kPa-MPa), stagnation temperature (K), or velocity (km/s).

Wallace D. Hayes developed a similarity parameter, similar to the Whitcomb area rule, which allowed similar configurations to be compared.

Regimes

Hypersonic flow can be approximately separated into a number of regimes. The selection of these regimes is rough, due to the blurring of the boundaries where a particular effect can be found.

Perfect gas

In this regime, the gas can be regarded as an ideal gas. Flow in this regime is still Mach number dependent. Simulations start to depend on the use of a constant-temperature wall, rather than the adiabatic wall typically used at lower speeds. The lower border of this region is around Mach 5, where Ramjets become inefficient, and the upper border around Mach 10-12.

Two-temperature ideal gas

This is a subset of the perfect gas regime, where the gas can be considered chemically perfect, but the rotational and vibrational temperatures of the gas must be considered separately, leading to two

temperature models. See particularly the modeling of supersonic nozzles, where vibrational freezing becomes important.

Dissociated gas

In this regime, multimolecular gases begin to dissociate as they come into contact with the bow shock generated by the body. The type of gas selected begins to have an effect on the flow. Surface catalyticity plays a role in the calculation of surface heating, meaning that the selection of the surface material also begins to have an effect on the flow. The lower border of this regime is where the first component of a gas mixture begins to dissociate in the stagnation point of a flow (Nitrogen~2000 K). The upper border of this regime is where the effects of ionization start to have an effect on the flow.

Ionized gas

In this regime the ionized electron population of the stagnated flow becomes significant, and the electrons must be modeled separately. Often the electron temperature is handled separately from the temperature of the remaining gas components. This region occurs for freestream velocities around 10-12 km/s. Gases in this region are modeled as non-radiating plasmas.

Radiation-dominated regime

Above around 12 km/s, the heat transfer to a vehicle changes from being conductively dominated to radiatively dominated. The modeling of gases in this regime is split into two classes:

1. Optically thin: where the gas does not re-absorb radiation emitted from other parts of the gas
2. Optically thick: where the radiation must be considered as a separate source of energy.

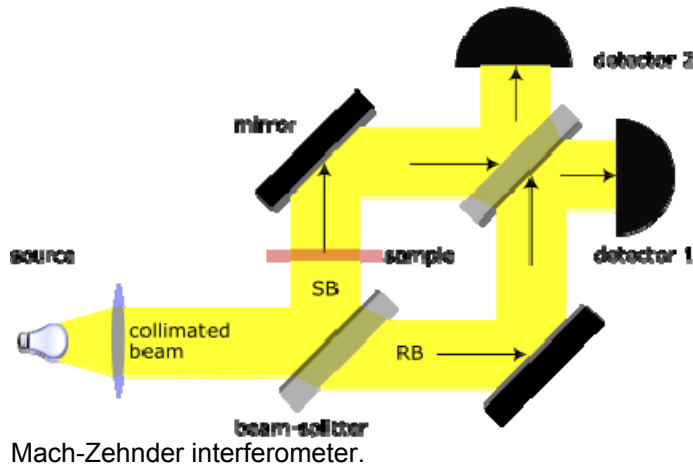
The modeling of optically thick gases is extremely difficult, since, due to the calculation of the radiation at each point, the computation load theoretically expands exponentially as the number of points considered increases.

References

- Anderson, John (2006). *Hypersonic and High-Temperature Gas Dynamics Second Edition*. AIAA Education Series. ISBN 1563477807.

Mach-Zehnder Interferometer

From Wikipedia, the free encyclopedia



Mach-Zehnder interferometer.

The **Mach-Zehnder interferometer** (named after physicists Ludwig Mach (son of Ernst Mach) and Ludwig Zehnder) is a device used to determine the phase shift caused by a small sample which is placed in the path of one of two collimated beams (thus having plane wavefronts) from a coherent light source.

In contrast to the Michelson interferometer, there are two output ports.

How it works

Set-up

A collimated beam is split by a half-silvered mirror. The two resulting beams (the "sample beam" and the "reference beam") are each reflected by a mirror. The two beams then pass a second half-silvered mirror and enter two detectors ("detector 1" and "detector 2"). It is important that the fully-silvered and half-silvered surfaces of all mirrors, except the last, face the inbound beam, and that the half-silvered surface of the last mirror faces the outbound beam exiting in the same orientation as the original collimated beam. That is, if the original beam is horizontal, the half-silvered surface of the last mirror should face the horizontally outbound beam.

Properties

It is important to consider that the medium of a mirror is what lies behind it; that is, if a glass substrate has its half-silvered or fully-silvered surface facing the inbound beam, then the inbound beam travels through air and is reflected off the surface of a glass medium – if, however, the half-silvered or fully-silvered surface faces away from the inbound beam, then the inbound beam travels through glass and is reflecting off the surface of an air medium.

The following rules apply to phase shifts due to material:

- Reflection or refraction at the surface of a medium with a lower refractive index causes no phase shift.
- Reflection at the surface of a medium with a higher refractive index causes a phase shift of half of a wavelength.
- The speed of light is slower in media with an index of refraction greater than that of a vacuum, which is 1. Specifically, its speed is: $v = \frac{c}{n}$, where c is the speed of light in vacuum and n is the index of refraction. This causes a phase shift proportional to $n * \text{length traveled}$.

Given the above rules, mirrors, including half-silvered mirrors, have the following properties:

- A $\frac{1}{2}$ wavelength phase shift occurs upon reflection from the front of a mirror, since the medium behind the mirror (glass) has a higher refractive index than the medium the light is traveling in (air).
- If k is the constant phase shift incurred by passing through a glass plate on which a mirror resides, a total of $2k$ phase shift occurs when reflecting off the rear of a mirror. This is because light traveling toward the rear of a mirror will enter the glass plate, incurring k phase shift, and then reflect off the mirror with no additional phase shift since only air is now behind the mirror, and travel again back through the glass plate incurring an additional k phase shift.

Observing the effect of a sample

Without a sample, there is no phase difference in the two beams in detector 1, yielding constructive interference. Both beams will have undergone a phase shift of wavelength $+k$ due to two front-side reflections and one transmission through a glass plate. At detector 2, there is a phase difference of $0.5 * \text{wavelength}$, yielding complete destructive interference. The reference beam into detector 2 has undergone a phase shift of $0.5 * \text{wavelength} + 2k$ due to one front-side reflection and two transmissions. The sample beam into detector 2 has undergone a wavelength $+ 2k$ phase shift due to two front-side reflections and one rear-side reflection. Therefore, when there is no sample, only detector 1 receives light.

If a sample is placed in the path of the sample beam, the intensities of the beams entering the two detectors will change, allowing the calculation of the phase shift caused by the sample.

References

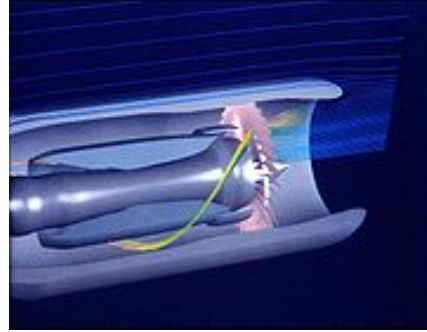
- Ludwig Zehnder, Z. Instrumentenkunde **11** (1891) 275.
- Ludwig Mach, Z. Instrumentenkunde **12** (1892) 89.
- Mach, Ernst (2003). *The Principles of Physical Optics*. Dover. ISBN 0-486-49559-0. p. 170. (First published in German in 1926.)

Jet engine

From Wikipedia, the free encyclopedia



A Pratt & Whitney F100 turbofan engine for the F-15 Eagle and the F-16 Falcon being tested in the hush house at Robins Air Force Base, Georgia, USA. The tunnel behind the engine muffles noise and allows exhaust to escape



Simulation of a low bypass turbofan's airflow

A **jet engine** is a reaction engine that discharges a fast moving jet of fluid to generate thrust in accordance with Newton's laws of motion. This broad definition of jet engines includes turbojets, turbofans, rockets, ramjets, pulse jets and pump-jets. In general, most jet engines are internal combustion engines^[1] but non-combusting forms also exist.

In some common parlance, the term 'jet engine' is loosely referred to an internal combustion duct engine, which typically consists of an engine with a rotary (rotating) air compressor powered by a turbine ("Brayton cycle"), with the leftover power providing thrust via a propelling nozzle. These types of jet engines are primarily used by jet aircraft for long distance travel. The early jet aircraft used turbojet engines which were relatively inefficient for subsonic flight. Modern subsonic jet aircraft usually use high-bypass turbofan engines which help give high speeds as well as, over long distances, giving better fuel efficiency than many other forms of transport.

About 7.2% of the oil used in 2004 was ultimately consumed by jet engines.^[2] In 2007, the cost of jet fuel, while highly variable from one airline to another, averaged 26.5% of total operating costs, making it the single largest operating expense for most airlines.^[3]

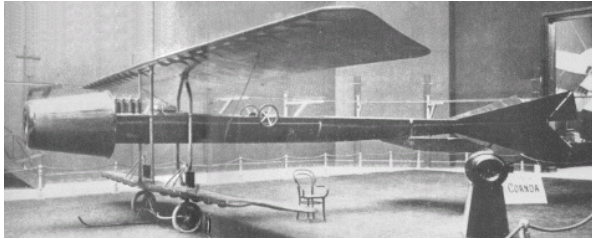
History

Jet engines can be dated back to the first century AD, when Hero of Alexandria (a Greek mathematician) invented the aeolipile. This used steam power directed through two jet nozzles so as to cause a sphere to spin rapidly on its axis. So far as is known, it was little used for supplying mechanical power, and the potential practical applications of Hero's invention of the jet engine were not recognized. It was simply considered a curiosity.

Jet propulsion only literally and figuratively took off with the invention of the rocket by the Chinese in the 13th century. Rocket exhaust was initially used in a modest way for fireworks but gradually progressed to propel formidable weaponry; and there the technology stalled for hundreds of years.

Archytas, the founder of mathematical mechanics, as described in the writings of Aulus Gellius five centuries after him, was reputed to have designed and built the first artificial, self-propelled flying device. This device was a bird-shaped model propelled by a jet of what was probably steam, said to have actually flown some 200 meters.

In Ottoman Turkey in 1633 Lagari Hasan Çelebi took off with what was described to be a cone shaped rocket and then glided with wings into a successful landing winning a position in the Ottoman army. However, this was essentially a stunt. The problem was that rockets are simply too inefficient at low speeds to be useful for general aviation.



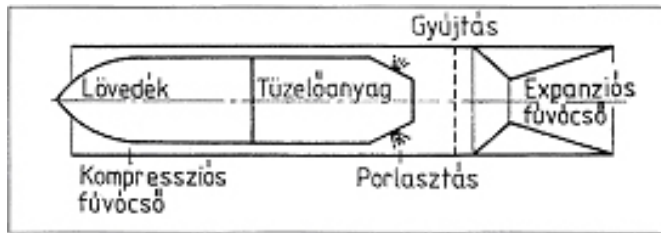
The Coandă-1910.

In 1910 Henri Coandă designed, built and piloted the first 'thermojet' powered aircraft, known as the Coandă-1910, which he demonstrated publicly at the second International Aeronautic Salon in Paris. The powerplant used a 4-cylinder piston engine to power a compressor, which fed two burners for thrust, instead of using a propeller. It would be nearly 30 years until the next thermojet powered aircraft, the Caproni Campini N.1 (sometimes referred to as C.C.2).

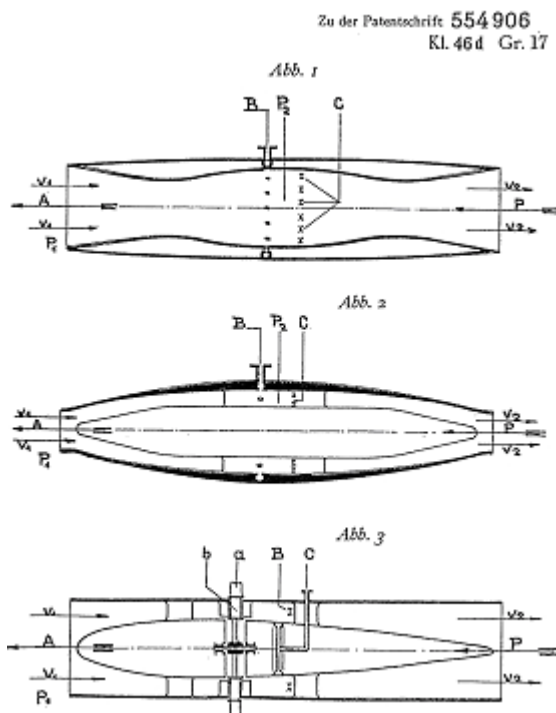
At the airport of Issy-les-Moulineaux near Paris, Coandă lost control of the jet plane, which went off of the runway and caught fire. Fortunately, he escaped with minor injuries to his face and hands. Around that time, Coandă abandoned his experiments due to a lack of interest from the public, scientific and engineering institutions.

In 1913 René Lorin came up with a form of jet engine, the subsonic pulsejet, which would have been somewhat more efficient, but he had no way to achieve high enough speeds for it to operate, and the concept remained theoretical for quite some time. However, engineers were beginning to realize that the piston engine was self-limiting in terms of the maximum performance which could be attained; the limit was essentially one of propeller efficiency.^[4] This seemed to peak as blade tips approached the speed of sound. If engine, and thus aircraft, performance were ever to increase beyond such a barrier, a way would have to be found to radically improve the design of the piston engine, or a wholly new type of powerplant would have to be developed. This was the motivation behind the development of the gas turbine engine, commonly called a "jet" engine, which would become almost as revolutionary to aviation as the Wright brothers' first flight.

The earliest attempts at jet engines were hybrid designs in which an external power source first compressed air, which was then mixed with fuel and burned for jet thrust. In one such system, called a thermojet by Secondo Campini but more commonly, motorjet, the air was compressed by a fan driven by a conventional piston engine. Examples of this type of design were Henri Coandă's Coandă-1910 aircraft, and the much later Campini Caproni CC.2, and the Japanese Tsu-11 engine intended to power Ohka kamikaze planes towards the end of World War II. None were entirely successful and the CC.2 ended up being slower than the same design with a traditional engine and propeller combination.



Albert Fonó's ramjet-cannonball from 1915



Albert Fonó's German patent for jet Engines (January 1928- granted 1932). The third illustration is a turbojet

The key to a practical jet engine was the gas turbine, used to extract energy from the engine itself to drive the compressor. The gas turbine was not an idea developed in the 1930s: the patent for a stationary turbine was granted to John Barber in England in 1791. The first gas turbine to successfully run self-sustaining was built in 1903 by Norwegian engineer Ægidius Elling. Limitations in design and practical engineering and metallurgy prevented such engines reaching manufacture. The main problems were safety, reliability, weight and, especially, sustained operation.

In Hungary, Albert Fonó In 1915 devised a solution for increasing the range of artillery, comprising a gun-launched projectile which was to be united with a ramjet propulsion unit. This was to make it possible to obtain a long range with low initial muzzle velocities, allowing heavy shells to be fired from relatively lightweight guns. Fonó submitted his invention to the Austro-Hungarian Army but the proposal was rejected. In 1928 he applied for a German patent on aircraft powered by supersonic ramjets, and this was awarded in 1932.^{[5][6][7]}

The first patent for using a gas turbine to power an aircraft was filed in 1921 by Frenchman Maxime Guillaume.^[8] His engine was an axial-flow turbojet.

In 1923, Edgar Buckingham of the US National Bureau of Standard published a report^[9] expressing scepticism that jet engines would be economically competitive with prop driven aircraft at the low altitudes and airspeeds of the period: "there does not appear to be, at present, any prospect whatever that jet propulsion of the sort here considered will ever be of practical value, even for military purposes."

Instead, by the 1930s, the piston engine in its many different forms (rotary and static radial, aircooled and liquid-cooled inline) was the only type of powerplant available to aircraft designers. This was acceptable as long as only low performance aircraft were required, and indeed all that were available.



The Whittle W.2/700 engine flew in the Gloster E.28/39, the first British aircraft to fly with a turbojet engine, and the Gloster Meteor

In 1928, RAF College Cranwell cadet^[10] Frank Whittle formally submitted his ideas for a turbo-jet to his superiors. In October 1929 he developed his ideas further.^[11] On 16 January 1930 in England, Whittle submitted his first patent (granted in 1932).^[12] The patent showed a two-stage axial compressor feeding a single-sided centrifugal compressor. Practical axial compressors were made possible by ideas from A.A.Griffith in a seminal paper in 1926 ("An Aerodynamic Theory of Turbine Design"). Whittle would later concentrate on the simpler centrifugal compressor only, for a variety of practical reasons. Whittle had his first engine running in April 1937. It was liquid-fuelled, and included a self-contained fuel pump. Whittle's team experienced near-panic when the engine would not stop, accelerating even after the fuel was switched off. It turned out that fuel had leaked into the engine and accumulated in pools. So the engine would not stop until all the leaked fuel had burned off. Whittle was unable to interest the government in his invention, and development continued at a slow pace.

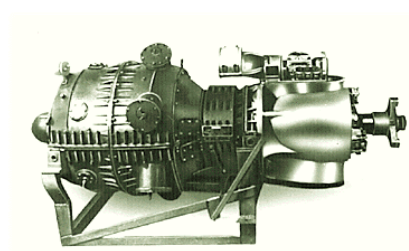


The world's first aircraft to fly purely on turbojet power, the Heinkel He 178. Its first true flight was on 27 August, 1939.

Slide 10. Heinkel 178 aircraft side view.

Heinkel He 178, the world's first aircraft to fly purely on turbojet power

In 1935 Hans von Ohain started work on a similar design in Germany, apparently unaware of Whittle's work.^[13] His first engine was strictly experimental and could only run under external power, but he was able to demonstrate the basic concept. Ohain was then introduced to Ernst Heinkel, one of the larger aircraft industrialists of the day, who immediately saw the promise of the design. Heinkel had recently purchased the Hirth engine company, and Ohain and his master machinist Max Hahn were set up there as a new division of the Hirth company. They had their first HeS 1 centrifugal engine running by September 1937. Unlike Whittle's design, Ohain used hydrogen as fuel, supplied under external pressure. Their subsequent designs culminated in the gasoline-fuelled HeS 3 of 1,100 lbf (5 kN), which was fitted to Heinkel's simple and compact He 178 airframe and flown by Erich Warsitz in the early morning of August 27, 1939, from Rostock-Marienehe aerodrome, an impressively short time for development. The He 178 was the world's first jet plane.

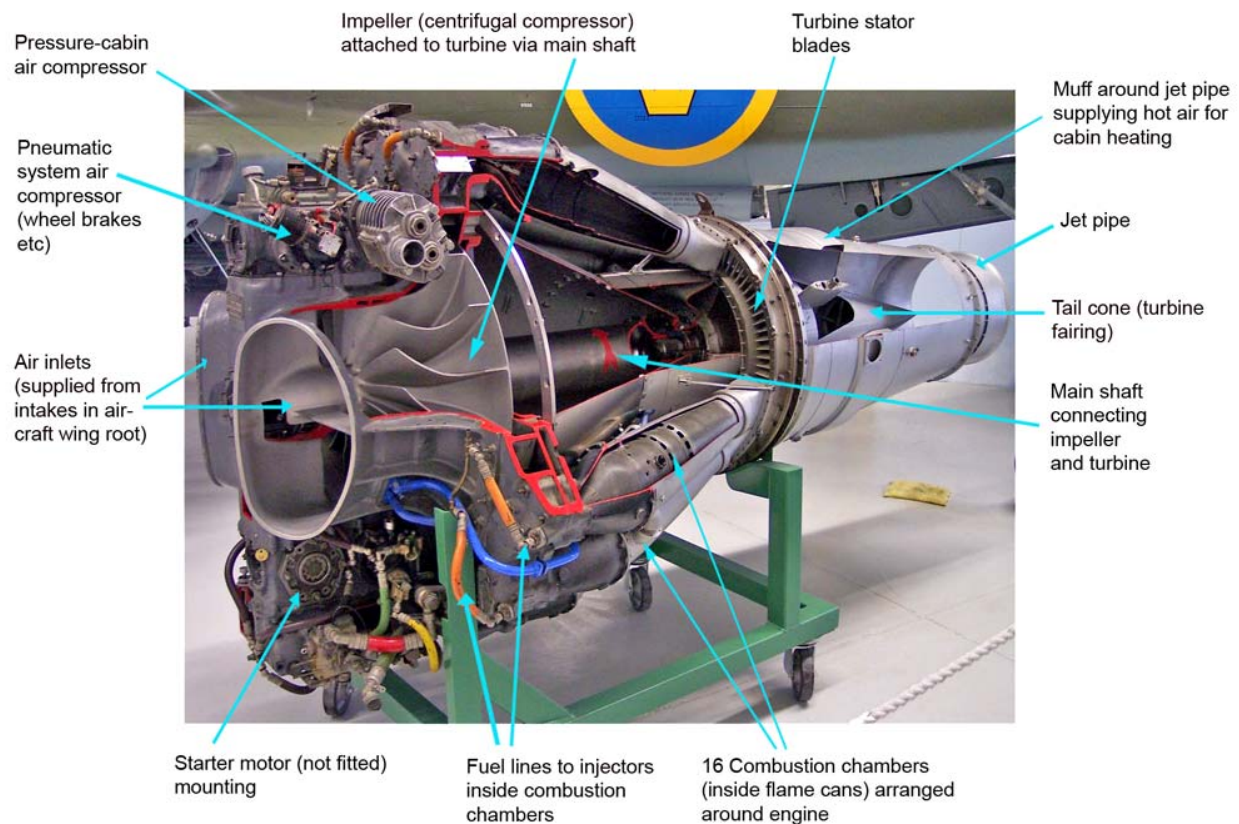


Jendrassik Cs-1, The first Turboprop engine. built in Hungarian Ganz works in 1938

The world's first turboprop was the Jendrassik Cs-1 designed by the Hungarian mechanical engineer György Jendrassik. It was produced and tested in the Ganz factory in Budapest between 1938 and 1942. It was planned to fit to the Varga RMI-1 X/H twin-engined reconnaissance bomber designed by László Varga in 1940, but the program was cancelled. Jendrassik had also designed a small-scale 75 kW turboprop in 1937.

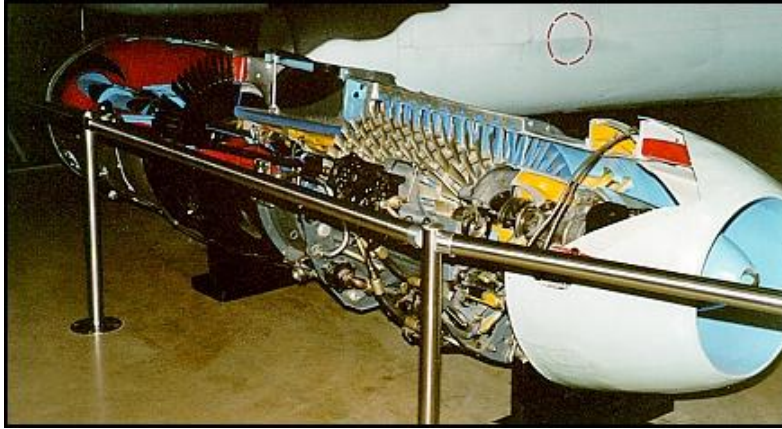
Whittle's engine was starting to look useful, and his **Power Jets Ltd.** started receiving Air Ministry money. In 1941 a flyable version of the engine called the **W.1**, capable of 1000 lbf (4 kN) of thrust, was fitted to the Gloster E28/39 airframe specially built for it, and first flew on May 15, 1941 at RAF Cranwell.

A Scottish aircraft engine designer, Frank Halford, working from Whittle's ideas developed a "straight through" version of the centrifugal jet; his design became the de Havilland Goblin.



A picture of an early centrifugal engine (DH Goblin II) sectioned to show its internal components

One problem with both of these early designs, which are called **centrifugal-flow** engines, was that the compressor worked by "throwing" (accelerating) air outward from the central intake to the outer periphery of the engine, where the air was then compressed by a divergent duct setup, converting its velocity into pressure. An advantage of this design was that it was already well understood, having been implemented in centrifugal superchargers, then in widespread use on piston engines. However, given the early technological limitations on the shaft speed of the engine, the compressor needed to have a very large diameter to produce the power required. This meant that the engines had a large frontal area, which made it less useful as an aircraft powerplant due to drag. A further disadvantage was that the air flow had to be "bent" to flow rearwards through the combustion section and to the turbine and tailpipe, adding complexity and lowering efficiency. Nevertheless, these types of engines had the major advantages of light weight, simplicity and reliability, and development rapidly progressed to practical airworthy designs.



A cutaway of the Junkers Jumo 004 engine.

Austrian Anselm Franz of Junkers' engine division (*Junkers Motoren* or **Jumo**) addressed these problems with the introduction of the axial-flow compressor. Essentially, this is a turbine in reverse. Air coming in the front of the engine is blown towards the rear of the engine by a fan stage (convergent ducts), where it is crushed against a set of non-rotating blades called *stators* (divergent ducts). The process is nowhere near as powerful as the centrifugal compressor, so a number of these pairs of fans and stators are placed in series to get the needed compression. Even with all the added complexity, the resulting engine is much smaller in diameter and thus, more aerodynamic. Jumo was assigned the next engine number in the RLM numbering sequence, 4, and the result was the Jumo 004 engine. After many lesser technical difficulties were solved, mass production of this engine started in 1944 as a powerplant for the world's first jet-fighter aircraft, the Messerschmitt Me 262 (and later the world's first jet-bomber aircraft, the Arado Ar 234). A variety of reasons conspired to delay the engine's availability, this delay caused the fighter to arrive too late to decisively impact Germany's position in World War II. Nonetheless, it will be remembered as the first use of jet engines in service.

In the UK, their first axial-flow engine, the Metrovick F.2, ran in 1941 and was first flown in 1943. Although more powerful than the centrifugal designs at the time, the Ministry considered its complexity and unreliability a drawback in wartime. The work at Metrovick led to the Armstrong Siddeley Sapphire engine which would be built in the US as the J65.

Following the end of the war the German jet aircraft and jet engines were extensively studied by the victorious allies and contributed to work on early Soviet and US jet fighters. The legacy of the axial-flow engine is seen in the fact that practically all jet engines on fixed wing aircraft have had some inspiration from this design.

Centrifugal-flow engines have improved since their introduction. With improvements in bearing technology the shaft speed of the engine was increased, greatly reducing the diameter of the centrifugal compressor. The short engine length remains an advantage of this design, particularly for use in helicopters where overall size is more important than frontal area. Also as their engine components are more robust they are less liable to foreign object damage than axial-flow compressor engines.

Although German designs were more advanced aerodynamically, the combination of simplicity and Britain's war-time availability of requisite rare metals for the necessary advanced metallurgy (such as tungsten, chromium and titanium) for high-stress components such as turbine blades and bearings, etc) meant that Whittle-derived designs were generally more reliable than their German

counterparts. British engines were also widely manufactured under license in the US (see Tizard Mission), and were sold to Soviet Russia who reverse engineered them with the Nene going on to power the famous MiG-15. American and Soviet designs, independent axial-flow types for the most part, would strive to attain superior performance until the 1960s, although the General Electric J47 provided excellent service in the F-86 Sabre in the 1950s.

By the 1950s the jet engine was almost universal in combat aircraft, with the exception of cargo, liaison and other specialty types. By this point some of the British designs were already cleared for civilian use, and had appeared on early models like the de Havilland Comet and Avro Canada Jetliner. By the 1960s all large civilian aircraft were also jet powered, leaving the piston engine in such low-cost niche roles such as cargo flights.

Relentless improvements in the turboprop pushed the piston engine (an internal combustion engine) out of the mainstream entirely, leaving it serving only the smallest general aviation designs and some use in drone aircraft. The ascension of the jet engine to almost universal use in aircraft took well under twenty years.

However, the story was not quite at an end, for the efficiency of turbojet engines was still rather worse than piston engines, but by the 1970s with the advent of high bypass jet engines, an innovation not foreseen by the early commentators like Edgar Buckingham, at high speeds and high altitudes that seemed absurd to them, only then did the fuel efficiency finally exceed that of the best piston and propeller engines,^[14] and the dream of fast, safe, economical travel around the world finally arrived, and their dour, if well founded for the time, predictions that jet engines would never amount to much, were killed forever.

Types

There are a large number of different types of jet engines, all of which achieve forward thrust from the principle of *jet propulsion*.

Type	Description	Advantages	Disadvantages
Water jet	For propelling water rockets and jetboats; squirts water out the back through a nozzle	In boats, can run in shallow water, high acceleration, no risk of engine overload (unlike propellers), less noise and vibration, highly maneuverable at all boat speeds, high speed efficiency, less vulnerable to damage from debris, very reliable, more load flexibility, less harmful to wildlife	Can be less efficient than a propeller at low speed, more expensive, higher weight in boat due to entrained water, will not perform well if boat is heavier than the jet is sized for
Motorjet	Most primitive airbreathing jet engine. Essentially a supercharged piston engine with a jet exhaust.	Higher exhaust velocity than a propeller, offering better thrust at high speed	Heavy, inefficient and underpowered. Examples include: Coandă-1910 and Caproni Campini N.1.
Turbojet	A tube with a compressor and turbine sharing a common shaft with a burner in between and a propelling nozzle for the exhaust. ^[15] Uses a high exhaust gas velocity to produce thrust. Has a much higher core flow than bypass type engines	Simplicity of design, efficient at supersonic speeds (~M2)	A basic design, misses many improvements in efficiency and power for subsonic flight, relatively noisy.

Low-bypass Turbofan	One- or two-stage fan added in front bypasses a proportion of the air through a bypass duct straight to the nozzle/ afterburner, avoiding the combustion chamber, with the rest being heated in the combustion chamber and passing through the turbine. ^[16] Compared with its turbojet ancestor, this allows for more efficient operation with somewhat less noise. This is the engine of high-speed military aircraft, some smaller private jets, and older civilian airliners such as the Boeing 707, the McDonnell Douglas DC-8, and their derivatives.	As with the turbojet, the design is aerodynamic, with only a modest increase in diameter over the turbojet required to accommodate the bypass fan and chamber. It is capable of supersonic speeds with minimal thrust drop-off at high speeds and altitudes yet still more efficient than the turbojet at subsonic operation.	Noisier and less efficient than high-bypass turbofan, with less static (Mach 0) thrust. Added complexity to accommodate dual shaft designs. More inefficient than a turbojet around M2 due to higher cross-sectional area.
High-bypass Turbofan	First stage compressor drastically enlarged to provide bypass airflow around engine core, and it provides significant amounts of thrust. Compared to the low-bypass turbofan and no-bypass turbojet, the high-bypass turbofan works on the principle of moving a great deal of air somewhat faster, rather than a small amount extremely fast. ^[16] Most common form of jet engine in civilian use today- used in airliners like the Boeing 747, most 737s, and all Airbus aircraft.	Quieter around 10 to 20 percent more than the turbojet engine due to greater mass flow and lower total exhaust speed and more efficient for a useful range of subsonic airspeeds for same reason, cooler exhaust temperature. Less noisy and exhibit much better efficiency than low bypass turbofans.	Greater complexity (additional ducting, usually multiple shafts) and the need to contain heavy blades. Fan diameter can be extremely large, especially in high bypass turbofans such as the GE90. More subject to FOD and ice damage. Top speed is limited due to the potential for shockwaves to damage engine. Thrust lapse at higher speeds, which necessitates huge diameters and introduces additional drag.
Rocket	Carries all propellants and oxidants on-board, emits jet for propulsion ^[17]	Very few moving parts, Mach 0 to Mach 25+, efficient at very high speed (> Mach 5.0 or so), thrust/weight ratio over 100, no complex air inlet, high compression ratio, very high speed (hypersonic) exhaust, good cost/thrust ratio, fairly easy to test, works in a vacuum-indeed works best exo-atmospheric which is kinder on vehicle structure at high speed, fairly small surface area to keep cool, and no turbine in hot exhaust stream.	Needs lots of propellant- very low specific impulse — typically 100-450 seconds. Extreme thermal stresses of combustion chamber can make reuse harder. Typically requires carrying oxidiser on-board which increases risks. Extraordinarily noisy.
Ramjet	Intake air is compressed entirely by speed of oncoming air and duct shape (<i>divergent</i>), and then it goes through a burner section where it is heated and then passes through a propelling nozzle ^[18]	Very few moving parts, Mach 0.8 to Mach 5+, efficient at high speed (> Mach 2.0 or so), lightest of all air-breathing jets (thrust/weight ratio up to 30 at optimum speed), cooling much easier than turbojets as no turbine blades to cool.	Must have a high initial speed to function, inefficient at slow speeds due to poor compression ratio, difficult to arrange shaft power for accessories, usually limited to a small range of speeds, intake flow must be slowed to subsonic speeds, noisy, fairly difficult to test, finicky to keep lit.
Turboprop (Turboshaft similar)	Strictly not a jet at all — a gas turbine engine is used as a powerplant to drive a propeller shaft (or rotor in the case of a helicopter)	High efficiency at lower subsonic airspeeds (300 knots plus), high shaft power to weight	Limited top speed (aeroplanes), somewhat noisy, complex transmission
Propfan/Unducted	Turbojet engine that also drives	Higher fuel efficiency, potentially	Development of propfan engines

Fan	one or more propellers. Similar to a turbofan without the fan cowlings.	less noisy than turbofans, could lead to higher-speed commercial aircraft, popular in the 1980s during fuel shortages	has been very limited, typically more noisy than turbofans, complexity
Pulsejet	Air is compressed and combusted intermittently instead of continuously. Some designs use valves.	Very simple design, commonly used on model aircraft	Noisy, inefficient (low compression ratio), works poorly on a large scale, valves on valved designs wear out quickly
Pulse detonation engine	Similar to a pulsejet, but combustion occurs as a detonation instead of a deflagration, may or may not need valves	Maximum theoretical engine efficiency	Extremely noisy, parts subject to extreme mechanical fatigue, hard to start detonation, not practical for current use
Air-augmented rocket	Essentially a ramjet where intake air is compressed and burnt with the exhaust from a rocket	Mach 0 to Mach 4.5+ (can also run exoatmospheric), good efficiency at Mach 2 to 4	Similar efficiency to rockets at low speed or exoatmospheric, inlet difficulties, a relatively undeveloped and unexplored type, cooling difficulties, very noisy, thrust/weight ratio is similar to ramjets.
Scramjet	Similar to a ramjet without a diffuser; airflow through the entire engine remains supersonic	Few mechanical parts, can operate at very high Mach numbers (Mach 8 to 15) with good efficiencies ^[19]	Still in development stages, must have a very high initial speed to function (Mach >6), cooling difficulties, very poor thrust/weight ratio (~2), extreme aerodynamic complexity, airframe difficulties, testing difficulties/expense
Turborocket	A turbojet where an additional oxidizer such as oxygen is added to the airstream to increase maximum altitude	Very close to existing designs, operates in very high altitude, wide range of altitude and airspeed	Airspeed limited to same range as turbojet engine, carrying oxidizer like LOX can be dangerous. Much heavier than simple rockets.
Precooled jets / LACE	Intake air is chilled to very low temperatures at inlet in a heat exchanger before passing through a ramjet and/or turbojet and/or rocket engine.	Easily tested on ground. Very high thrust/weight ratios are possible (~14) together with good fuel efficiency over a wide range of airspeeds, mach 0-5.5+; this combination of efficiencies may permit launching to orbit, single stage, or very rapid, very long distance intercontinental travel.	Exists only at the lab prototyping stage. Examples include RB545, Reaction Engines SABRE, ATREX. Requires liquid hydrogen fuel which has very low density and heavily insulated tankage.

Uses

Jet engines are usually used as aircraft engines for jet aircraft. They are also used for cruise missiles and unmanned aerial vehicles.

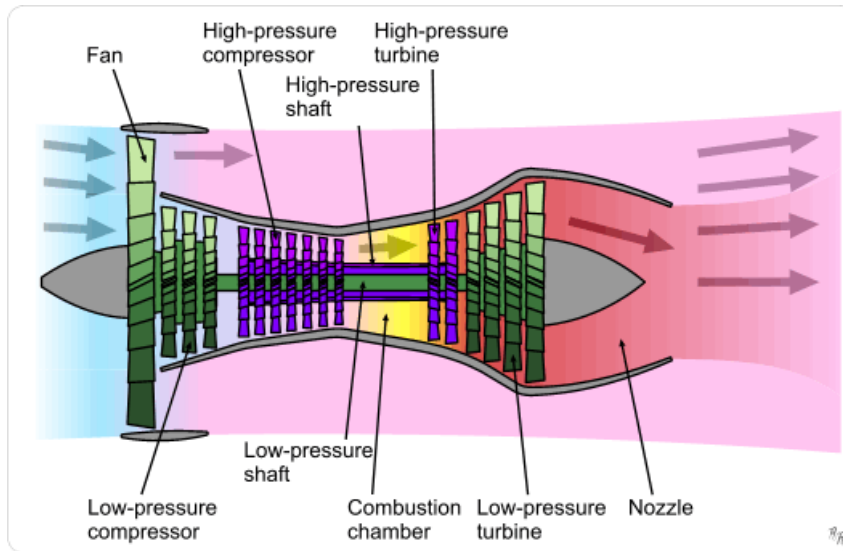
In the form of rocket engines they are used for fireworks, model rocketry, spaceflight, and military missiles.

Jet engines have also been used to propel high speed cars, particularly drag racers, with the all-time record held by a rocket car. A turbofan powered car ThrustSSC currently holds the land speed record.

Jet engine designs are frequently modified to turn them into gas turbine engines which are used in a wide variety of industrial applications. These include electrical power generation, powering water, natural gas, or oil pumps, and providing propulsion for ships and locomotives. Industrial gas turbine can create up to 50,000 shaft horsepower. Many of these engines are derived from older military

turbojets such as the Pratt & Whitney J57 and J75 models. There is also a derivative of the P&W JT8D low-bypass turbofan that creates up to 35,000 HP.

Major components



Components of jet engines

The major components of a jet engine are similar across the major different types of engines, although not all engine types have all components. The major parts include:

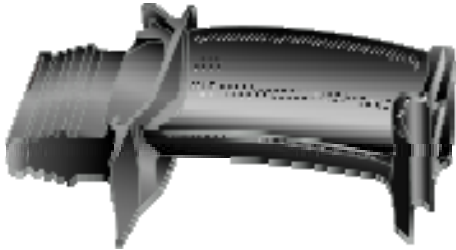
- **Cold Section:**

- **Air intake (Inlet)** — For subsonic aircraft, the air intake to a jet engine consists essentially of an opening which is designed to minimise drag. The air reaching the compressor of a normal jet engine must be travelling below the speed of sound, even for supersonic aircraft, to allow smooth flow through compressor and turbine blades. At supersonic flight speeds, shockwaves form in the intake system, these help compress the air, but also there is some inevitable reduction in the recovered pressure at inlet to the compressor. Some supersonic intakes use devices, such as a cone or a ramp, to increase pressure recovery.
- **Compressor or Fan** — The compressor is made up of stages. Each stage consists of vanes which rotate, and stators which remain stationary. As air is drawn deeper through the compressor, its heat and pressure increases. Energy is derived from the **turbine** (see below), passed along the **shaft**.
- **Bypass ducts** — Much of the thrust of essentially all modern jet engines comes from air from the front compressor that bypasses the combustion chamber and gas turbine section that leads directly to the nozzle or afterburner (where fitted).

- **Common:**

- **Shaft** — The shaft connects the **turbine** to the **compressor**, and runs most of the length of the engine. There may be as many as three concentric shafts, rotating at independent speeds, with as many sets of turbines and compressors. Other services, like a bleed of cool air, may also run down the shaft.

- **Diffuser section:** - This section is a divergent duct that utilizes Bernoulli's principle to decrease the velocity of the compressed air to allow for easier ignition. And, at the same time, continuing to increase the air pressure before it enters the combustion chamber.
- **Hot section:**
 - **Combustor or Can or Flameholders or Combustion Chamber** — This is a chamber where fuel is continuously burned in the compressed air.



A blade with internal cooling as applied in the high-pressure turbine

- **Turbine** — The turbine is a series of bladed discs that act like a windmill, gaining energy from the hot gases leaving the **combustor**. Some of this energy is used to drive the **compressor**, and in some turbine engines (ie turboprop, turboshaft or turbofan engines), energy is extracted by additional turbine discs and used to drive devices such as propellers, bypass fans or helicopter rotors. One type, a **free turbine**, is configured such that the turbine disc driving the compressor rotates independently of the discs that power the external components. Relatively cool air, bled from the compressor, may be used to cool the turbine blades and vanes, to prevent them from melting.
- **Afterburner or reheat** (chiefly UK) — (mainly military) Produces extra thrust by burning extra fuel, usually inefficiently, to significantly raise Nozzle Entry Temperature at the **exhaust**. Owing to a larger volume flow (i.e. lower density) at exit from the afterburner, an increased nozzle flow area is required, to maintain satisfactory engine matching, when the afterburner is alight.
- **Exhaust or Nozzle** — Hot gases leaving the engine exhaust to atmospheric pressure via a nozzle, the objective being to produce a high velocity jet. In most cases, the nozzle is convergent and of fixed flow area.
- **Supersonic nozzle** — If the Nozzle Pressure Ratio (Nozzle Entry Pressure/Ambient Pressure) is very high, to maximize thrust it may be worthwhile, despite the additional weight, to fit a convergent-divergent (de Laval) nozzle. As the name suggests, initially this type of nozzle is convergent, but beyond the throat (smallest flow area), the flow area starts to increase to form the divergent portion. The expansion to atmospheric pressure and supersonic gas velocity continues downstream of the throat, whereas in a convergent nozzle the expansion beyond sonic velocity occurs externally, in the exhaust plume. The former process is more efficient than the latter.

The various components named above have constraints on how they are put together to generate the most efficiency or performance. The performance and efficiency of an engine can never be taken in isolation; for example fuel/distance efficiency of a supersonic jet engine maximises at about mach 2, whereas the drag for the vehicle carrying it is increasing as a square law and has much extra drag

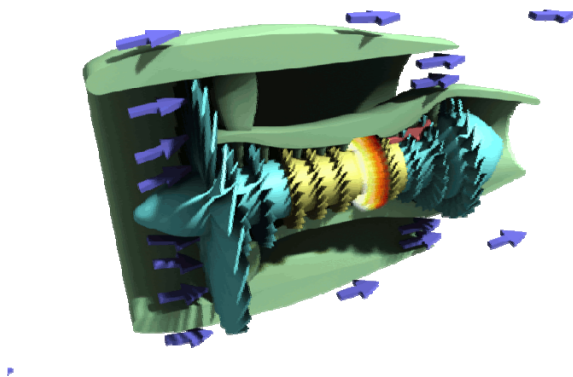
in the transonic region. The highest fuel efficiency for the overall vehicle is thus typically at Mach ~ 0.85 .

For the engine optimisation for its intended use, important here is air intake design, overall size, number of compressor stages (sets of blades), fuel type, number of exhaust stages, metallurgy of components, amount of bypass air used, where the bypass air is introduced, and many other factors. For instance, let us consider design of the air intake.

Common types

There are two types of jet engine that are seen commonly today, the turbofan which is used on almost all commercial airliners, and rocket engines which are used for spaceflight and other terrestrial uses such as ejector seats, flares, fireworks etc.

Turbofan engines



Turbofan engine

Most modern jet engines are actually turbofans, where the low pressure compressor acts as a fan, supplying supercharged air not only to the engine core, but to a bypass duct. The bypass airflow either passes to a separate 'cold nozzle' or mixes with low pressure turbine exhaust gases, before expanding through a 'mixed flow nozzle'.

Turbofans are used for airliners because they give an exhaust speed that is better matched for subsonic airliners. At airliners' flight speed, conventional turbojet engines generate an exhaust that ends up travelling very fast backwards, and this wastes energy. By emitting the exhaust so that it ends up travelling more slowly, better fuel consumption is achieved as well as higher thrust at low speeds. In addition, the lower exhaust speed gives much lower noise.

In the 1960s there was little difference between civil and military jet engines, apart from the use of afterburning in some (supersonic) applications. Civil turbofans today have a low exhaust speed (low *specific thrust* - net thrust divided by airflow) to keep jet noise to a minimum and to improve fuel efficiency. Consequently the bypass ratio (bypass flow divided by core flow) is relatively high (ratios from 4:1 up to 8:1 are common). Only a single fan stage is required, because a low specific thrust implies a low fan pressure ratio.

Today's military turbofans, however, have a relatively high specific thrust, to maximize the thrust for a given frontal area, jet noise being of less concern in military uses relative to civil uses. Multistage fans are normally needed to reach the relatively high fan pressure ratio needed for high specific thrust. Although high turbine inlet temperatures are often employed, the bypass ratio tends to be low, usually significantly less than 2.0.

Rocket engines

A common form of jet engine is the rocket engine. Rocket engines are used for high altitude flights because they give very high thrust and their lack of reliance on atmospheric oxygen allows them to operate at arbitrary altitudes. This is used for launching satellites, space exploration and manned access, and permitted landing on the moon in 1969.

However, the high exhaust speed and the heavier, oxidiser-rich propellant results in more propellant use than turbojets, and their use is largely restricted to very high altitudes, very high speeds, or where very high accelerations are needed as rocket engines themselves have a very high thrust-to-weight ratio.

An approximate equation for the net thrust of a rocket engine is:

$$F = \dot{m}g_0 I_{sp-vac} - A_e P$$

Where F is the thrust, $I_{sp(vac)}$ is the specific impulse, g_0 is a standard gravity, \dot{m} is the propellant flow in kg/s, A_e is the area of the exhaust bell at the exit, and P is the atmospheric pressure.

General physical principles

All jet engines are reaction engines that generate thrust by emitting a jet of fluid rearwards at relatively high speed. The forces on the inside of the engine needed to create this jet give a strong thrust on the engine which pushes the craft forwards.

Jet engines make their jet from propellant from tankage that is attached to the engine (as in a 'rocket') as well as in **duct engines** (those commonly used on aircraft) by ingesting an external fluid (very typically air) and expelling it at higher speed.

Thrust

The motion impulse of the engine is equal to the fluid mass multiplied by the speed at which the engine emits this mass:

$$I = m c$$

where m is the fluid mass per second and c is the exhaust speed. In other words, a vehicle gets the same thrust if it outputs a lot of exhaust very slowly, or a little exhaust very quickly. (In practice parts of the exhaust may be faster than others, but it is the *average* momentum that matters, and thus the important quantity is called the **effective exhaust speed** - c here.)

However, when a vehicle moves with certain velocity v , the fluid moves towards it, creating an opposing ram drag at the intake:

$$m v$$

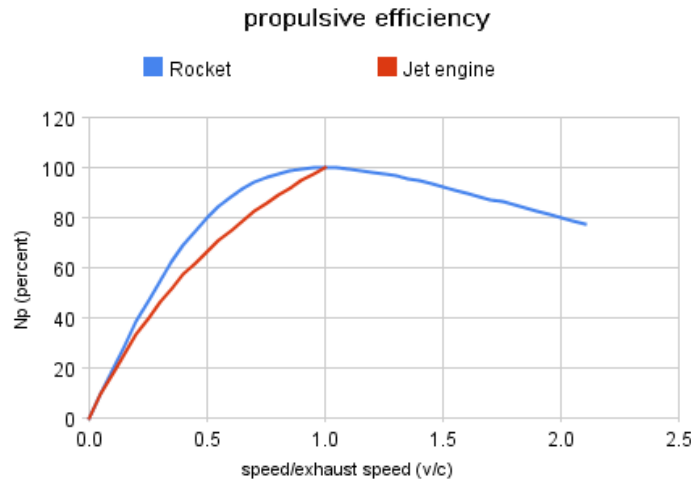
Most types of jet engine have an intake, which provides the bulk of the fluid exiting the exhaust. Conventional rocket motors, however, do not have an intake, the oxidizer and fuel both being carried within the vehicle. Therefore, rocket motors do not have ram drag; the gross thrust of the nozzle is the net thrust of the engine. Consequently, the thrust characteristics of a rocket motor are different from that of an air breathing jet engine, and thrust is independent of speed.

The jet engine with an intake duct is only useful if the velocity of the gas from the engine, c , is greater than the vehicle velocity, v , as the net engine thrust is the same as if the gas were emitted with the velocity $c-v$. So the thrust is actually equal to

$$S = m(c-v)$$

This equation implies that as v approaches c , a greater mass of fluid must go through the engine to continue to accelerate at the same rate, but all engines have a designed limit on this. Additionally, the equation implies that the vehicle can't accelerate past its exhaust velocity as it would have negative thrust.

Energy efficiency



Dependence of the energy efficiency (η) upon the vehicle speed/exhaust speed ratio (v/c)
for air-breathing jet and rocket engines

Energy efficiency (η) of jet engines installed in vehicles has two main components, *cycle efficiency* (η_c)- how efficiently the engine can accelerate the jet, and *propulsive efficiency* (η_p)-how much of the energy of the jet ends up in the vehicle body rather than being carried away as kinetic energy of the jet.

Even though overall energy efficiency η is simply:

$$\eta = \eta_p \eta_c$$

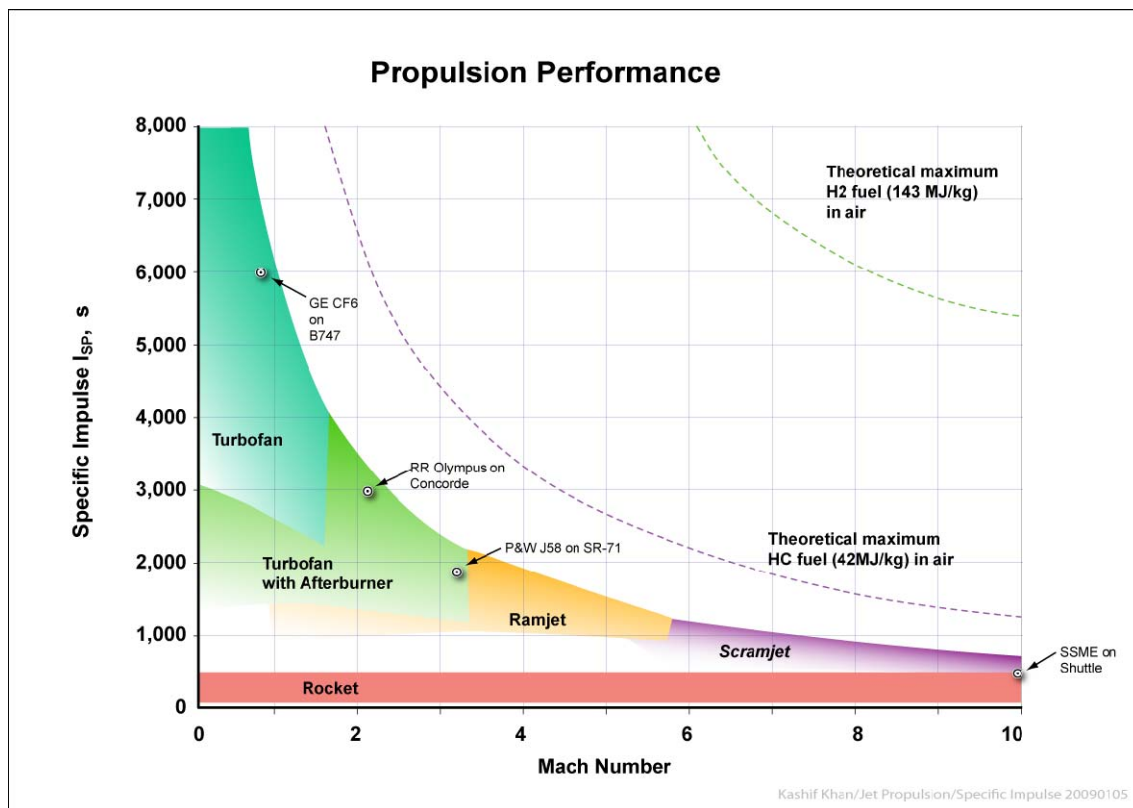
For all jet engines the *propulsive efficiency* is highest when the engine emits an exhaust jet at a speed that is the same as, or nearly the same as, the vehicle velocity as this gives the smallest residual kinetic energy.(Note:^[20]) The exact formula for air-breathing engines moving at speed v with an exhaust velocity c is given in the literature as:^[21] is

$$\eta_p = \frac{2}{1 + \frac{c}{v}}$$

And for a rocket:

$$\eta_p = \frac{2\frac{v}{c}}{1 + \left(\frac{v}{c}\right)^2} [22]$$

In addition to propulsive efficiency, another factor is cycle efficiency; essentially a jet engine is typically a form of heat engine. Heat engine efficiency is determined by the ratio of temperatures that are reached in the engine to that they are exhausted at from the nozzle, which in turn is limited by the overall pressure ratio that can be achieved. Cycle efficiency is highest in rocket engines (~60+%), as they can achieve extremely high combustion temperatures and can have very large, energy efficient nozzles. Cycle efficiency in turbojet and similar is nearer to 30%, the practical combustion temperatures and nozzle efficiencies are much lower.



Specific impulse as a function of speed for different jet types with kerosene fuel (hydrogen I_{sp} would be about twice as high). Although efficiency plummets with speed, greater distances are covered, it turns out that efficiency per unit distance (per km or mile) is roughly independent of speed for jet engines as a group; however airframes become inefficient at supersonic speeds

Fuel/propellant consumption

A closely related (but different) concept to energy efficiency is the rate of consumption of propellant mass. Propellant consumption in jet engines is measured by **Specific Fuel Consumption**, **Specific impulse** or **Effective exhaust velocity**. They all measure the same thing, specific impulse and effective exhaust velocity are strictly proportional, whereas specific fuel consumption is inversely proportional to the others.

For airbreathing engines such as turbojets energy efficiency and propellant (fuel) efficiency are much the same thing, since the propellant is a fuel and the source of energy. In rocketry, the propellant is also the exhaust, and this means that a high energy propellant gives better propellant efficiency but can in some cases actually can give *lower* energy efficiency.

Engine type	scenario	SFC in lb/(lbf·h)	SFC in g/(kN·s)	Isp in s	Effective exhaust velocity (m/s)
NK-33 rocket engine	vacuum	10.9	309	330	3,240
SSME rocket engine	Space Shuttle vacuum	7.95	225	453	4,423
Ramjet	M1	4.5	127	800	7,877
J-58 turbojet	SR-71 at M3.2 (wet)	1.9	53.8	1,900	18,587
Rolls-Royce/Snecma Olympus 593	Concorde M2 cruise (dry)	1.195 ^[23]	33.8	3,012	29,553
CF6-80C2B1F turbofan	Boeing 747-400 cruise	0.605 ^[23]	17.1	5,950	58,400
General Electric CF6 turbofan	sea level	0.307	8.696	11,700	115,000

[23]

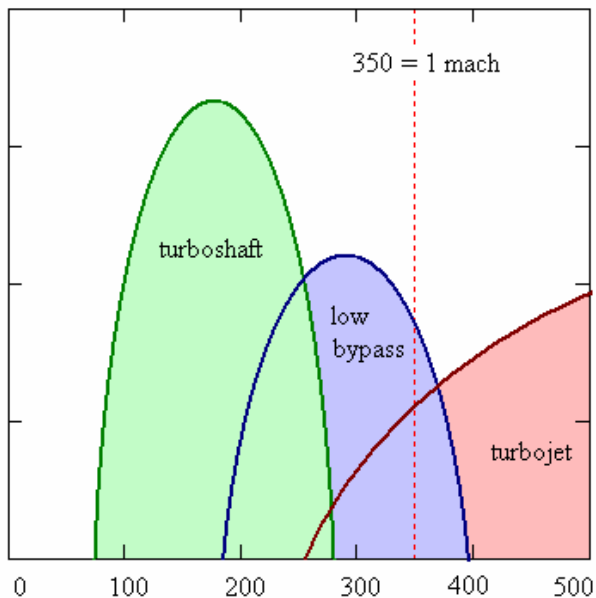
Thrust-to-weight ratio

The thrust to weight ratio of jet engines of similar principles varies somewhat with scale, but mostly is a function of engine construction technology. Clearly for a given engine, the lighter the engine, the better the thrust to weight is, the less fuel is used to compensate for drag due to the lift needed to carry the engine weight, or to accelerate the mass of the engine.

As can be seen in the following table, rocket engines generally achieve very much higher thrust to weight ratios than duct engines such as turbojet and turbofan engines. This is primarily because rockets almost universally use dense liquid or solid reaction mass which gives a much smaller volume and hence the pressurisation system that supplies the nozzle is much smaller and lighter for the same performance. Duct engines have to deal with air which is 2-3 orders of magnitude less dense and this gives pressures over much larger areas, and which in turn results in more engineering materials being needed to hold the engine together and for the air compressor.

Engine	Thrust-to-weight ratio
Concorde's Rolls-Royce/Snecma Olympus 593 turbojet	4.0 with reheat ^[24]
J-58 (SR-71 Blackbird jet engine)	5.2 ^[25]
Space shuttle's SSME rocket engine	73.12 ^[26]
RD-180 rocket engine	73.4
NK-33 rocket engine	136.66 ^[27]

Comparison of types



Comparative suitability for (left to right) turboshaft, low bypass and turbojet to fly at 10 km altitude in various speeds. Horizontal axis - speed, m/s. Vertical axis displays engine efficiency.

Turboprops obtain little thrust from jet effect, but are useful for comparison. They are gas turbine engines that have a rotating fan that takes and accelerates the large mass of air but by a relatively small change in speed. This low speed limits the speed of any propeller driven airplane. When the plane speed exceeds this limit, propellers no longer provide any thrust ($c-v < 0$). However, because they accelerate a large mass of air, turboprops are very efficient.

Turbojets accelerate a much smaller mass of the air and burned fuel, but they emit it at the much higher speeds possible with a de Laval nozzle. This is why they are suitable for supersonic and higher speeds.

Low bypass turboprops have the mixed exhaust of the two air flows, running at different speeds (c_1 and c_2). The thrust of such engine is

$$S = m_1 (c_1 - v) + m_2 (c_2 - v)$$

where m_1 and m_2 are the air masses, being blown from the both exhausts. Such engines are effective at lower speeds, than the pure jets, but at higher speeds than the turboshafts and propellers in general. For instance, at the 10 km altitude, turboshafts are most effective at about Mach 0.4 (0.4 times the speed of sound), low bypass turboprops become more effective at about Mach 0.75 and turbojets become more effective than mixed exhaust engines when the speed approaches Mach 2-3.

Rocket engines have extremely high exhaust velocity and thus are best suited for high speeds (hypersonic) and great altitudes. At any given throttle, the thrust and efficiency of a rocket motor improves slightly with increasing altitude (because the back-pressure falls thus increasing net thrust at the nozzle exit plane), whereas with a turbojet (or turboprop) the falling density of the air entering the intake (and the hot gases leaving the nozzle) causes the net thrust to decrease with increasing altitude. Rocket engines are more efficient than even scramjets above roughly Mach 15.^[28]

Altitude and speed

With the exception of scramjets, jet engines, deprived of their inlet systems can only accept air at around half the speed of sound. The inlet system's job for transonic and supersonic aircraft is to slow the air and perform some of the compression.

The limit on maximum altitude for engines is set by flammability- at very high altitudes the air becomes too thin to burn, or after compression, too hot. For turbojet engines altitudes of about 40 km appear to be possible, whereas for ramjet engines 55 km may be achievable. Scramjets may theoretically manage 75 km.^[29] Rocket engines of course have no upper limit.

Flying faster compresses the air in at the front of the engine, but ultimately the engine cannot go any faster without melting. The upper limit is usually thought to be about Mach 5-8, except for scramjets which may be able to achieve about Mach 15 or more, as they avoid slowing the air.

Noise

Noise is due to shockwaves that form when the exhaust jet interacts with the external air. The intensity of the noise is proportional to the thrust as well as proportional to the fourth power of the jet velocity. Generally then, the lower speed exhaust jets emitted from engines such as high bypass turbofans are the quietest, whereas the fastest jets are the loudest.

Although some variation in jet speed can often be arranged from a jet engine (such as by throttling back and adjusting the nozzle) it is difficult to vary the jet speed from an engine over a very wide range. Therefore since engines for supersonic vehicles such as Concorde, military jets and rockets inherently need to have supersonic exhaust at top speed, so these vehicles are especially noisy even at low speeds.

Advanced designs

J-58 combined ramjet/turbojet

The SR-71 Blackbird's Pratt & Whitney J58 engines were rather unusual. They could convert in flight from being largely a turbojet to being largely a compressor-assisted ramjet. At high speeds (above Mach 2.4), the engine used variable geometry vanes to direct excess air through 6 bypass pipes from downstream of the fourth compressor stage into the afterburner.^[30] 80% of the SR-71's thrust at high speed was generated in this way, giving much higher thrust, improving specific impulse by 10-15%, and permitting continuous operation at Mach 3.2. The name coined for this setup is *turbo-ramjet*.

Hydrogen fuelled air-breathing jet engines

Jet engines can be run on almost any fuel. Hydrogen is a highly desirable fuel, as, although the energy per mole is not unusually high, the molecule is very much lighter than other molecules. The energy per kg of hydrogen is twice that of more common fuels and this gives twice the specific impulse. In addition, jet engines running on hydrogen are quite easy to build—the first ever turbojet

was run on hydrogen. Also, although not duct engines, hydrogen-fueled rocket engines have seen extensive use.

However, in almost every other way, hydrogen is problematic. The downside of hydrogen is its density; in gaseous form the tanks are impractical for flight, but even in the form of liquid hydrogen it has a density one fourteenth that of water. It is also deeply cryogenic and requires very significant insulation that precludes it being stored in wings. The overall vehicle would end up being very large, and difficult for most airports to accommodate. Finally, pure hydrogen is not found in nature, and must be manufactured either via steam reforming or expensive electrolysis. Nevertheless, research is ongoing and hydrogen-fueled aircraft designs do exist that may be feasible.

Precooled jet engines

An idea originated by Robert P. Carmichael in 1955^[31] is that hydrogen-fueled engines could theoretically have much higher performance than hydrocarbon-fueled engines if a heat exchanger were used to cool the incoming air. The low temperature allows lighter materials to be used, a higher mass-flow through the engines, and permits combustors to inject more fuel without overheating the engine.

This idea leads to plausible designs like Reaction Engines SABRE, that might permit single-stage-to-orbit launch vehicles,^[32] and ATREX, which could permit jet engines to be used up to hypersonic speeds and high altitudes for boosters for launch vehicles. The idea is also being researched by the EU for a concept to achieve non-stop antipodal supersonic passenger travel at Mach 5 (Reaction Engines A2).

Nuclear-powered ramjet

Project Pluto was a nuclear-powered ramjet, intended for use in a cruise missile. Rather than combusting fuel as in regular jet engines, air was heated using a high-temperature, unshielded nuclear reactor. This dramatically increased the engine burn time, and the ramjet was predicted to be able to cover any required distance at supersonic speeds (Mach 3 at tree-top height).

However, there was no obvious way to stop it once it had taken off, which would be a great disadvantage in any non-disposable application. Also, because the reactor was unshielded, it was dangerous to be in or around the flight path of the vehicle (although the exhaust itself wasn't radioactive). These disadvantages limit the application to warhead delivery system for all-out nuclear war, which it was being designed for.

Scramjets

Scramjets are an evolution of ramjets that are able to operate at much higher speeds than any other kind of airbreathing engine. They share a similar structure with ramjets, being a specially-shaped tube that compresses air with no moving parts through ram-air compression. Scramjets, however, operate with supersonic airflow through the entire engine. Thus, scramjets do not have the diffuser required by ramjets to slow the incoming airflow to subsonic speeds.

Scramjets start working at speeds of at least Mach 4, and have a maximum useful speed of approximately Mach 17.^[33] Due to aerodynamic heating at these high speeds, cooling poses a challenge to engineers.

Environmental considerations

Jet engines are usually run on fossil fuel propellant, and in that case, are a net source of carbon to the atmosphere. Some scientists believe that jet engines are also a source of global dimming due to the water vapour in the exhaust causing cloud formations. Nitrogen compounds are also formed from the combustion process from atmospheric nitrogen. At low altitudes this is not thought to be especially harmful, but for supersonic aircraft that fly in the stratosphere some destruction of ozone may occur. Sulphates are also emitted if the fuel contains sulphur.

Safety and reliability

Jet engines are usually very reliable and have a very good safety record. However, failures do sometimes occur.

Compressor blade containment

The most likely failure is compressor blade failure, and modern jet engines are designed with structures that can catch these blades and keep them contained within the engine casing. Verification of a jet engine design involves testing that this system works correctly.

Bird strike

Bird strike is an aviation term for a collision between a bird and an aircraft. It is a common threat to aircraft safety and has caused a number of fatal accidents. In 1988 an Ethiopian Airlines Boeing 737 sucked pigeons into both engines during take-off and then crashed in an attempt to return to the Bahir Dar airport; of the 104 people aboard, 35 died and 21 were injured. In another incident in 1995, a Dassault Falcon 20 crashed at a Paris airport during an emergency landing attempt after sucking lapwings into an engine, which caused an engine failure and a fire in the airplane fuselage; all 10 people on board were killed. A US Airways Airbus A320 aircraft sucked in one bird in each engine. The plane landed in the Hudson River after taking off from LaGuardia International Airport in New York City. There were no fatalities.^[34]

Modern jet engines have the capability of surviving an ingestion of a bird. Small fast planes, such as military jet fighters, are at higher risk than big heavy multi-engine ones. This is due to the fact that the fan of a high-bypass turbofan engine, typical on transport aircraft, acts as a centrifugal separator to force ingested materials (birds, ice, etc.) to the outside of the fan's disc. As a result, such materials go through the relatively unobstructed bypass duct, rather than through the core of the engine, which contains the smaller and more delicate compressor blades. Military aircraft designed for high-speed flight typically have pure turbojet, or low-bypass turbofan engines, increasing the risk that ingested materials will get into the core of the engine to cause damage.

The highest risk of the bird strike is during the takeoff and landing, in low altitudes, which is in the vicinity of the airports.

Uncontained failures

One class of failures that has caused accidents in particular is uncontained failures, where rotary parts of the engine break off and exit through the case. These can cut fuel or control lines, and can penetrate the cabin. Although fuel and control lines are usually duplicated for reliability, the crash of United Airlines Flight 232 was caused when hydraulic fluid lines for all three independent hydraulic systems were simultaneously severed by shrapnel from an uncontained engine failure. Prior to the United 232 crash, the probability of a simultaneous failure of all three hydraulic systems was considered as high as a billion-to-one. However, the statistical models used to come up with this figure did not account for the fact that the number-two engine was mounted at the tail close to all the hydraulic lines, nor the possibility that an engine failure would release many fragments in many directions. Since then, more modern aircraft engine designs have focused on keeping shrapnel from penetrating the cowling or ductwork, and have increasingly utilized high-strength composite materials to achieve the required penetration resistance while keeping the weight low.

References

1. ^ Encyclopedia Britannica: Internal Combustion Engine
2. ^ How many air-miles are left in the world's fuel tank?
3. ^ U.S. Airlines: Operating in an Era of High Jet Fuel Prices
4. ^ propeller efficiency
5. ^ Patent number 554,906
6. ^ Gyorgy, Nagy Istvan, "Albert Fono: A Pioneer of Jet Propulsion", International Astronautical Congress, 1977, IAF/IAA
7. ^ Dugger, Gordon L. (1969). Ramjets. American Institute of Aeronautics and Astronautics, p. 15.
8. ^ Maxime Guillaume, "Propulseur par réaction sur l'air," French patent no. 534,801 (filed: 3 May 1921; issued: 13 January 1922). Available on-line (in French) at:
<http://v3.espacenet.com/origdoc?DB=EPODOC&IDX=FR534801&F=0&QPN=FR534801> .
9. ^ sod1280.tmp
10. ^ PBS - Chasing the Sun - Frank Whittle
11. ^ BBC - History - Frank Whittle (1907 - 1996)
12. ^ Frank Whittle, "Improvements relating to the propulsion of aircraft and other vehicles," British patent no. 347,206 (filed: 16 January 1930). Available on-line at:
<http://v3.espacenet.com/origdoc?DB=EPODOC&IDX=GB347206&F=0&QPN=GB347206> .
13. ^ The History of the Jet Engine - Sir Frank Whittle - Hans Von Ohain Ohain said that he had not read Whittle's patent and Whittle believed him (Frank Whittle 1907-1996) however the Whittle patent was in German libraries and Whittle's son had suspicions that Ohain had read or heard of it (The History of the Jet Engine - Sir Frank Whittle a genius betrayed -)
14. ^ ch10-3
15. ^ [1]
16. ^ ^{a b} [2]
17. ^ [3]
18. ^ [4]
19. ^ Merging Air and Space

20. ^ In Newtonian mechanics kinetic energy is frame dependent. The speed must be measured in the center of mass frame of the vehicle and less obviously its *reaction mass*, which it is typically in at take-off.
 21. ^ K.Honicke, R.Lindner, P.Anders, M.Krahl, H.Hadrich, K.Rohricht. Beschreibung der Konstruktion der Triebwerksanlagen. Interflug, Berlin, 1968
 22. ^ Rocket Propulsion elements- seventh edition, pg 37-38
 23. ^ ^{a b c} Data from: <http://adg.stanford.edu/aa241/propulsion/largefan.html>
 24. ^ http://www.faa.gov/about/office_org/headquarters_offices/AEP/supersonic_noise/media/1-Panel3-Brines_Smith-AADC.pdf
 25. ^ Aircraft: Lockheed SR-71A Blackbird
 26. ^ SSME
 27. ^ Astronautix NK-33 entry
 28. ^ High Speed Propulsion
 29. ^ SCRAMJET
 30. ^ J58
 31. ^ NASA history Other Interests in Hydrogen
 32. ^ The Skylon Spaceplane
 33. ^ Astronautix X30
 34. ^ Transport Canada - Sharing the Skies
- John Golley (1997). *Genesis of the Jet: Frank Whittle and the Invention of the Jet Engine*. Crowood Press. ISBN 1-85310-860-X.
 - David S Brooks (1997). *Vikings at Waterloo: Wartime Work on the Whittle Jet Engine by the Rover Company*. Rolls-Royce Heritage Trust. ISBN 1-872922-08-2

Mach wave

From Wikipedia, the free encyclopedia

In fluid dynamics, a **Mach wave** is a pressure wave traveling with the speed of sound caused by a slight change of pressure added to a compressible flow. These weak waves can combine in supersonic flow to become a shock wave if sufficient Mach waves are present at any location. Thus it is possible to have shockless compression or expansion in a supersonic flow by having the production of Mach waves sufficiently spaced (cf isentropic compression in supersonic flows). A Mach wave is the weak limit of an oblique shock wave (a normal shock is the other limit). They propagate across the flow at the **Mach angle** μ ^[1]:

$$\mu = \arcsin\left(\frac{1}{M}\right),$$

where M is the Mach number.

Mach waves can be used in schlieren or shadowgraph observations to determine the local Mach number of the flow. Early observations by Ernst Mach used grooves in the wall of a duct to produce Mach waves in a duct, which were then photographed by the schlieren method, to obtain data about the flow in nozzles and ducts.

References

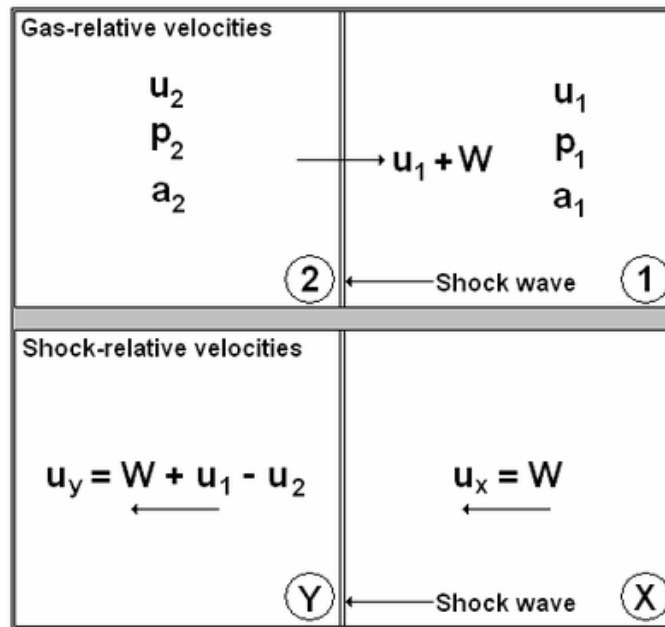
- [^] Mach angle at NASA

Moving Shock Wave

From Wikipedia, the free encyclopedia

In fluid dynamics, a **moving shock** is a shock wave that is traveling through a fluid (often gaseous) medium with a velocity relative to the velocity of the fluid already making up the medium. As such, the normal shock relations require modification to calculate the properties before and after the moving shock. A knowledge of moving shocks is important for studying the phenomena surrounding detonation, among other applications.

Theory



This diagram shows the gas-relative and shock-relative velocities used for the theoretical moving shock equations.

To derive the theoretical equations for a moving shock, one may start by denoting the region in front of the shock as subscript 1, with the subscript 2 defining the region behind the shock. This is shown in the figure, with the shock wave propagating to the right. The speed of the shock wave relative to the gas is W , making the total velocity equal to $u_1 + W$. Additionally, the pressure is denoted by p and the local speed of sound by a .

Next, suppose a reference frame is then fixed to the shock so it appears stationary as the gas in regions 1 and 2 move with a velocity relative to it. Redefining region 1 as x and region 2 as y leads to the following shock-relative velocities:

$$\begin{aligned} u_y &= W + u_1 - u_2, \\ u_x &= W. \end{aligned}$$

With these shock-relative velocities, the properties of the regions before and after the shock can be defined below introducing the temperature as T , the density as ρ , and the Mach number as M :

$$\begin{aligned} p_1 &= p_x \quad ; \quad p_2 = p_y \quad ; \quad T_1 = T_x \quad ; \quad T_2 = T_y, \\ \rho_1 &= \rho_x \quad ; \quad \rho_2 = \rho_y \quad ; \quad a_1 = a_x \quad ; \quad a_2 = a_y, \\ M_x &= \frac{u_x}{a_x} = \frac{W}{a_1}, \\ M_y &= \frac{u_y}{a_y} = \frac{W + u_1 - u_2}{a_2}. \end{aligned}$$

Introducing the heat capacity ratio as γ , the speed of sound, density, and pressure ratios can be derived:

$$\begin{aligned} \frac{a_2}{a_1} &= \sqrt{1 + \frac{2(\gamma - 1)}{(\gamma + 1)^2} \left[\gamma M_x^2 - \frac{1}{M_x^2} - (\gamma - 1) \right]}, \\ \frac{\rho_2}{\rho_1} &= \frac{1}{1 - \frac{2}{\gamma + 1} \left[1 - \frac{1}{M_x^2} \right]}, \\ \frac{p_2}{p_1} &= 1 + \frac{2\gamma}{\gamma + 1} \left[M_x^2 - 1 \right]. \end{aligned}$$

One must keep in mind that the above equations are for a shock wave moving towards the right. For a shock moving towards the left, the x and y subscripts must be switched and:

$$\begin{aligned} u_y &= W - u_1 + u_2, \\ M_y &= \frac{W - u_1 + u_2}{a_2}. \end{aligned}$$

References

Shapiro, Ascher H., *Dynamics and Thermodynamics of Compressible Fluid Flow*, Krieger Pub. Co; Reprint ed., with corrections (June 1983), ISBN 0898745667.

Oblique Shock Wave

From Wikipedia, the free encyclopedia

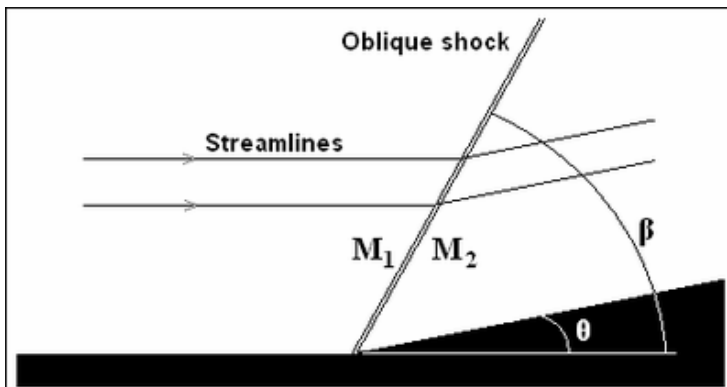


A small scale X-15 placed in a NASA supersonic wind tunnel produces an oblique shock wave at the nose of the model (along with other shocks).

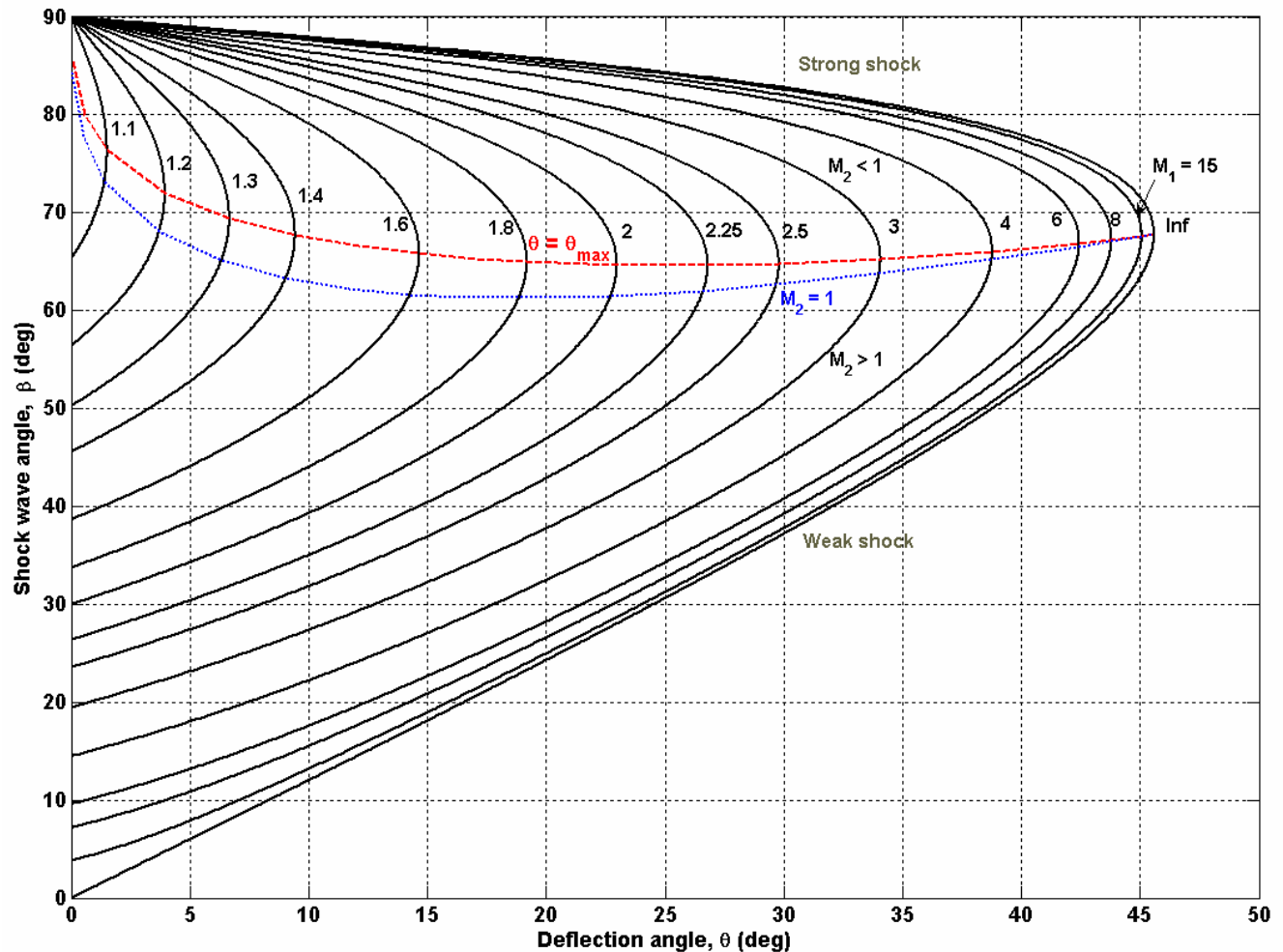
An **oblique shock** wave, unlike a normal shock, is inclined with respect to the incident upstream flow direction. It will occur when a supersonic flow encounters a corner that effectively turns the flow into itself and compresses. The upstream streamlines are uniformly deflected after the shock wave. The most common way to produce an oblique shock wave is to place a wedge into supersonic, compressible flow. Similar to a normal shock wave, the oblique shock wave consists of a very thin region across which nearly discontinuous changes in the thermodynamic properties of a gas occur. While the upstream and downstream flow directions are unchanged across a normal shock, they are different for flow across an oblique shock wave.

It is always possible to convert an oblique shock into a normal shock by a Galilean transformation.

Oblique Shock Wave Theory



Supersonic flow encounters a wedge and is uniformly deflected forming an oblique shock.



This chart shows the oblique shock angle, β , as a function of the corner angle, θ , for a few constant M_1 lines. The blue line separates the strong and weak solutions.

For a given Mach number, M_1 , and corner angle, θ , the oblique shock angle, β , and the downstream Mach number, M_2 , can be calculated. M_2 is always less than M_1 . Unlike after a normal shock, M_2 can still be supersonic. Discontinuous changes also occur in the pressure, density and temperature, which all rise downstream of the oblique shock wave.

Using the continuity equation and the fact that the tangential velocity component does not change across the shock, trigonometric relations eventually lead to the θ - β - M equation which shows θ as a function of M_1 and β . It is more intuitive to want to solve for β as a function of M_1 and θ , but this approach is more complicated, the results of which are often contained in tables or calculated through an applet.

$$\tan \theta = 2 \cot \beta \frac{M_1^2 \sin^2 \beta - 1}{M_1^2 (\gamma + \cos 2\beta) + 2}$$

Within the θ - β - M equation, a maximum corner angle, θ_{MAX} , exists for any upstream Mach number. When $\theta > \theta_{MAX}$, the oblique shock wave is no longer attached to the corner and is replaced by a detached bow shock. A θ - β - M diagram, common in most compressible flow textbooks, shows a

series of curves that will indicate θ_{MAX} for each Mach number. The θ - β -M relationship will produce two β angles for a given θ and M_1 , with the larger angle called a strong shock and the smaller called a weak shock. The weak shock is almost always seen experimentally.

The rise in pressure, density, and temperature after an oblique shock can be calculated as follows:

$$\frac{p_2}{p_1} = 1 + \frac{2\gamma}{\gamma + 1}(M_1^2 \sin^2 \beta - 1)$$

$$\frac{\rho_2}{\rho_1} = \frac{(\gamma + 1)M_1^2 \sin^2 \beta}{(\gamma - 1)M_1^2 \sin^2 \beta + 2}$$

$$\frac{T_2}{T_1} = \frac{p_2 \rho_1}{p_1 \rho_2}.$$

M_2 is solved for as follows:

$$M_2 = \frac{1}{\sin(\beta - \theta)} \sqrt{\frac{1 + \frac{\gamma-1}{2}M_1^2 \sin^2 \beta}{\gamma M_1^2 \sin^2 \beta - \frac{\gamma-1}{2}}}.$$

Oblique Shock Wave Applications

Oblique shock waves are used predominantly in engineering applications when compared with normal shock waves. This can be attributed to the fact that using one or a combination of oblique shock waves results in more favorable post-shock conditions (lower post-shock temperature, etc.) when compared to utilizing a single normal shock. An example of this technique can be seen in the design of supersonic aircraft engine inlets, which are wedge-shaped to compress air flow into the combustion chamber while minimizing thermodynamic losses. Early supersonic aircraft jet engine inlets were designed using compression from a single normal shock, but this approach caps the maximum achievable Mach number to roughly 1.6. The wedge-shaped inlets are clearly visible on the sides of the F-14 Tomcat, which has a maximum speed of Mach 2.34.

Many supersonic aircraft wings are designed around a thin diamond shape. Placing a diamond-shaped object at an angle of attack relative to the supersonic flow streamlines will result in two oblique shocks propagating from the front tip over the top and bottom of the wing, with Prandtl-Meyer expansion fans created at the two corners of the diamond closest to the front tip. When correctly designed, this generates lift.

Oblique Shock Waves and the Hypersonic Limit

As the Mach number of the upstream flow becomes hypersonic, the equations for the pressure, density, and temperature after the oblique shock wave reach a mathematical limit. The pressure and density ratios can then be expressed as:

$$\frac{p_2}{p_1} \approx \frac{2\gamma}{\gamma + 1} M_1^2 \sin^2 \beta$$

$$\frac{\rho_2}{\rho_1} \approx \frac{\gamma + 1}{\gamma - 1}.$$

For a perfect atmospheric gas approximation using $\gamma = 1.4$, the hypersonic limit for the density ratio is 6. However, hypersonic post-shock dissociation of O_2 and N_2 into O and N lowers γ , allowing for higher density ratios in nature. The hypersonic temperature ratio is:

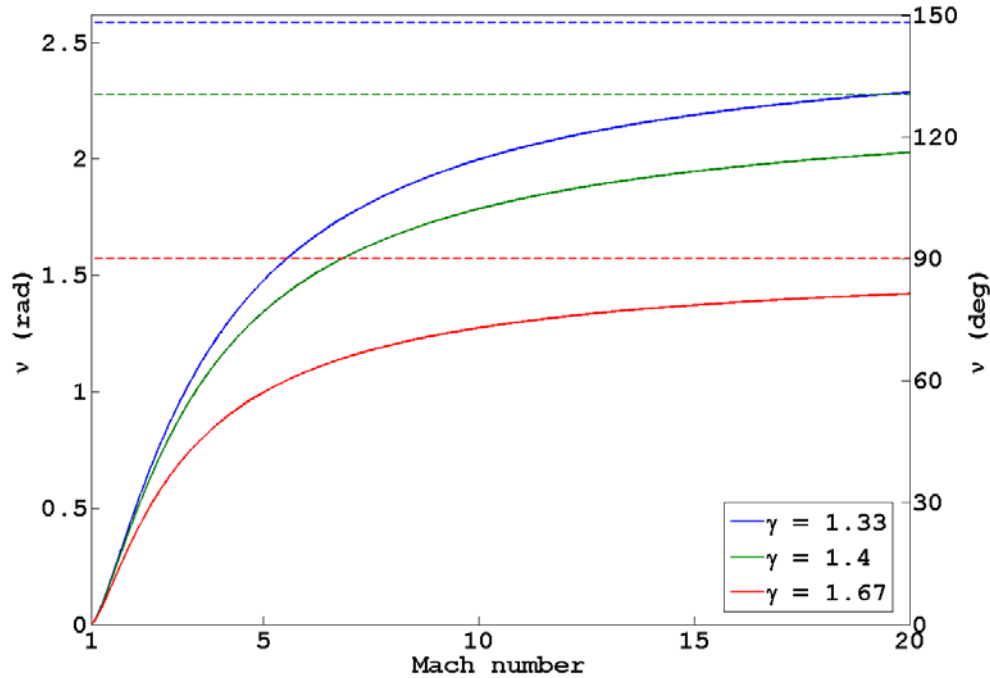
$$\frac{T_2}{T_1} \approx \frac{2\gamma(\gamma - 1)}{(\gamma + 1)^2} M_1^2 \sin^2 \beta.$$

References

- Liepmann, Hans W.; Roshko, A. (2001) [1957]. *Elements of Gasdynamics*. Dover Publications. ISBN 0-486-41963-0.
- Anderson, John D. Jr. (January 2001) [1984]. *Fundamentals of Aerodynamics* (3rd Edition ed.). McGraw-Hill Science/Engineering/Math. ISBN 0-07-237335-0.
- Shapiro, Ascher H.. *The Dynamics and Thermodynamics of Compressible Fluid Flow, Volume 1*. Ronald Press. ISBN 978-0-471-06691-0.

Prandtl–Meyer Function

From Wikipedia, the free encyclopedia



Variation in the Prandtl–Meyer function (ν) with Mach number (M) and ratio of specific heat capacity (γ). The dashed lines show the limiting value ν_{\max} as Mach number tends to infinity.

Prandtl–Meyer function describes the angle through which a flow can turn isentropically for the given initial and final Mach number. It is the maximum angle through which a sonic ($M = 1$) flow can be turned around a convex corner. For an ideal gas, it is expressed as follows,

$$\begin{aligned}\nu(M) &= \int \frac{\sqrt{M^2 - 1}}{1 + \frac{\gamma-1}{2}M^2} \frac{dM}{M} \\ &= \sqrt{\frac{\gamma+1}{\gamma-1}} \cdot \arctan \sqrt{\frac{\gamma-1}{\gamma+1}(M^2 - 1)} - \arctan \sqrt{M^2 - 1}\end{aligned}$$

where, ν is the Prandtl–Meyer function, M is the Mach number of the flow and γ is the ratio of the specific heat capacities.

By convention, the constant of integration is selected such that $\nu(1) = 0$.

As Mach number varies from 1 to ∞ , ν takes values from 0 to ν_{\max} , where

$$\nu_{\max} = \frac{\pi}{2} \left(\sqrt{\frac{\gamma+1}{\gamma-1}} - 1 \right)$$

For isentropic expansion, $\nu(M_2) = \nu(M_1) + \theta$

For isentropic compression, $\nu(M_2) = \nu(M_1) - \theta$

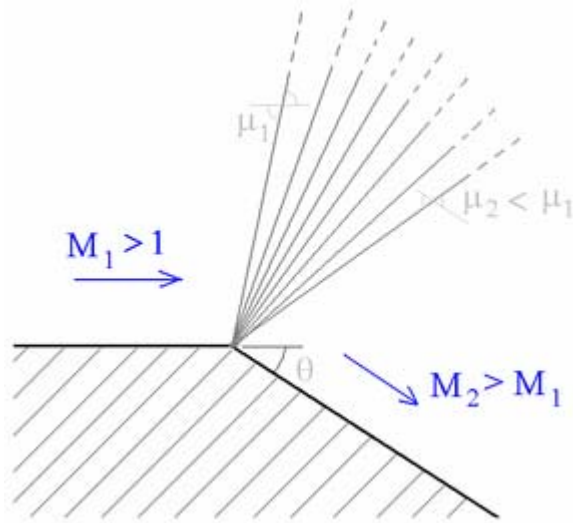
where, θ is the absolute value of the angle through which the flow turns, M is the flow Mach number and the suffixes "1" and "2" denote the initial and final conditions respectively.

References

- Liepmann, Hans W.; Roshko, A. (2001) [1957]. *Elements of Gasdynamics*. Dover Publications. ISBN 0-486-41963-0.

Prandtl–Meyer Expansion Fan

From Wikipedia, the free encyclopedia



When a supersonic flow encounters a convex corner, it forms an expansion fan, which consist of an infinite number of expansion waves centered at the corner. The figure shows one such ideal expansion fan.

A **Prandtl-Meyer expansion fan** is a centered expansion process, which turns a supersonic flow around a convex corner. The fan consists of an infinite number of Mach waves, diverging from a sharp corner. In case of a smooth corner, these waves can be extended backwards to meet at a point. Each wave in the expansion fan turns the flow gradually (in small steps). It is physically impossible to turn the flow away from itself through a single "shock" wave because it will violate the second law of thermodynamics.^[1] Across the expansion fan, the flow accelerates (velocity increases) and the Mach number increases, while the static pressure, temperature and density decrease. Since the process is isentropic, the stagnation properties remain constant across the fan.

Flow properties

The expansion fan consists of infinite number of expansion waves or Mach lines.^[2] The first Mach

line is at an angle $\mu_1 = \arcsin\left(\frac{1}{M_1}\right)$ with respect to the flow direction and the last Mach line is

at an angle $\mu_2 = \arcsin\left(\frac{1}{M_2}\right)$ with respect to final flow direction. Since the flow turns in small angles and the changes across each expansion wave are small, the whole process is isentropic.^[1]

This simplifies the calculations of the flow properties significantly. Since the flow is isentropic, the stagnation properties like stagnation pressure (p_0), stagnation temperature (T_0) and stagnation density (ρ_0) remain constant. The final static properties are a function of the final flow Mach number (M_2) and can be related to the initial flow conditions as follows,

$$\begin{aligned}\frac{T_2}{T_1} &= \left(\frac{1 + \frac{\gamma-1}{2} M_1^2}{1 + \frac{\gamma-1}{2} M_2^2} \right) \\ \frac{p_2}{p_1} &= \left(\frac{1 + \frac{\gamma-1}{2} M_1^2}{1 + \frac{\gamma-1}{2} M_2^2} \right)^{\gamma/(\gamma-1)} \\ \frac{\rho_2}{\rho_1} &= \left(\frac{1 + \frac{\gamma-1}{2} M_1^2}{1 + \frac{\gamma-1}{2} M_2^2} \right)^{1/(\gamma-1)}.\end{aligned}$$

The Mach number after the turn (M_2) is related to the initial Mach number (M_1) and the turn angle (θ) by,

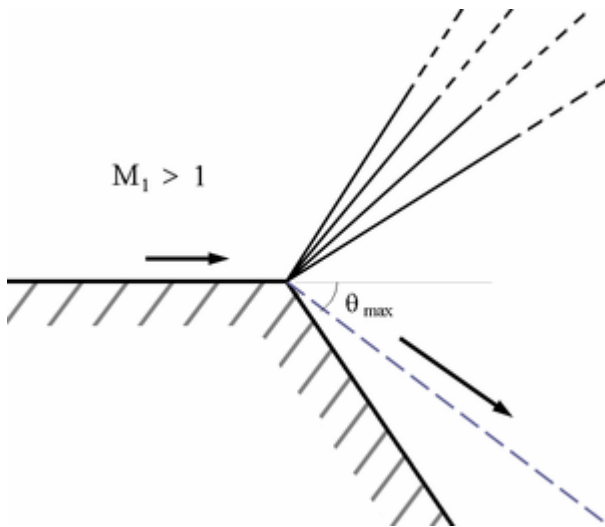
$$\theta = \nu(M_2) - \nu(M_1)$$

where, $\nu(M)$ is the Prandtl-Meyer function. This function determines the angle through which a sonic flow ($M = 1$) must turn to reach a particular Mach number (M). Mathematically,

$$\begin{aligned}\nu(M) &= \int \frac{\sqrt{M^2 - 1}}{1 + \frac{\gamma-1}{2} M^2} \frac{dM}{M} \\ &= \sqrt{\frac{\gamma+1}{\gamma-1}} \cdot \arctan \sqrt{\frac{\gamma-1}{\gamma+1} (M^2 - 1)} - \arctan \sqrt{M^2 - 1}.\end{aligned}$$

By convention, $\nu(1) = 0$. Thus, given the initial Mach number (M_1), one can calculate $\nu(M_1)$ and using the turn angle find $\nu(M_2)$. From the value of $\nu(M_2)$ one can obtain the final Mach number (M_2) and the other flow properties.

Maximum turn angle



There is a limit on the maximum angle (θ_{max}) through which a supersonic flow can turn.

As Mach number varies from 1 to ∞ , ν takes values from 0 to ν_{\max} , where

$$\nu_{\max} = \frac{\pi}{2} \left(\sqrt{\frac{\gamma+1}{\gamma-1}} - 1 \right).$$

This places a limit on how much a supersonic flow can turn through, with the maximum turn angle given by,

$$\theta_{\max} = \nu_{\max} - \nu(M_1).$$

One can also look at it as follows. A flow has to turn so that it can satisfy the boundary conditions. In an ideal flow, there are two kinds of boundary condition that the flow has to satisfy,

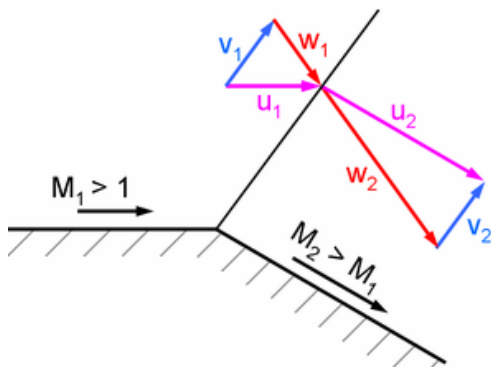
1. Velocity boundary condition, which dictates that the component of the flow velocity normal to the wall be zero. It is also known as no-penetration boundary condition.
2. Pressure boundary condition, which states that there cannot be a discontinuity in the static pressure inside the flow (since there are no shocks in the flow).

If the flow turns enough so that it becomes parallel to the wall, we do not need to worry about this boundary condition. However, as the flow turns, its static pressure decreases (as described earlier). If there is not enough pressure to start with, the flow won't be able to complete the turn and will not be parallel to the wall. This shows up as the maximum angle through which a flow can turn. The lower the Mach number is to start with (i.e. small M_1), the greater the maximum angle through which the flow can turn.

The streamline which separates the final flow direction and the wall is known as a **slipstream** (shown as the dashed line in the figure). Across this line there is a jump in the temperature, density and tangential component of the velocity (normal component being zero). Beyond the slipstream the flow is stagnant (which automatically satisfies the velocity boundary condition at the wall). In case of real flow, a shear layer is observed instead of a slipstream, because of the additional no-slip boundary condition.

Notes

1. $\wedge a b$



An expansion process through a single "shock" is impossible, because it will violate the second law of thermodynamics.

Impossibility of expanding a flow through a single "shock" wave:

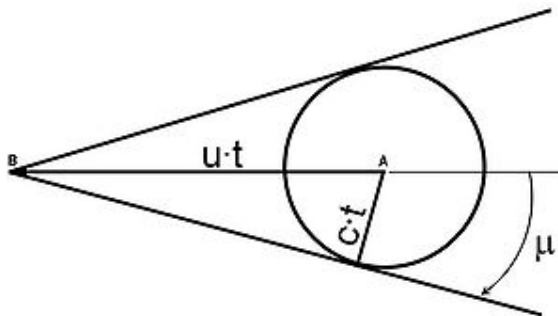
Consider the scenario shown in the adjacent figure. As a supersonic flow turns, the normal component of the velocity increases ($w_2 > w_1$), while the tangential component remains constant ($v_2 = v_1$). The corresponding change in the entropy ($\Delta s = s_2 - s_1$) can be expressed as follows,

$$\begin{aligned}\frac{\Delta s}{R} &= \ln \left[\left(\frac{p_2}{p_1} \right)^{1/(\gamma-1)} \left(\frac{\rho_2}{\rho_1} \right)^{-\gamma/(\gamma-1)} \right] \\ &\approx \frac{\gamma+1}{12\gamma^2} \left(\frac{p_2 - p_1}{p_1} \right)^3 \\ &\approx \frac{\gamma+1}{12\gamma^2} \left[\frac{\rho_1 w_1^2}{p_1} \left(1 - \frac{w_2}{w_1} \right) \right]^3\end{aligned}$$

where, R is the universal gas constant, γ is the ratio of specific heat capacities, ρ is the static density, p is the static pressure, s is the static entropy, and w is the component of flow velocity normal to the "shock". The suffix "1" and "2" refer to the initial and final conditions respectively.

Since $w_2 > w_1$, this would mean that $\Delta s < 0$. Since this is not possible it means that it is impossible to turn a flow through a single shock wave. The argument may be further extended to show that such an expansion process can occur only if we consider a turn through infinite number of expansion waves in the limit $\Delta s \rightarrow 0$. Accordingly an expansion process is an isentropic process.

2. ^



For an object moving at supersonic speeds ($u > c$) as it moves from point A to B (distance $u \cdot t$), the disturbances originating from point A travel a distance $c \cdot t$. The corresponding angle is known as Mach angle and the lines enclosing the disturbed region are known as Mach lines (in 2-D case) or Mach cone (in 3-D).

Mach lines (cone) and Mach angle:

Mach lines are a concept usually encountered in 2-D supersonic flows (i.e. $M \geq 1$). They are a pair of bounding lines which separate the region of disturbed flow from the undisturbed part of the flow. These lines occur in pair and are oriented at an angle

$$\mu = \arcsin\left(\frac{c}{u}\right) = \arcsin\left(\frac{1}{M}\right)$$

with respect to the direction of motion (also known as the **Mach angle**). In case of 3-D flow field these lines form a surface known as **Mach cone**, with Mach angle as the half angle of the cone.

To understand the concept better, consider the case sketched in the figure. We know that when an object moves in a flow, it causes pressure disturbances (which travel at the speed of sound, also known as Mach waves). The figure shows an object moving from point A to B along the line AB at supersonic speeds ($u > c$). By the time the object reaches point B, the pressure disturbances from point A have traveled a distance $c \cdot t$ and are now at circumference of the circle (with center at point A). There are infinite such circles with their center on the line AB, each representing the location of the disturbances due to the motion of the object. The lines propagating outwards from point B and tangent to all these circles are known as Mach lines.

Note: These concepts have a physical meaning only for supersonic flows ($u \geq c$). In case of subsonic flows the disturbances will travel faster than the source and the argument of the $\arcsin()$ function will be greater than one.

References

- Liepmann, Hans W.; Roshko, A. (2001) [1957]. *Elements of Gasdynamics*. Dover Publications. ISBN 0-486-41963-0.
- Anderson, John D. Jr. (January 2001) [1984]. *Fundamentals of Aerodynamics* (3rd Edition ed.). McGraw-Hill Science/Engineering/Math. ISBN 0-07-237335-0.
- Shapiro, Ascher H.. *The Dynamics and Thermodynamics of Compressible Fluid Flow, Volume 1*. Ronald Press. ISBN 978-0-471-06691-0.

Real Gas

From Wikipedia, the free encyclopedia

Real gas, as opposed to a Perfect or Ideal Gas, effects refers to an assumption base where the following are taken into account:

- Compressibility effects
- Variable heat capacity
- Van der Waals forces
- Non-equilibrium thermodynamic effects
- Issues with molecular dissociation and elementary reactions with variable composition.

For most applications, such a detailed analysis is "over-kill" and the ideal gas approximation is used. Real-gas models have to be used near condensation point of gases, near critical point, at very high pressures, and in several other less usual cases.

Modelisation

Van der Waals modelisation

Real gases are often modeled by taking into account their molar weight and molar volume

$$RT = (P + \frac{a}{V_m^2})(V_m - b)$$

Where P is the pressure, T is the temperature, R the ideal gas constant, and V_m the molar volume. a and b are parameters that are determined empirically for each gas, but are sometimes estimated from their critical temperature (T_c) and critical pressure (P_c) using these relations:

$$a = \frac{27R^2T_c^2}{64P_c}$$

$$b = \frac{RT_c}{8P_c}$$

Redlich–Kwong modelisation

The Redlich–Kwong equation is another two-parameters equation that is used to modelize real gases. It is almost always more accurate than the Van der Waals equation, and often more accurate than some equation with more than two parameters. The equation is

$$RT = P + \frac{a}{V_m(V_m + b)T^{\frac{1}{2}}}(V_m - b)$$

where a and b two empirical parameters that are **not** the same parameters as in the Van der Waals equation.

Berthelot and modified Berthelot modelisation

The Berthelot Equation is very rarely used,

$$P = \frac{RT}{V - b} - \frac{a}{TV^2}$$

but the modified version is somewhat more accurate

$$P = \frac{RT}{V} \left(1 + \frac{9PT_c}{128P_cT} \frac{(1 - 6T_c^2)}{T^2} \right)$$

Dieterici modelisation

This modelisation fell out of usage in recent years

$$P = RT \frac{\exp\left(\frac{-a}{V_m RT}\right)}{V_m - b}$$

Clausius modelisation

The Clausius equation is a very simple three-parameter equation used to model gases.

$$RT = \left(P + \frac{a}{T(V_m + c)^2} \right) (V_m - b)$$

where

$$a = \frac{V_c - RT_c}{4P_c}$$

$$b = \frac{3RT_c}{8P_c} - V_c$$

$$c = \frac{27R^2T_c^3}{64P_c}$$

Virial Modelisation

The Virial equation derives from a perturbative treatment of statistical mechanics.

$$PV_m = RT \left(1 + \frac{B(T)}{V_m} + \frac{C(T)}{V_m^2} + \frac{D(T)}{V_m^3} + \dots \right)$$

or alternatively

$$PV_m = RT \left(1 + \frac{B'(T)}{P} + \frac{C'(T)}{P^2} + \frac{D'(T)}{P^3} + \dots \right)$$

where A, B, C, A', B', and C' are temperature dependent constants.

Peng-Robinson Modelisation

This two parameter equation has the interesting property being useful in modeling some liquids as well as real gases.

$$P = \frac{RT}{V_m - b} - \frac{a(T)}{V_m(V_m + b) + b(V_m - b)}$$

Wohl modelisation

The Wohl equation is formulated in terms of critical values, making it useful when real gas constants are not available.

$$RT = \left(P + \frac{a}{TV_m(V_m - b)} - \frac{c}{T^2V_m^3} \right) (V_m - b)$$

where

$$a = 6P_cT_cV_c^2$$

$$b = \frac{V_c}{4}$$

$$c = 4P_cT_c^2V_c^3$$

Beattie-Bridgeman Modelisation

The Beattie-Bridgeman equation

$$P = RTd + (BRT - A - \frac{Rc}{T^2})d^2 + (-BbRT + Aa - \frac{RBc}{T^2})d^3 + \frac{RBbcd^4}{T^2}$$

where d is the molal density and a, b, c, A, and B are empirical parameters.

Benedict-Webb-Rubin Modelisation

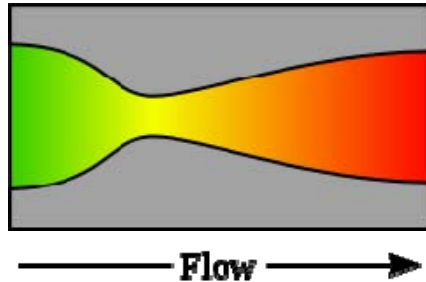
The BWR equation, sometimes referred to as the BWRS equation

$$P = RTd + d^2 \left(RT(B + bd) - (A + ad - a\alpha d^4) - \frac{1}{T^2} [C - cd(1 + \gamma d^2) \exp(-\gamma d^2)] \right)$$

Where d is the molal density and where a, b, c, A, B, C, α , and γ are empirical constants.

Rocket Engine Nozzle

From Wikipedia, the free encyclopedia



A de Laval nozzle, showing approximate flow velocity increasing from green to red in the direction of flow

A **rocket engine nozzle** is a propelling nozzle usually of the de Laval type used in a rocket engine to expand and accelerate the combustion gases, from burning propellants, so that the exhaust gases exit the nozzle at hypersonic velocities.

History

The de Laval nozzle was first used in an early rocket engine developed by Robert Goddard, one of the fathers of modern rocketry. Subsequently, almost all rocket engines used this idea, including Walter Thiel's implementation which made possible Germany's V2 rocket.

Atmospheric use

The optimal size of a rocket engine nozzle to be used within the atmosphere is when the exit pressure equals ambient pressure, which decreases with altitude. For rockets travelling from the Earth to orbit, a simple nozzle design is only optimal at one altitude, losing efficiency and wasting fuel at other altitudes.

If the pressure of the jet leaving the nozzle is above ambient pressure then a nozzle is said to be 'underexpanded'; if the jet is below ambient pressure then it is 'overexpanded'.

Slight overexpansion causes a slight reduction in efficiency, but otherwise does little harm. However, if the jet pressure is approximately 40 percent of ambient then 'flow separation' occurs. This can cause jet instabilities that can cause damage to the nozzle or simply cause control difficulties of the vehicle or the engine.

In some cases it is desirable for reliability and safety reasons to ignite a rocket engine on the ground that will be used all the way to orbit. In most cases the optimal pressure is ambient, however if most of the thrust comes from (ambient pressure) boosters at takeoff, then the trades push to using an overexpanded nozzle. This is the technique used on the Space shuttle's main engines.

Vacuum use

For nozzles that are used in vacuum or at very high altitude, it is impossible to match ambient pressure and rather larger area ratio nozzles are usually more efficient. However, a very long nozzle has significant mass and a length that optimises overall vehicle performance can always be found.

Additionally, as the temperature of the gas in the nozzle decreases some components of the exhaust gases (such as water vapour from the combustion process) may liquefy or even freeze. This is highly undesirable and needs to be avoided.

Magnetic nozzles have been proposed for some types of propulsion (for example VASIMR), in which the flow of plasma or ions are directed by magnetic fields instead of walls made of solid materials. These can be advantageous since a magnetic field itself cannot melt and the plasma can be at millions of kelvins. But there are often thermal problems in the coils, particularly if superconducting coils are used to form the throat and expansion fields.

1-D Analysis of gas flow in rocket engine nozzles

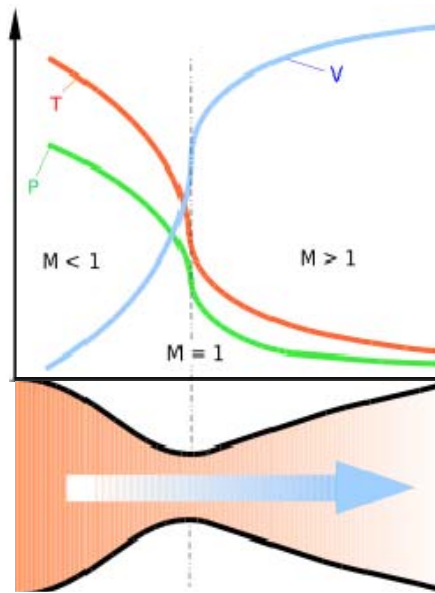


Diagram of a de Laval nozzle, showing flow velocity (v) increasing in the direction of flow, with decreases in temperature (t) and pressure (p). The Mach number (M) increases from subsonic, to sonic at the throat, to supersonic.

The analysis of gas flow through de Laval nozzles involves a number of concepts and assumptions:

- For simplicity, the combustion gas is assumed to be an ideal gas.
- The gas flow is isentropic (i.e., at constant entropy), frictionless, and adiabatic (i.e., there is little or no heat gained or lost)
- The gas flow is constant (i.e., steady) during the period of the propellant burn.
- The gas flow is along a straight line from gas inlet to exhaust gas exit (i.e., along the nozzle's axis of symmetry)
- The gas flow behavior is compressible since the flow is at very high velocities.

As the combustion gas enters the rocket nozzle, it is traveling at subsonic velocities. As the throat contracts down the gas is forced to accelerate until at the nozzle throat, where the cross-sectional area is the smallest, the linear velocity becomes sonic. From the throat the cross-sectional area then increases, the gas expands and the linear velocity becomes progressively more supersonic.

The linear velocity of the exiting exhaust gases can be calculated using the following equation
[1][2][3]

$$V_e = \sqrt{\frac{T}{M} \cdot \frac{R}{k-1} \cdot \left[1 - (P_e/P)^{(k-1)/k} \right]}$$

where:

V_e = Exhaust velocity at nozzle exit, m/s

T = absolute temperature of inlet gas, K

R = Universal gas law constant = 8314.5 J/(kmol·K)

M = the gas molecular mass, kg/kmol (also known as the molecular weight)

$k = c_p / c_v$ = isentropic expansion factor

c_p = specific heat of the gas at constant pressure

c_v = specific heat of the gas at constant volume

P_e = absolute pressure of exhaust gas at nozzle exit, Pa

P = absolute pressure of inlet gas, Pa

Some typical values of the exhaust gas velocity V_e for rocket engines burning various propellants are:

- 1.7 to 2.9 km/s (3800 to 6500 mi/h) for liquid monopropellants
- 2.9 to 4.5 km/s (6500 to 10100 mi/h) for liquid bipropellants
- 2.1 to 3.2 km/s (4700 to 7200 mi/h) for solid propellants

As a note of interest, V_e is sometimes referred to as the *ideal exhaust gas velocity* because it is based on the assumption that the exhaust gas behaves as an ideal gas.

As an example calculation using the above equation, assume that the propellant combustion gases are: at an absolute pressure entering the nozzle of $P = 7.0$ MPa and exit the rocket exhaust at an absolute pressure of $P_e = 0.1$ MPa; at an absolute temperature of $T = 3500$ K; with an isentropic expansion factor of $k = 1.22$ and a molar mass of $M = 22$ kg/kmol. Using those values in the above equation yields an exhaust velocity $V_e = 2802$ m/s or 2.80 km/s which is consistent with above typical values.

The technical literature can be very confusing because many authors fail to explain whether they are using the universal gas law constant R which applies to any ideal gas or whether they are using the gas law constant R_s which only applies to a specific individual gas. The relationship between the two constants is $R_s = R/M$.

Specific Impulse

Thrust is the force which moves a rocket through the air, and through space. Thrust is generated by the propulsion system of the rocket through the application of Newton's third law of motion: "For

every action there is an equal and opposite reaction". A gas or working fluid is accelerated out the rear of the rocket engine nozzle and the rocket is accelerated in the opposite direction. The thrust of a rocket engine nozzle can be defined as:^{[1][2][4][5]}

$$\begin{aligned} F &= \dot{m} V_e + (P_e - P_o) A_e \\ &= \dot{m} \left[V_e + \left(\frac{P_e - P_o}{\dot{m}} \right) A_e \right] \end{aligned}$$

and for perfectly expanded nozzles, this reduces to:

$$F = \dot{m} V_{eq}$$

The specific impulse, I_{sp} , is the ratio of the amount of thrust produced to the weight flow of the propellants. It is a measure of the fuel efficiency of a rocket engine. It can be obtained from:^[6]

$$I_{sp} = \frac{F}{\dot{m} g_o} = \frac{\dot{m} V_{eq}}{\dot{m} g_o} = \frac{V_{eq}}{g_o}$$

where:

F = gross rocket engine thrust, N

\dot{m} = mass flow rate of exhaust gas, kg/s

V_e = exhaust gas velocity at nozzle exit, m/s

P_e = exhaust gas pressure at nozzle exit, Pa

P_o = external ambient pressure, Pa (also known as free stream pressure)

A_e = cross-sectional area of nozzle exhaust exit, m²

V_{eq} = equivalent (or effective) exhaust gas velocity at nozzle exit, m/s

I_{sp} = specific impulse, s

g_o = Gravitational acceleration at sea level on Earth = 9.807 m/s²

In certain cases, where P_e equals P_o , then:

$$I_{sp} = \frac{F}{\dot{m} g_o} = \frac{\dot{m} V_e}{\dot{m} g_o} = \frac{V_e}{g_o}$$

In cases where this may not be the case since for a rocket nozzle P_e is proportional to \dot{m} , then it is possible to define a constant quantity which is the vacuum $I_{sp}(vac)$ for any given engine thus:

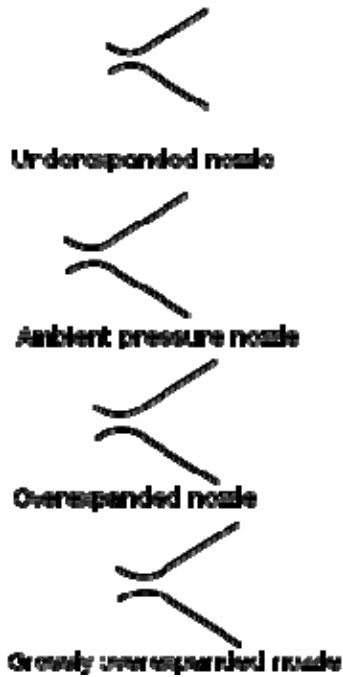
$$I_{sp}(vac) = \frac{V_e}{g_o} + \frac{P_e A_e}{\dot{m} g_o}$$

and hence:

$$F = I_{sp}(vac) g_o \dot{m} - A_e P_o$$

which is simply the vacuum thrust minus the force of the ambient atmospheric pressure acting over the exit plane.

Essentially then, for rocket nozzles, the ambient pressure acting over the engine largely cancels but effectively acts over the exit plane of the rocket engine in a rearward direction, while the exhaust jet generates forward thrust.



Nozzles can be underexpanded, ambient or overexpanded. If under or overexpanded then loss of efficiency occurs. Grossly overexpanded nozzles have improved efficiency, but the exhaust jet is unstable.^[7]

Aerostatic back-pressure and optimum expansion

As the gas travels down the expansion part of the nozzle the pressure and temperature decreases and the speed of the gas increases.

The supersonic nature of the exhaust jet means that the pressure of the exhaust can be significantly different from ambient pressure- the outside air is unable to equalize the pressure upstream due to the very high jet velocity. Therefore, for supersonic nozzles, it is actually possible for the pressure of the gas exiting the nozzle to go significantly below or very greatly above ambient pressure.

If the exit pressure is too low, then the jet can separate from the nozzle. This is often unstable and the jet will generally cause large off-axis thrusts, and may mechanically damage the nozzle.

This separation generally occurs if the exit pressure goes below roughly 30-45% of ambient, but may be delayed to far lower pressures if the nozzle is designed to increase the pressure at the rim, as is achieved with the SSME (1-2 psi at 15 psi ambient).^[8]

Other things also very modestly affect the efficiency of a rocket nozzle, it's important that the throat be a smooth radius, the angle of the narrowing down to the throat also has a very slight affect on the overall efficiency, but this is small. The exit of the nozzle needs to be as sharp as possible to minimize the chances of separation problems at low exit pressures.

Advanced designs

A number of more sophisticated designs have been proposed and they can be categorised by the method with which they achieve altitude compensation.

Nozzles with an atmospheric boundary include:

- the expansion-deflection nozzle^[9],
- the plug nozzle and
- the aerospike^{[9] [10]}.

Each of these allows the supersonic flow to adapt to the ambient pressure by expanding or contracting, thereby changing the exit ratio so that it is at (or near) optimal exit pressure for the corresponding altitude. The plug and aerospike nozzles are very similar in that they are radial in-flow designs but plug nozzles feature a solid centrebody (sometimes truncated) and aerospike nozzles have a 'base-bleed' of gases to simulate a solid centre-body. ED nozzles are radial out-flow nozzles with the flow deflected by a centre pintle.

Controlled flow-separation nozzles include:

- the expanding nozzle,
- bell nozzles with a removable insert and
- the Stepped nozzles or dual-bell nozzles^[11].

These are generally very similar to bell nozzles but include an insert or mechanism by which the exit area ratio can be increased as ambient pressure is reduced.

Dual-mode nozzles include:

- the dual-expander nozzle and
- the dual-throat nozzle.

These have either two throats or two thrust chamber (with corresponding throats). The central throat is of a standard design but it is surrounded by an annular throat which exhausts gases from the same (dual-throat) or a separate (dual-expander) thrust chamber. Both throats would, in either case, discharge into a bell nozzle. At higher altitudes where the ambient pressure is lower, the central nozzle would be shut off reducing the throat area and thereby increasing the nozzle area ratio. These designs require additional complexity but an advantage of having two thrust chambers is that they

can be configured to burn different propellants or different fuel mixture ratios. Similarly, Aerojet has also designed a nozzle called the 'Thrust Augmented Nozzle'^[12] which injects propellant and oxidiser directly into the nozzle section for combustion allowing larger area ratio nozzles to be used deeper in an atmosphere than they would without augmentation due to effects of flow separation. They would again allow multiple propellants to be used (such as RP-1) further increasing thrust.

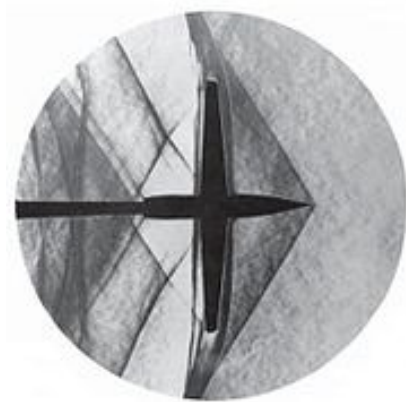
There is also a SERN (Single Expansion Ramp Nozzle), a linear expansion nozzle where the gas pressure transfers work only on one side and which could be described as a single-sided aerospike nozzle.

References

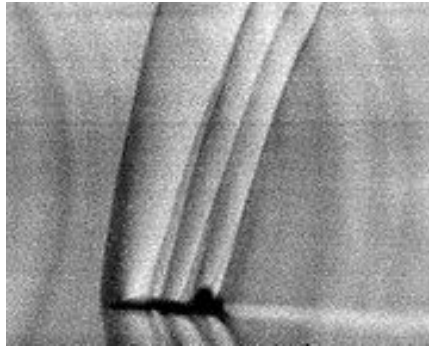
1. ^ a b Richard Nakka's Equation 12
2. ^ a b Robert Braeuning's Equation 2.22
3. ^ Sutton, George P. (1992). *Rocket Propulsion Elements: An Introduction to the Engineering of Rockets* (6th Edition ed.). Wiley-Interscience. p. 636. ISBN 0471529389.
4. ^ NASA: Rocket thrust
5. ^ NASA: Rocket thrust summary
6. ^ NASA: Rocket specific impulse
7. ^ Huzel, D. K. and Huang, D. H. (1971). *NASA SP-125, Design of Liquid Propellant Rocket Engines* (2nd Edition ed.). NASA. Technical report
8. ^ PWR Engineering: Nozzle Design
9. ^ a b Sutton, George P. (2001). *Rocket Propulsion Elements: An Introduction to the Engineering of Rockets* (7th Edition ed.). Wiley-Interscience. p. 84. ISBN 0471326429. <http://books.google.co.uk/books?id=LQbDOxg3XZcC&printsec=frontcover&dq=rocket+propulsion&ei=wIEhScL4EYykwSVv5SCDw#PPA84,M1-->
10. ^ Journal of Propulsion and Power Vol.14 No.5, "Advanced Rocket Nozzles", Hagemann et al.
11. ^ Journal of Propulsion and Power Vol.18 No.1, "Experimental and Analytical Design Verification of the Dual-Bell Concept", Hagemann et al.
12. ^ Thrust Augmented Nozzle

Schlieren Photography

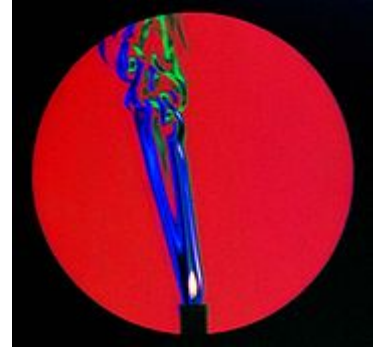
From Wikipedia, the free encyclopedia



A schlieren photograph showing the compression in front of an unswept wing at Mach 1.2



Shock waves produced by a T-38 Talon during flight



Color schlieren image of the thermal plume from a burning candle, disturbed by a breeze from the right. Photographed by Gary S. Settles, Penn State University

Schlieren photography is a visual process that is used to photograph the flow of fluids of varying density. Invented by the German physicist August Toepler in 1864 to study supersonic motion, it is widely used in aeronautical engineering to photograph the flow of air around objects. Its role is changing due to the increasing use of computational fluid dynamics, where the same principle is used to display the computed results as flow images.

Optical system

The basic optical schlieren system uses light from a single collimated source shining on, or from behind, a target object. Variations in refractive index caused by density gradients in the fluid distort the collimated light beam. This distortion creates a spatial variation in the intensity of the light, which can be visualised directly with a shadowgraph system.

In schlieren photography, the collimated light is focused with a lens, and a knife-edge is placed at the focal point, positioned to block about half the light. In flow of uniform density this will simply make the photograph half as bright. However in flow with density variations the distorted beam focuses imperfectly, and parts which have focussed in an area covered by the knife-edge are blocked. The result is a set of lighter and darker patches corresponding to positive and negative fluid density gradients in the direction normal to the knife-edge. When a knife-edge is used, the system is generally referred to as a *schlieren system*, which measures the first derivative of density in the direction of the knife-edge. If a knife-edge is not used, the system is generally referred to as a *shadowgraph system*, which measures the second derivative of density

If the fluid flow is uniform the image will be steady, but any turbulence will cause scintillation, the shimmering effect that can be seen on hot surfaces on a sunny day. To visualise instantaneous density profiles, a short duration flash (rather than continuous illumination) may be used.

Variations

Variations on the optical schlieren method include the replacement of the knife-edge by a colored "bullseye" target, resulting in *Rainbow Schlieren* which can assist in visualising the flow. The adaptive optics pyramid wavefront sensor is a modified form of schlieren (having two perpendicular knife edges formed by the vertices of a refracting square pyramid).

Few complete schlieren optical systems are commercially available today, but details of theory and construction are given in Settles' 2001 book.^[1] The USSR produced a number of sophisticated schlieren systems based on the Maksutov telescope principle, many of which still survive in the former Soviet Union and China.

Synthetic schlieren

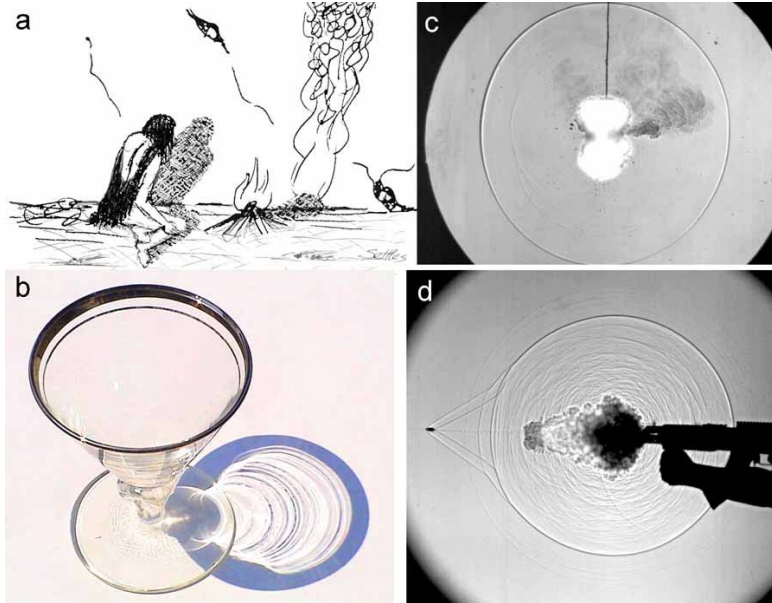
The synthetic schlieren method is a technique similar to schlieren photography which makes use of digital photography and image processing rather than optics to visualize the density variations of a fluid.

References

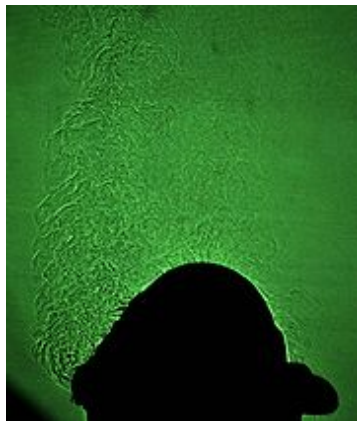
1. ^ Settles, G. S., *Schlieren and shadowgraph techniques: Visualizing phenomena in transparent media*, Berlin:Springer-Verlag, 2001.

Shadowgraph

From Wikipedia, the free encyclopedia



a) prehistoric shadowgraphy, b) sunlight shadowgram of a martini glass, c) "focused" shadowgram of a common firecracker explosion, d) "Edgerton" shadowgram of the firing of an AK-47 assault rifle (images and artwork by Gary S. Settles, Penn State Gas Dynamics Lab)



Shadowgram of the turbulent plume of hot air rising from a home-barbecue gas grill. Photograph by Gary S. Settles, Penn State University.

Shadowgraph is an optical method that reveals non-uniformities in transparent media like air, water, or glass. It is related to, but simpler than, the schlieren and schlieren photography methods that perform a similar function. Shadowgraph is a type of flow visualisation.

In principle, we cannot directly see a difference in temperature, a different gas, or a shock wave in the transparent air. However, all these disturbances refract light rays, so they can cast shadows. The plume of hot air rising from a fire, for example, can be seen by way of its shadow cast upon a nearby surface by the uniform sunlight.

Sunlight shadowgraph

This technique is as old as nature itself. For example, some aquatic predators detect their transparent prey by way of their shadows cast upon the ocean floor. Nevertheless it was Robert Hooke^[1] who first scientifically demonstrated the sunlight shadowgraph and Jean-Paul Marat^[2] who first used it to study fire. A modern account of shadowgraphy is given by G.S. Settles.^[3]

Applications

Applications of shadowgraphy in science and technology are very broad. It is used in aeronautical engineering to see the flow about high-speed aircraft and missiles, as well as in combustion research, ballistics, explosions, and in the testing of glass.

Shadowgram

According to F. J. Weinberg,^[4] the result of applying the shadowgraph technique should be known as a *shadowgram*. A shadowgram is not a focused image, rather it is a mere shadow. In the shadowgram, the differences in light intensity are proportional to the second spatial derivative (Laplacian) of the refractive index field in the transparent medium under study. Once the distance from the transparent disturbance to the cast shadow becomes too large, then the shadow no longer constitutes a useful representation of the disturbance that caused it.

Cartoons

The Shadowgraph, and shadowgram have been used in animation, where they reinforce the cartoon's realism. One first use was made by Disney Studios on the *Three Blind Mouseketeers* (1936) Silly Symphonies.^[5]

Postcards

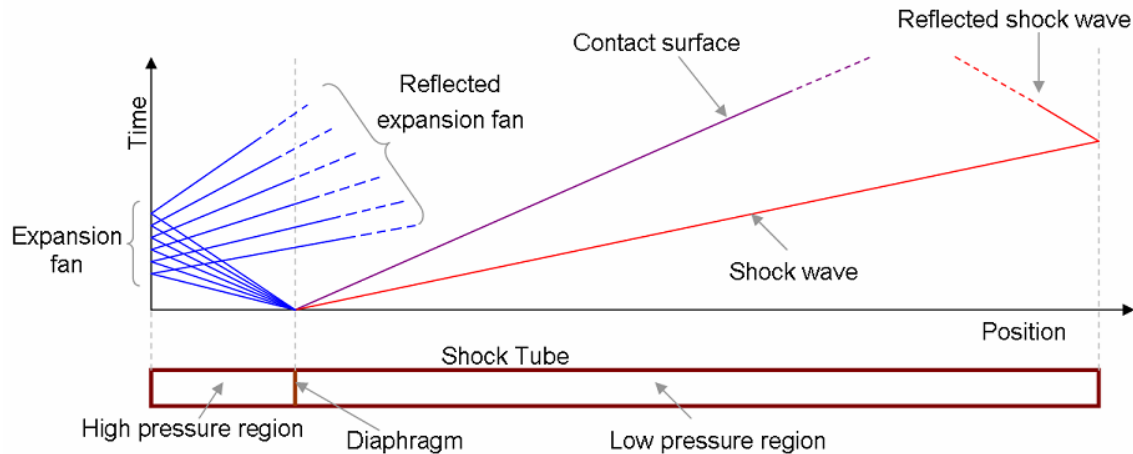
Additionally the term *Shadowgraph* was used by English postcard publishers E.T.W. Dennis & Sons Ltd. of London and Scarborough for a series of 'Hold up to the Light' postcards in the 1950s. In these a saucy image can be seen through what seems an innocent picture when a light is shone through the card.^[6]

References

1. ^ Hooke, R., "Of a New Property in the Air," *Micrographia*, Observation LVIII, 217-219, London (1665).
2. ^ Marat, J.-P., *Recherches physiques sur le feu*, Paris, France: Cl. Ant. Jombert, 1780.
3. ^ Settles, G. S., *Schlieren and shadowgraph techniques: Visualizing phenomena in transparent media*, Berlin: Springer-Verlag, 2001.
4. ^ Weinberg, F.J., *Optics of flames: including methods for the study of refractive index fields in combustion and aerodynamics*, London: Butterworths, 1963.
5. ^ Russel Merritt & JB Kaufman, *Walt Disney's Silly Symphonies : A Companion to the classic cartoons series*, Italy: La Cinecitta del Friuli, 2006, ISBN 88-86155-27-1 p 46
6. ^ "MetroPostcard Publishers D". Metropolitan Postcard Club of New York City. <http://www.metropostcard.com/publishersd.html>. Retrieved on 2008-10-02.

Shock tube

From Wikipedia, the free encyclopedia



An idealized shock tube. The plot shows different waves which are formed in the tube once the diaphragm is ruptured.

A **shock tube** is a device used primarily to study gas phase combustion reactions. Shock tubes (and related impulse facilities: shock tunnels, expansion tubes, and expansion tunnels) can also be used to study aerodynamic flow under a wide range of temperatures and pressures that are difficult to obtain in other types of testing facilities.

Working

A simple shock tube is a metal tube in which a gas at low pressure and a gas at high pressure are separated using a diaphragm. This diaphragm suddenly bursts open under predetermined conditions to produce a shock wave that travels down the low pressure section of the tube. This shock wave increases the temperature and pressure of the gas and induces a flow in the direction of the shock wave, creating the conditions desired for the testing being done.

The low-pressure gas, referred to as the *driven gas*, is subjected to the shock wave. The high pressure gas is known as the *driver gas*. The corresponding sections of the tube are likewise called the driver and driven sections. These gases (which do not necessarily need to be the same chemical composition) are pumped into the tube sections or loaded from pressurized gas supply lines, or (if the desired pressure is less than atmospheric) the gas is pumped out of the tube section until the desired pressure is reached. The diaphragm between the tube sections must be strong enough to hold the initial pressure difference but must also burst cleanly to yield good test results.

The test being conducted begins with the bursting of the diaphragm. There are three common methods used to burst the diaphragm.

- A plunger with a bladed cutting edge on the end can be built into the driver tube; actuating the plunger (electrically, hydraulically, or pneumatically) drives the blade through the diaphragm material to burst it. However, this requires a somewhat complex mechanism.

- Another method is to use diaphragms (such as aluminum discs) that have been scored in a cross-shaped pattern to a calibrated depth, designed to rupture when the pressure difference across the diaphragm is the difference specified for the test being conducted.
- A third method is to use a combustible mixture of gasses in the driver; initiating combustion creates a sudden increase in pressure that bursts the diaphragm (shock tubes of this design are said to use a *combustion driver*).

After the diaphragm is burst a compression wave travels down the tube into the driven gas, which then rapidly steepens to form a shock front, known as the incident shock wave. This shock wave increases the temperature and pressure of the driven gas and induces a flow in the direction of the shock wave (but at lower velocity than the shock wave itself). Simultaneously, a rarefaction wave, often referred to as an expansion fan, travels back in to the driver gas. The circular section that represents the interface separating the experimental (driven) gas and the driver gas is called the contact surface; the contact surface moves rapidly along the tube behind the shock front.

Once the incident shock wave reaches the end of the shock tube, it is reflected back in to the already heated gas, resulting in a further rise in the temperature, pressure and density of the gas. This effectively creates a high temperature and high pressure reaction zone to which the driver gas is subjected. This reaction can be quenched by using a 'dump tank' which swallows the reflected shock wave. The gas samples are then collected from the tube and analyzed.

Applications

Other than study of gas samples at high temperatures and pressures, shock tubes have numerous applications in combustion and aerodynamics studies. Often solid particles may be injected into the driven section of the shock tube prior to the diaphragm burst. The properties of the combustion reaction of these particles resulting from the sudden increase in temperature and pressure due to the shock wave can be analyzed using data collected with pressure transducers and spectrometers.

For aerodynamic testing, the fluid flow induced in the driven gas behind the shock wave can be used much as a wind tunnel is used. Shock tubes allow the study of fluid flow at temperatures and pressures that would be difficult to obtain in wind tunnels (for example, to replicate the conditions in the turbine sections of jet engines). The duration of the testing is limited, though, by the time available between the passage of the shock wave and the arrival of either the contact surface or the reflection of the shock wave off the end of the tube. In practice, this usually limits the available test time to a few milliseconds.

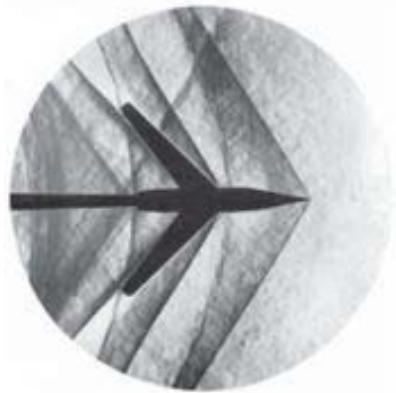
A further development for aerodynamic testing is the shock tunnel, where a nozzle is placed between the end of the tube and a dump tank. As the shock wave reflects off the end of the tube it creates a region of very high pressure and temperature. Since the dump tank is pumped down to a low pressure (near vacuum), there is a very large pressure difference across the nozzle. Using a shock tunnel, very high temperature hypersonic flow can be created in the test section, located immediately behind the nozzle. This allows testing in conditions that can simulate re-entry of spacecraft or hypersonic transport; but again testing time is limited to the order of milliseconds.

References

- Liepmann, Hans W.; Roshko, A. (2001) [1957]. *Elements of Gasdynamics*. Dover Publications. pp. 79–83. ISBN 0-486-41963-0.
- Anderson, John D. Jr. (August 2000) [1989]. *Hypersonic and High Temperature Gas Dynamics*. AIAA. pp. 368–369. ISBN 1-56347-459-X.

Shock wave

From Wikipedia, the free encyclopedia



Schlieren photograph of an attached shock on a sharp-nosed supersonic body.

A **shock wave** (also called **shock front** or simply "**shock**") is a type of propagating disturbance. Like an ordinary wave, it carries energy and can propagate through a medium (solid, liquid or gas) or in some cases in the absence of a material medium, through a field such as the electromagnetic field. Shock waves are characterized by an abrupt, nearly discontinuous change in the characteristics of the medium.^[1] Across a shock there is always an extremely rapid rise in pressure, temperature and density of the flow. In supersonic flows, expansion is achieved through an expansion fan. A shock wave travels through most media at a higher speed than an ordinary wave.

Unlike solitons (another kind of nonlinear wave), the energy of a shock wave dissipates relatively quickly with distance. Also, the accompanying expansion wave approaches and eventually merges with the shock wave, partially cancelling it out. Thus the sonic boom associated with the passage of a supersonic aircraft is the sound wave resulting from the degradation and merging of the shock wave and the expansion wave produced by the aircraft.

When a shock wave passes through matter, the total energy is preserved but the energy which can be extracted as work decreases and entropy increases. This, for example, creates additional drag force on aircraft with shocks.

Terminology

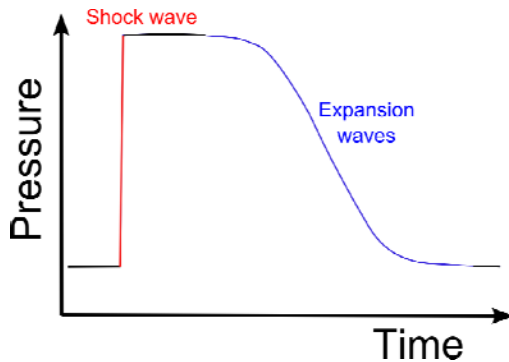
Shock waves can be

- Normal: at 90° (perpendicular) to the shock medium's flow direction.
- Oblique: at an angle to the direction of flow.
- Bow: Occurs upstream of the front (bow) of a blunt object when the upstream velocity exceeds Mach 1.

Some other terms

- Shock Front: an alternative name for the shock wave itself
- Contact Front: in a shock wave caused by a driver gas (for example the "impact" of a high explosive on the surrounding air), the boundary between the driver (explosive products) and the driven (air) gases. The Contact Front trails the Shock Front.

In supersonic flows



Pressure-time diagram at an external observation point for the case of a supersonic object propagating past the observer. The leading edge of the object causes a shock (left, in red) and the trailing edge of the object causes an expansion (right, in blue).

When an object (or disturbance) moves faster than the information about it can be propagated into the surrounding fluid, fluid near the disturbance cannot react or "get out of the way" before the disturbance arrives. In a shock wave the properties of the fluid (density, pressure, temperature, velocity, Mach number) change almost instantaneously. Measurements of the thickness of shock waves have resulted in values approximately one order of magnitude greater than the mean free path of the gas investigated.

Shock waves form when the speed of a gas changes by more than the speed of sound.^[2] At the region where this occurs sound waves traveling against the flow reach a point where they cannot travel any further upstream and the pressure progressively builds in that region, and a high pressure shock wave rapidly forms.

Shock waves are not conventional sound waves; a shock wave takes the form of a very sharp change in the gas properties on the order of a few mean free paths (roughly micro-meters at atmospheric conditions) in thickness. Shock waves in air are heard as a loud "crack" or "snap" noise. Over longer distances a shock wave can change from a nonlinear wave into a linear wave, degenerating into a conventional sound wave as it heats the air and loses energy. The sound wave is heard as the familiar "thud" or "thump" of a sonic boom, commonly created by the supersonic flight of aircraft.

The shock wave is one of several different ways in which a gas in a supersonic flow can be compressed. Some other methods are isentropic compressions, including Prandtl-Meyer compressions. The method of compression of a gas results in different temperatures and densities for a given pressure ratio, which can be analytically calculated for a non-reacting gas. A shock wave

compression results in a loss of total pressure, meaning that it is a less efficient method of compressing gases for some purposes, for instance in the intake of a scramjet. The appearance of pressure-drag on supersonic aircraft is mostly due to the effect of shock compression on the flow.

Due to nonlinear steepening

Shock waves can form due to steepening of ordinary waves. The best-known example of this phenomenon is ocean waves that form breakers on the shore. In shallow water, the speed of surface waves is dependent on the depth of the water. An incoming ocean wave has a slightly higher wave speed near the crest of each wave than near the troughs between waves, because the wave height is not infinitesimal compared to the depth of the water. The crests overtake the troughs until the leading edge of the wave forms a vertical face and spills over to form a turbulent shock (a breaker) that dissipates the wave's energy as sound and heat.

Similar phenomena affect strong sound waves in gas or plasma, due to the dependence of the sound speed on temperature and pressure. Strong waves heat the medium near each pressure front, due to adiabatic compression of the air itself, so that high pressure fronts outrun the corresponding pressure troughs. While shock formation by this process does not normally happen to sound waves in Earth's atmosphere, it is thought to be one mechanism by which the solar chromosphere and corona are heated, via waves that propagate up from the solar interior.

Analogies

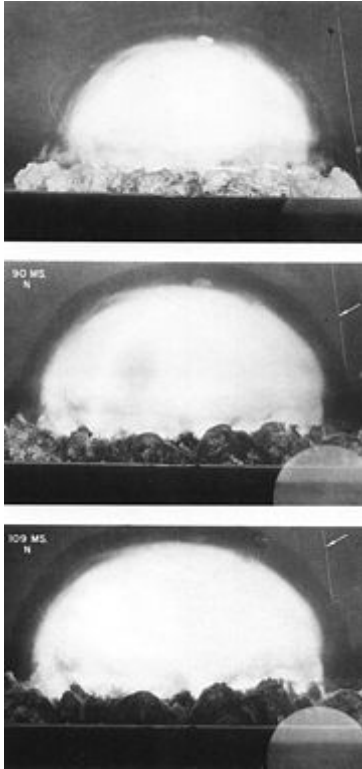
A shock wave may be described as the furthest point upstream of a moving object which "knows" about the approach of the object. In this description, the shock wave position is defined as the boundary between the zone having no information about the shock-driving event, and the zone aware of the shock-driving event, analogous with the light cone described in the theory of special relativity.

To get a shock wave something has to be travelling faster than the local speed of sound. In that case some parts of the air around the aircraft are travelling at exactly the speed of sound with the aircraft, so that the sound waves leaving the aircraft pile up on each other, similar to a tailback on a road, and a shock wave forms, the pressure increases, and then spreads out sideways. Because of this amplification effect, a shock wave is very intense, more like an explosion when heard (not coincidentally, since explosions create shock waves).

Analogous phenomena are known outside fluid mechanics. For example, particles accelerated beyond the speed of light in a refractive medium (where the speed of light is less than that in a vacuum, such as water) create visible shock effects, a phenomenon known as Cherenkov radiation.

Examples

Below are a number of examples of shock waves, broadly grouped with similar shock phenomena:



Shock wave propagating into a stationary medium, ahead of the fireball of an explosion. The shock is made visible by the shadow effect (Trinity explosion.)

Moving shock

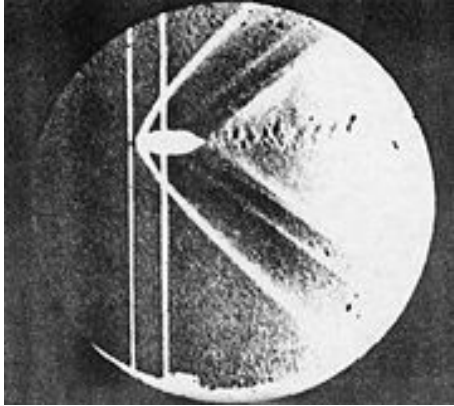
- usually consists of a shockwave propagating into a stationary medium
- In this case, the gas ahead of the shock is stationary (in the laboratory frame), and the gas behind the shock is supersonic in the laboratory frame. The shock propagates with a wave front which is normal (at right angles) to the direction of flow. The speed of the shock is a function of the original pressure ratio between the two bodies of gas.
- Moving shocks are usually generated by the interaction of two bodies of gas at different pressure, with a shock wave propagating into the lower pressure gas, and an expansion wave propagating into the higher pressure gas.
- Examples: Balloon bursting, Shock tube, shock wave from explosion

Detonation wave

- A detonation wave is essentially a shock supported by a trailing exothermic reaction. It involves a wave traveling through a highly combustible or chemically unstable medium, such as an oxygen-methane mixture or a high explosive. The chemical reaction of the medium occurs following the shock wave, and the chemical energy of the reaction drives the wave forward.
- A detonation wave follows slightly different rules from an ordinary shock since it is driven by the chemical reaction occurring behind the shock wave front. In the simplest theory for detonations, an unsupported, self-propagating detonation wave proceeds at the Chapman-

Jouguet velocity. A detonation will also cause a shock of type 1, above to propagate into the surrounding air due to the overpressure induced by the explosion.

- When a shockwave is created by high explosives such as TNT (which has a detonation velocity of 6,900 m/s), it will always travel at high, supersonic velocity from its point of origin.



Shadowgraph of the detached shock on a bullet in supersonic flight, published by Ernst Mach in 1887.

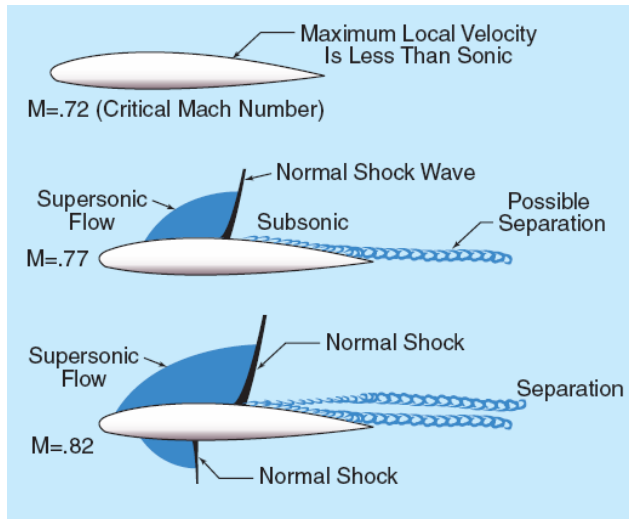
Detached shock

- These shocks are curved, and form a small distance in front of the body. Directly in front of the body, they stand at 90 degrees to the oncoming flow, and then curve around the body. Detached shocks allow the same type of analytic calculations as for the attached shock, for the flow near the shock. They are a topic of continuing interest, because the rules governing the shock's distance ahead of the blunt body are complicated, and are a function of the body's shape. Additionally, the shock standoff distance varies drastically with the temperature for a non-ideal gas, causing large differences in the heat transfer to the thermal protection system of the vehicle. See the extended discussion on this topic at Atmospheric reentry. These follow the "strong-shock" solutions of the analytic equations, meaning that for some oblique shocks very close to the deflection angle limit, the downstream Mach number is subsonic. See also bow shock or oblique shock
- Such a shock occurs when the maximum deflection angle is exceeded. A detached shock is commonly seen on blunt bodies, but may also be seen on sharp bodies at low Mach numbers.
- Examples: Space return vehicles (Apollo, Space shuttle), bullets, the boundary (Bow shock) of a magnetosphere. The name "bow shock" comes from the example of a bow wave, the detached shock formed at the bow (front) of a ship or boat moving through water, whose slow surface wave speed is easily exceeded (see ocean surface wave).

Attached shock

- These shocks appear as "attached" to the tip of a sharp body moving at supersonic speeds.
- Examples: Supersonic wedges and cones with small apex angles
- The attached shock wave is a classic structure in aerodynamics because, for a perfect gas and inviscid flow field, an analytic solution is available, such that the pressure ratio, temperature ratio, angle of the wedge and the downstream Mach number can all be

calculated knowing the upstream Mach number and the shock angle. Smaller shock angles are associated with higher upstream Mach numbers, and the special case where the shock wave is at 90 degrees to the oncoming flow (Normal shock), is associated with a Mach number of one. These follow the "weak-shock" solutions of the analytic equations.



Recompression shock on a transonic flow airfoil, at and above critical Mach number.

Recompression shock

- These shocks appear when the flow over a transonic body is decelerated to subsonic speeds.
- Examples: Transonic wings, turbines
- Where the flow over the suction side of a transonic wing is accelerated to a supersonic speed, the resulting re-compression can be by either Prandtl-Meyer compression or by the formation of a normal shock. This shock is of particular interest to makers of transonic devices because it can cause separation of the boundary layer at the point where it touches the transonic profile. This can then lead to full separation and stall on the profile, higher drag, or shock-buffet, a condition where the separation and the shock interact in a resonance condition, causing resonating loads on the underlying structure.

Shock in a pipe flow

- This shock appears when supersonic flow in a pipe is decelerated.
- Examples: Supersonic ramjet, scramjet, needle valve
- In this case the gas ahead of the shock is supersonic (in the laboratory frame), and the gas behind the shock system is either supersonic (*oblique shocks*) or subsonic (a *normal shock*) (Although for some oblique shocks very close to the deflection angle limit, the downstream Mach number is subsonic.) The shock is the result of the deceleration of the gas by a converging duct, or by the growth of the boundary layer on the wall of a parallel duct.

Shock waves in rapid granular flows

Shock waves can also occur in rapid flows of dense granular materials down inclined channels or slopes. Strong shocks in rapid dense granular flows can be studied theoretically and analyzed to compare with experimental data. Consider a configuration in which the rapidly moving material down the chute impinges on an obstruction wall erected perpendicular at the end of a long and steep channel. Impact leads to a sudden change in the flow regime from a fast moving supercritical thin layer to a stagnant thick heap. This flow configuration is particularly interesting because it is analogous to some hydraulic and aerodynamic situations associated with flow regime changes from supercritical to subcritical flows. Such study is important in estimating impact pressures exerted by avalanches and granular flows on defense structures or infrastructure along the channel and in the run-out zones, and to study the complex flow dynamics around the obstacles and in depositions when the mass comes suddenly to a standstill.^{[3][4]}

Shock waves in astrophysics

Astrophysical environments feature many different types of shock waves. Some common examples are Supernovae remnant shock waves traveling through the interstellar medium, the bow shock caused by the earth's magnetic field colliding with the solar wind and shock waves caused by galaxies colliding with each other.

References

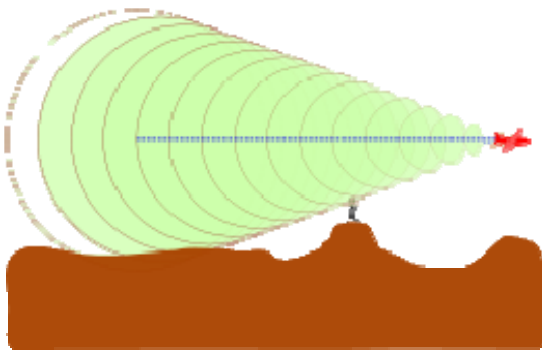
1. ^ Anderson, John D. Jr. (January 2001) [1984]. *Fundamentals of Aerodynamics* (3rd ed.). McGraw-Hill Science/Engineering/Math. ISBN 0-07-237335-0.
2. ^ Settles, Gary S. (2006), *High-speed Imaging of Shock Wave, Explosions and Gunshots*, **94**, American Scientist, pp. 22–31
3. ^ Shiva P. Pudasaini, et al., (2007), *Rapid Flow of Dry Granular Materials down Inclined Chutes Impinging on Rigid Walls*, *Physics of Fluids*, **19**, American Institute of Physics
4. ^ Shiva P. Pudasaini, Christian Kroener (2008), *Shock waves in rapid flows of dense granular materials: Theoretical predictions and experimental results*, *Physical Review E*, **78**, American Physical Society

Sonic Boom

From Wikipedia, the free encyclopedia



Rapid condensation of water vapor due to a sonic shock produced at sub-sonic speed creates a vapor cone (known as a Prandtl–Glauert singularity), which can be seen with the naked eye



A sonic boom produced by an aircraft moving at $M=2.92$, calculated from the cone angle of 20 deg. An observer hears the boom when the shock wave, on the edges of the cone, crosses his or her location.



Mach cone angle

The term **sonic boom** is commonly used to refer to the shocks caused by the supersonic flight of an aircraft. Sonic booms generate enormous amounts of sound energy, sounding much like an

explosion. Thunder is a type of natural sonic boom, created by the rapid heating and expansion of air in a lightning discharge.^[1]

Causes

When an object passes through the air, it creates a series of pressure waves in front of it and behind it, similar to the bow and stern waves created by a boat. These waves travel at the speed of sound, and as the speed of the object increases, the waves are forced together, or compressed, because they cannot "get out of the way" of each other, eventually merging into a single shock wave at the speed of sound. This critical speed is known as Mach 1 and is approximately 1,225 kilometers per hour (761 mph) at sea level at room temperature. In smooth flight, the shock wave starts at the nose of the aircraft and ends at the tail. Because directions around the aircraft's direction of travel are equivalent, the shock forms a Mach cone with the aircraft at its tip. The half-angle (between direction of flight and the shock wave) α is given by

$$\sin(\alpha) = \frac{v_{sound}}{v_{object}},$$

where v_{sound} is the plane's Mach number. So the faster it goes, the finer, (more pointed) the cone.

There is a rise in pressure at the nose, decreasing steadily to a negative pressure at the tail, followed by a sudden return to normal pressure after the object passes. This "overpressure profile" is known as an N-wave because of its shape. The "boom" is experienced when there is a sudden change in pressure, so the N-wave causes two booms, one when the initial pressure rise from the nose hits, and another when the tail passes and the pressure suddenly returns to normal. This leads to a distinctive "double boom" from supersonic aircraft. When maneuvering, the pressure distribution changes into different forms, with a characteristic U-wave shape.

Since the boom is being generated continually as long as the aircraft is supersonic, it fills out a narrow path on the ground following the aircraft's flight path, a bit like an unrolling celebrity carpet and hence known as the "boom carpet". Its width depends on the altitude of the aircraft.^[2] The distance from the point on the ground where the boom is heard to the aircraft depends on its altitude and the angle α .

Characteristics

The power, or volume, of the shock wave is dependent on the quantity of air that is being accelerated, and thus the size and shape of the aircraft. As the aircraft increases speed the shocks grow "tighter" around the craft and do not become much "louder". At very high speeds and altitudes the Mach cone does not intersect the ground and no boom is heard. The "length" of the boom from front to back is dependent on the length of the aircraft to a factor of 3:2. Longer aircraft therefore "spread out" their booms more than smaller ones, which leads to a less powerful boom which has a less "spread out" boom.

Several smaller shock waves can, and usually do, form at other points on the aircraft, primarily any convex points or curves, the leading wing edge and especially the inlet to engines. These secondary shockwaves are caused by the air being forced to turn around these convex points, which generates a shock wave in supersonic flow.

The later shock waves are somehow faster than the first one, travel faster and add to the main shockwave at some distance away from the aircraft to create a much more defined N-wave shape. This maximizes both the magnitude and the "rise time" of the shock which makes the boom seem louder. On most designs the characteristic distance is about 40,000 feet (12,000 m), meaning that below this altitude the sonic boom will be "softer". However, the drag at this altitude or below makes supersonic travel particularly inefficient, which poses a serious problem.

Measurement and examples

Sonic booms caused by aircraft are often a few pounds per square foot. A vehicle flying at greater altitude will generate lower pressures on the ground, because the shock wave reduces in intensity as it spreads out away from the vehicle, but the sonic booms are less affected by vehicle speed.

Aircraft	speed	altitude	pressure (psf)
SR-71	Mach 3	80,000 feet	0.9
Concorde SST	Mach 2	52,000	1.94
F-104	Mach 1.93	48,000 feet	0.8
Space Shuttle	Mach 1.5	60,000 feet	1.25

[3]

Abatement

In the late 1950s when supersonic transport (SST) designs were being actively pursued, it was thought that although the boom would be very large, the problems could be avoided by flying higher. This premise was proven false when the North American B-70 *Valkyrie* started flying, and it was found that the boom was a problem even at 70,000 feet (21,000m). It was during these tests that the N-wave was first characterized.

Richard Seebass and his colleague Albert George at Cornell University studied the problem extensively and eventually defined a "figure of merit" (FM) to characterize the sonic boom levels of different aircraft. FM is a function of the aircraft weight and the aircraft length. The lower this value, the less boom the aircraft generates, with figures of about 1 or lower being considered acceptable. Using this calculation, they found FM's of about 1.4 for Concorde and 1.9 for the Boeing 2707. This eventually doomed most SST projects as public resentment mixed with politics eventually resulted in laws that made any such aircraft impractical (flying only over water for instance). Another way to express this is wing span. The fuselage of even large supersonic aeroplanes is very sleek and with enough angle of attack and wing span the plane can fly so high that the boom by the fuselage is not important. The larger the wing span, the greater the downwards impulse which can be applied to the air, the greater the boom felt. A smaller wing span favors small aeroplane designs like business jets. Seebass and George also worked on the problem from another

angle, trying to spread out the N-wave laterally and temporally (longitudinally), by producing a strong and downwards-focused (SR-71 Blackbird, Boeing X-43) shock at a sharp, but wide angle nosecone, which will travel at slightly supersonic speed (bow shock), and using a swept back flying wing or an oblique flying wing to smooth out this shock along the direction of flight (the tail of the shock travels at sonic speed). To adapt this principle to existing planes, which generate a shock at their nose-cone and an even stronger one at their wing leading edge, the fuselage below the wing is shaped according to the area rule. Ideally this would raise the characteristic altitude from 40,000 feet to 60,000 feet (from 12,000 m to 18,000 m), which is where most SST aircraft fly.

This remained untested for decades, until DARPA started the Quiet Supersonic Platform project and funded the Shaped Sonic Boom Demonstration (SSBD) aircraft to test it. SSBD used an F-5 Freedom Fighter. The F-5E was modified with a highly refined shape which lengthened the nose to that of the F-5F model. The fairing extended from the nose all the way back to the inlets on the underside of the aircraft. The SSBD was tested over a two year period culminating in 21 flights and was an extensive study on sonic boom characteristics. After measuring the 1,300 recordings, some taken inside the shock wave by a chase plane, the SSBD demonstrated a reduction in boom by about one-third. Although one-third is not a huge reduction, it could have reduced Concorde below the $FM = 1$ limit for instance.

As a follow-on to SSBD, in 2006 a NASA-Gulfstream Aerospace team tested the Quiet Spike on NASA-Dryden's F-15B aircraft 836. The Quiet Spike is a telescoping boom fitted to the nose of an aircraft specifically designed to weaken the strength of the shock waves forming on the nose of the aircraft at supersonic speeds. Over 50 test flights were performed. Several flights included probing of the shockwaves by a second F-15B, NASA's Intelligent Flight Control System testbed, aircraft 837.

There are theoretical designs that do not appear to create sonic booms at all, such as the Busemann's Biplane.

Perception and noise

The sound of a sonic boom depends largely on the distance between the observer and the aircraft shape producing the sonic boom. A sonic boom is usually heard as a deep double "boom" as the aircraft is usually some distance away. However, as those who have witnessed landings of space shuttles have heard, when the aircraft is nearby the sonic boom is a sharper "bang" or "crack". The sound is much like the "aerial bombs" used at firework displays.

In 1964, NASA and the Federal Aviation Administration began the Oklahoma City sonic boom tests, which caused eight sonic booms per day over a period of six months. Valuable data was gathered from the experiment, but 15,000 complaints were generated and ultimately entangled the government in a class action lawsuit, which it lost on appeal in 1969.

There has been recent work in this area, notably under DARPA's Quiet Supersonic Platform studies. Research by acoustics experts under this program began looking more closely at the composition of sonic booms, including the frequency content. Several characteristics of the traditional sonic boom "N" wave can influence how loud and irritating it can be perceived by listeners on the ground. Even strong N-waves such as those generated by Concorde or military aircraft can be far less

objectionable if the rise time of the overpressure is sufficiently long. A new metric has emerged, known as *perceived* loudness, measured in PLdB. This takes into account the frequency content, rise time, etc. A well known example is the snapping of your fingers in which the "perceived" sound is nothing more than an annoyance.

The composition of the atmosphere is also a factor. Temperature variations, humidity, pollution, and winds can all have an effect on how a sonic boom is perceived on the ground. Even the ground itself can influence the sound of a sonic boom. Hard surfaces such as concrete, pavement, and large buildings can cause reflections which may amplify the sound of a sonic boom. Similarly grassy fields and lots of foliage can help attenuate the strength of the overpressure of a sonic boom.

Currently there are no industry accepted standards for the acceptability of a sonic boom. Until such metrics can be established, either through further study or supersonic overflight testing, it is doubtful that legislation will be enacted to remove the current prohibition on supersonic overflight in place in several countries, including the United States.

Bullwhip

The cracking sound a bullwhip makes when properly wielded is, in fact, a small sonic boom. The end of the whip, known as the "*popper*", moves faster than the speed of sound, thus resulting in the sonic boom.^[4] The whip is quite possibly the first human invention to break the sound barrier.

A bullwhip tapers down from the handle section to the cracker. The cracker has much less mass than the handle section. When the whip is sharply swung, the energy is transferred down the length of the tapering whip. In accordance with the formula for kinetic energy $E_k = \frac{mv^2}{2}$, the velocity of the whip increases with the decrease in mass, which is how the whip reaches the speed of sound and causes a sonic boom.

References

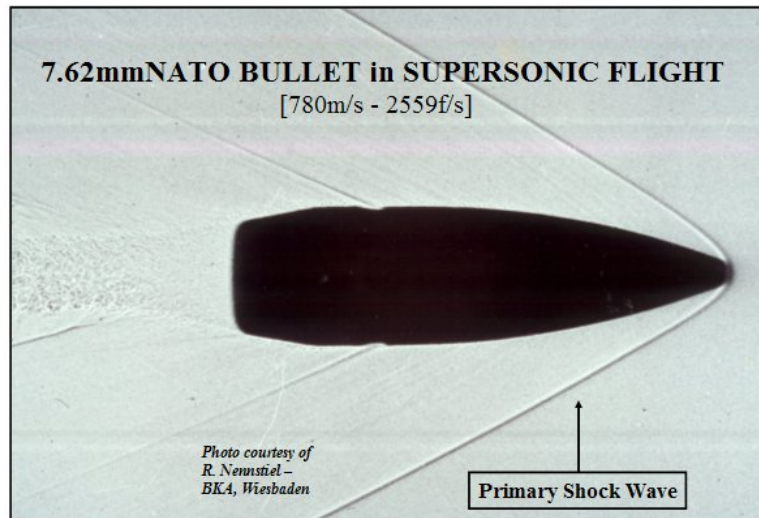
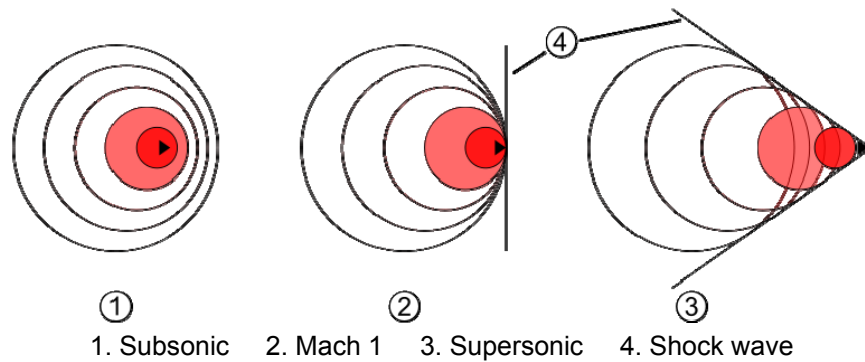
1. ^ "The Science of Thunder". http://www.lightningsafety.com/nlsi_info/thunder2.html. Retrieved on 2008-02-20.
2. ^ "boom forest". <http://au.answers.yahoo.com/question/index?qid=20080429010916AARjbl7>. Retrieved on 2008-07-12.
3. ^ Dryden Flight Research Center Fact Sheet: Sonic Booms
4. ^ Mike May, *Crackin' Good Mathematics*, American Scientist, Volume 90, Number 5, 2002

Sound Barrier

From Wikipedia, the free encyclopedia



U.S. Navy F/A-18 breaking the sound barrier. The white halo is formed by condensed water droplets which are thought to result from a drop in air pressure around the aircraft (see Prandtl-Glauert Singularity).^{[1][2]}



Shadowgraph of a 7,62 x 51 NATO bullet in supersonic flight at Mach 2.4. Notice the shockwave (Mach cone) from the bullet's tip, a secondary shockwave coining from the cannellure and the turbulence in the air behind the bullet

In aerodynamics, the **sound barrier** usually refers to the point at which an aircraft moves from transonic to supersonic speed. The term came into use during World War II when a number of

aircraft started to encounter the effects of compressibility, a grab-bag of unrelated aerodynamic effects. By the 1950s, aircraft started to routinely "break" the sound barrier.^[3]

History

Some common whips such as the bullwhip or sparewhip are able to move faster than sound: the tip of the whip breaks the sound barrier and causes a sharp crack—literally a sonic boom. Firearms since the 19th century have generally had a supersonic muzzle velocity. However, the sound barrier may have been first breached some 150 million years prior to the inventions of these implements. Some paleobiologists report that, based on computer models of their biomechanical capabilities, certain long-tailed dinosaurs such as *apatosaurus* and *diplodocus* may have possessed the ability to flick their tails at supersonic velocities, possibly used to generate an intimidating booming sound. This finding is theoretical and disputed by others in the field.^[4]

Early problems

The tip of the propeller on many early aircraft may reach supersonic speeds, producing a noticeable buzz that differentiates such aircraft. This is particularly noticeable on the Stearman, and noticeable on the T-6 Texan when it enters a sharp-breaking turn. This is undesirable, as the transonic air movement creates disruptive shock waves and turbulence. It is due to these effects that propellers are known to suffer from dramatically decreased performance as they approach the speed of sound. It is easy to demonstrate that the power needed to improve performance is so great that the weight of the required engine grows faster than the power output of the propeller. This problem was one of the issues that led to early research into jet engines, notably by Frank Whittle in England and Hans von Ohain in Germany, who were led to their research specifically in order to avoid these problems in high-speed flight.

Propeller aircraft were, nevertheless, able to approach the speed of sound in a dive. This led to numerous crashes for a variety of reasons. These included the rapidly increasing forces on the various control surfaces, which led to the aircraft becoming difficult to control to the point where many suffered from powered flight into terrain when the pilot was unable to overcome the force on the control stick. The Mitsubishi Zero was infamous for this^[citation needed] problem, and several attempts to fix it only made the problem worse. In the case of the Supermarine Spitfire, the wings suffered from low torsional stiffness, and when ailerons were moved the wing tended to flex such that they counteracted the control input, leading to a condition known as *control reversal*. This was solved in later models with changes to the wing. The P-38 Lightning suffered from a particularly dangerous interaction of the airflow between the wings and tail surfaces in the dive that made it difficult to "pull out", a problem that was later solved with the addition of a "dive flap" that upset the airflow under these circumstances. Flutter due to the formation of shock waves on curved surfaces was another major problem, which led most famously to the breakup of de Havilland Swallow and death of its pilot, Geoffrey de Havilland, Jr.

All of these effects, although unrelated in most ways, led to the concept of a "barrier" that makes it difficult for an aircraft to break the speed of sound.^[5]

Early claims

There are, however, several claims that the sound barrier was broken during World War II. Hans Guido Mutke claimed to have broken the sound barrier on April 9, 1945 in a Messerschmitt Me 262. Mütke reported not just transonic buffeting but the resumption of normal control once a certain speed was exceeded, then a resumption of severe buffeting once the Me 262 slowed again. He also

reported engine flame out. However, this claim is widely disputed by various experts believing the Me 262's structure could not support high transonic, let alone supersonic flight.^[6] The lack of area ruled fuselage and 10 percent thick wings did not prevent other aircraft from exceeding Mach 1 in dives. Chuck Yeager's Bell X1, the F-86 Sabre (with Me-262 profile ^{[7][8]}) and the Convair Sea Dart seaplane exceeded Mach 1 without area rule fuselages. Computational tests carried out by Professor Otto Wagner of the München Technical University in 1999 suggest the Me 262 was capable of supersonic flight during steep dives. Recovering from the dive and the resumption of severe buffeting once subsonic flight was resumed would have been very likely to damage the craft terminally.

On page 13 of the "Me 262 A-1 Pilot's Handbook" issued by Headquarters Air Materiel Command, Wright Field, Dayton, Ohio as Report No. F-SU-1111-ND on January 10, 1946:

"Speeds of 950 km/h (590 mph) are reported to have been attained in a shallow dive 20° to 30° from the horizontal. No vertical dives were made. At speeds of 950 to 1,000 km/h (590 to 620 mph) the air flow around the aircraft reaches the speed of sound, and it is reported that the control surfaces no longer affect the direction of flight. The results vary with different airplanes: some wing over and dive while others dive gradually. It is also reported that once the speed of sound is exceeded, this condition disappears and normal control is restored."

The comments about restoration of flight control and cessation of buffeting above Mach 1 are very significant in a 1946 document.

In his book *Me-163*, former Me-163 pilot Mano Ziegler claims that his friend, test pilot Heini Dittmar, broke the sound barrier when steep-diving the rocket plane and that several on the ground heard the sonic bangs. Heini Dittmar had been accurately and officially recorded at 1,004.5 km/h (623.8 mph) in level flight on October 2, 1941 in the prototype Me-163a V4. He reached this speed at less than full throttle as he was concerned by the transonic buffeting. The craft's Walter RII-203 cold rocket engine produced 7.34 kN (750 kgp / 1,650 lbf) thrust. The flight was made after a drop launch from a carrier plane to conserve fuel, a record that was kept secret until the war's end. The craft's potential performance in a powered dive is unknown but the Me 163B test version of the series rocket plane had an even more powerful engine (HWK 109-509 A-2) and a greater wing sweep as the Me 163 A. Ziegler claims that on July 6, 1944, Heini Dittmar flying a test Comet Me-163BV18 VA + SP was measured traveling at a speed of 1,130 km/h.^[9] Similar claims for the Spitfire and other propeller aircraft are more suspect. It is now known that traditional airspeed gauges using a pitot tube give inaccurately high readings in the transonic, apparently due to shock waves interacting with the tube or the static source. This led to problems then known as "Mach jump".^[10]

Attempts to break the sound barrier

The first self-propelled vehicle to break the sound barrier was probably the first successful test launch of the German V-2 ballistic missile on October 3, 1942, at Peenemünde in Germany. By September 1944, the V-2s routinely achieved Mach 4 (4,900 km/h) during terminal descent.

In 1942 the United Kingdom's Ministry of Aviation began a top secret project with Miles Aircraft to develop the world's first aircraft capable of breaking the sound barrier. The project resulted in the

development of the prototype Miles M.52 jet aircraft, which was designed to reach 1,000 mph (417 m/s; 1,600 km/h) at 36,000 feet (11 km) in 1 minute 30 sec.

The aircraft's design introduced many innovations which are still used on today's supersonic aircraft. The single most important development was the all-moving tailplane, giving extra control to counteract the Mach tuck which allowed control to be maintained to and beyond supersonic speeds. This was wind-tunnel tested at Mach 0.86 in 1944 in the UK.^[11] In the immediate postwar era new data from captured German records suggested that major savings in drag could be had through a variety of means such as swept wings, and Director of Scientific Research, Sir Ben Lockspeiser, decided to cancel the project in light of this new information. Later experimentation with the Miles M.52 design proved that the aircraft would indeed have broken the sound barrier, with an unpowered 3/10 scale replica of the M.52 achieving Mach 1.5 in October 1948.^[12] By that time, the sound barrier had been broken by the Americans, and also by the British De Havilland DH 108.

Sound barrier officially broken

U.S. efforts progressed apace soon after Britain had disclosed all its research and designs to the U.S. government, on the promise that U.S. information would be shared the other way.^[13] The U.S. betrayed by not disclosing any information in return, stating the Pentagon had deemed the project Top Secret.^[citation needed] They took the technological information provided by the British and began work on the Bell XS-1. The final version of the Bell XS-1 has many design similarities to the original Miles version. Also featuring the all-moving tail, the XS-1 was later known as the X-1. It was in the X-1 that Chuck Yeager was credited with being the first man to break the sound barrier in level flight on 14 October 1947, flying at an altitude of 45,000 ft (13.7 km). George Welch made a plausible but officially unverified claim to have broken the sound barrier on 1 October 1947, while flying an XP-86 Sabre. He also claimed to have repeated his supersonic flight on October 14, 1947, 30 minutes before Yeager broke the sound barrier in the Bell X-1. Although evidence from witnesses and instruments strongly imply that Welch achieved supersonic speed, the flights were not properly monitored and are not officially recognized. The XP-86 officially achieved supersonic speed on 26 April 1948.^[14]

On October 14, 1947, just under a month after the United States Air Force had been created as a separate service, the tests culminated in the first manned supersonic flight, piloted by Air Force Captain Charles "Chuck" Yeager in aircraft #46-062, which he had christened "Glamorous Glennis", after his wife. The rocket-powered aircraft was launched from the bomb bay of a specially modified B-29 and glided to a landing on a runway. XS-1 flight number 50 is the first one where the X-1 recorded supersonic flight, at Mach 1.06 (361 m/s, 1,299 km/h, 807.2 mph) peak speed; however, Yeager and many other personnel believe Flight #49 (also with Yeager piloting), which reached a top recorded speed of Mach 0.997 (339 m/s, 1,221 km/h), may have, in fact, exceeded Mach 1.^[citation needed] (The measurements were not accurate to three significant figures and no sonic boom was recorded for that flight.)

As a result of the X-1's initial supersonic flight, the National Aeronautics Association voted its 1948 Collier Trophy to be shared by the three main participants in the program. Honored at the White House by President Harry S. Truman were Larry Bell for Bell Aircraft, Captain Yeager for piloting the flights, and John Stack for the NACA contributions.

Jackie Cochran was the first woman to break the sound barrier on May 18, 1953, in a Canadair Sabre, with Yeager as her wingman.

The sound barrier fades



http://en.wikipedia.org/wiki/File:Yeager_supersonic_flight_1947.ogg

Chuck Yeager broke the sound barrier on October 14, 1947 in the Bell X-1, as shown in this newsreel.

As the science of high-speed flight became more widely understood, a number of changes led to the eventual disappearance of the "sound barrier". Among these were the introduction of swept wings, the area rule, and engines of ever increasing performance. By the 1950s many combat aircraft could routinely break the sound barrier in level flight, although they often suffered from control problems when doing so, such as Mach tuck. Modern aircraft can transition through the "barrier" without it even being noticeable.

By the late 1950s the issue was so well understood that many companies started investing in the development of supersonic airliners, or SSTs, believing that to be the next "natural" step in airliner evolution. History has proven this not to be the case, at least yet, but Concorde and the Tupolev Tu-144 both entered service in the 1970s regardless.

Although Concorde and the Tu-144 were the first aircraft to carry commercial passengers at supersonic speeds, they were not the first or only commercial airliners to break the sound barrier. On August 21, 1961, a Douglas DC-8 broke the sound barrier at Mach 1.012 or 1,240 km/h (776.2 mph) while in a controlled dive through 41,088 feet (12,510 m). The purpose of the flight was to collect data on a new leading-edge design for the wing.^[15] A China Airlines 747 almost certainly broke the sound barrier in an unplanned descent from 41,000 ft (12,500 m) to 9,500 ft (2,900 m) after an in-flight upset on February 19, 1985. It also reached over 5g.^[16]

Breaking the sound barrier on land

The sound barrier was first broken in a vehicle in a sustained way on land in 1948 by a rocket-powered test vehicle at Muroc Air Force Base (now Edwards AFB) in California, United States. It was powered by 6,000 lbs (27 kN) of thrust, reaching 1,019 mph (1,640 km/h).^[17]

On 15 October 1997, in a vehicle designed and built by a team led by Richard Noble, British driver (and Royal Air Force pilot) Andy Green became the first person to break the sound barrier in a land vehicle. The vehicle, called the ThrustSSC ("Super Sonic Car"), captured the record exactly 50 years and one day after Yeager's flight.

References

Notes

1. ^ APOD: 19 August 2007- A Sonic Boom
2. ^ <http://www.eng.vt.edu/fluids/msc/gallery/conden/mpegf14.htm>

3. ^ Refer to the speed of sound for the science behind the velocity referred to as the **sound barrier**, and to sonic boom for information on the sound associated with supersonic flight.
4. ^ Wilford, John Noble (1997-12-02). "Did Dinosaurs Break the Sound Barrier?". *The New York Times*. Archived from the original on 2009-01-15. <http://www.webcitation.org/5dq7UdVkC>. Retrieved 2009-01-15.
5. ^ Portway 1940, p. 18. Quote: "For various reasons it is fairly certain that the maximum attainable speed under self-propelled conditions will be that of sound in air," i.e., 750 mph (1,210 km/h).
6. ^ Me 262 and the Sound Barrier
7. ^ Willy Radinger and Schick 1996, p. 15.
8. ^ Willy and Schick 1996, p. 32.
9. ^ Käsmann, Ferdinand C.W. 1999, pp. 17, 122. Die schnellsten Jets der Welt (in German). Berlin: Aviatic-Verlag GmbH, 1999. ISBN 3-925505-26-1.
10. ^ The Amazing George Welch, First Through the Sonic Wall
11. ^ Comments by Eric "Winkle" Brown
12. ^ Brown 1980, p. 40.
13. ^ Brown 1980, pp. 38–40.
14. ^ Wagner 1963, p. 17.
15. ^ *Douglas Passenger Jet Breaks Sound Barrier*
16. ^ China Airlines Flight 006
17. ^ NASA Timeline

Bibliography

- "Breaking the Sound Barrier." *Modern Marvels (TV program)*. July 16, 2003.
- Brown, Eric. "Miles M.52: The Supersonic Dream." *Air Enthusiast Thirteen*, August-November 1980. ISSN 01443-5450.
- Hallion, Dr. Richard P. "Saga of the Rocket Ships." *AirEnthusiast Five*, November 1977-February 1978. Bromley, Kent, UK: Pilot Press Ltd., 1977.
- Miller, Jay. *The X-Planes: X-1 to X-45*, Hinckley, UK: Midland, 2001. ISBN 1-85780-109-1.
- Pisano, Dominick A., R. Robert van der Linden and Frank H. Winter. *Chuck Yeager and the Bell X-1: Breaking the Sound Barrier*. Washington, DC: Smithsonian National Air and Space Museum (in association with Abrams, New York), 2006. ISBN 0-8109-5535-0.
- Portway, Donald. *Military Science Today*. London: Oxford University Press, 1940.
- Wagner, Ray. *The North American Sabre*. London: Macdonald, 1963.
- Winchester, Jim. "Bell X-1." *Concept Aircraft: Prototypes, X-Planes and Experimental Aircraft* (The Aviation Factfile). Kent, UK: Grange Books plc, 2005. ISBN 1-84013-309-2.
- Wolfe, Tom. *The Right Stuff*. New York: Farrar, Straus and Giroux, 1979. ISBN 0-374-25033-2.
- Yeager, Chuck, Bob Cardenas, Bob Hoover, Jack Russell and James Young. *The Quest for Mach One: A First-Person Account of Breaking the Sound Barrier*. New York: Penguin Studio, 1997. ISBN 0-670-87460-4.
- Yeager, Chuck and Leo Janos. *Yeager: An Autobiography*. New York: Bantam, 1986. ISBN 0-553-25674-2.

Speed of Sound

From Wikipedia, the free encyclopedia

Sound is a vibration that travels through an elastic medium as a wave. The speed of sound describes how far this wave travels in a given amount of time. In dry air at 20 °C (68 °F), the speed of sound is 343 meters per second (1,125 ft/s). This equates to 1,236 kilometers per hour (768 mph) or about one mile in five seconds. This figure for air (or any given gas) increases with gas temperature (equations are given below), but is nearly independent of pressure or density for a given gas. For different gases, the speed of sound is dependent on the mean molecular weight of the gas, and to a lesser extent upon the ways in which the molecules of the gas can store heat energy from compression (since sound in gases is a type of compression).

Although "the speed of sound" is commonly used to refer specifically to the speed of sound waves in air, the speed of sound can be measured in virtually any substance. Sound travels faster in liquids and non-porous solids than it does in air, traveling about 4.4 times faster in water than in air.

Additionally, in solids, there occurs the possibility of two different types of sound waves: one type is associated with compression (the same as usual sound waves in fluids) and the other is associated with shear-stresses, which cannot occur in fluids. These two types of waves have different speeds, and (for example in an earthquake) may thus be initiated at the same time but arrive at distant points at appreciably different times. The speed of compression-type waves in all media is set by the medium's compressibility and density, and the speed of shear-waves in solids is set by the material's rigidity and density.

Sound measurements

Sound pressure p
Particle velocity v
Particle velocity level (SVL)
(Sound velocity level)
Particle displacement ζ
Sound intensity I
Sound intensity level (SIL)
Sound power P_{ac}
Sound power level (SWL)
Sound energy density E
Sound energy flux q
Surface S
Acoustic impedance Z
Speed of sound c

Basic concept



U.S. Navy F/A-18 breaking the sound barrier. The white halo is formed by condensed water droplets which are thought to result from a drop in air pressure around the aircraft (see Prandtl-Glauert Singularity).^{[1][2]}

The transmission of sound can be illustrated by using a toy model consisting of an array of balls interconnected by springs. For real material the balls represent molecules and the springs represent the bonds between them. Sound passes through the model by compressing and expanding the springs, transmitting energy to neighboring balls, which transmit energy to *their* springs, and so on. The speed of sound through the model depends on the stiffness of the springs (stiffer springs transmit energy more quickly). Effects like dispersion and reflection can also be understood using this model.

In a real material, the stiffness of the springs is called the elastic modulus, and the mass corresponds to the density. All other things being equal, sound will travel more slowly in denser materials, and faster in stiffer ones. For instance, sound will travel faster in iron than uranium, and faster in hydrogen than nitrogen, due to the lower density of the first material of each set. At the same time, sound will travel faster in solids than in liquids and faster in liquids than in gases, because the internal bonds in a solid are much stronger than the bonds in a liquid, as are the bonds in liquids compared to gases.

Some textbooks mistakenly state that the speed of sound increases with increasing density. This is usually illustrated by presenting data for three materials, such as air, water and steel, which also have vastly different compressibilities which more than make up for the density differences. An illustrative example of the two effects is that sound travels only 4.4 times faster in water than air, despite enormous differences in compressibility of the two media. The reason is that the larger density of water, which works to *slow* sound in water relative to air, nearly makes up for the compressibility difference in the two media.

General formula

In general, the speed of sound c is given by

$$c = \sqrt{\frac{C}{\rho}}$$

where

C is a coefficient of stiffness (or the modulus of bulk elasticity for gas mediums),
 ρ is the density

Thus the speed of sound increases with the stiffness (the resistance of an elastic body to deformation by an applied force) of the material, and decreases with the density. For general equations of state, if classical mechanics is used, the speed of sound c is given by

$$c^2 = \frac{\partial p}{\partial \rho}$$

where differentiation is taken with respect to adiabatic change.

If relativistic effects are important, the speed of sound may be calculated from the relativistic Euler equations.

In a **non-dispersive medium** sound speed is independent of sound frequency, so the speeds of energy transport and sound propagation are the same. For audible sounds air is a non-dispersive medium. But air does contain a small amount of CO₂ which *is* a dispersive medium, and it introduces dispersion to air at ultrasonic frequencies (> 28 kHz).^[3]

In a **dispersive medium** sound speed is a function of sound frequency, through the dispersion relation. The spatial and temporal distribution of a propagating disturbance will continually change. Each frequency component propagates at its own phase velocity, while the energy of the disturbance propagates at the group velocity. The same phenomenon occurs with light waves; see optical dispersion for a description.

Dependence on the properties of the medium

The speed of sound is variable and depends on the properties of the substance through of which the wave is traveling. In solids, the speed of longitudinal waves depend on the stiffness to shear stress, and the density of the medium. In fluids, the medium's compressibility and density are the important factors.

In gases, compressibility and density are related, making other compositional effects and properties important, such as temperature and molecular composition. In low molecular weight gases, such as helium, sound propagates faster compared to heavier gases, such as xenon (for monatomic gases the speed of sound is about 68% of the mean speed that molecules move in the gas). For a given ideal gas the sound speed depends only on its temperature. At a constant temperature, the ideal gas pressure has no effect on the speed of sound, because pressure and density (also proportional to pressure) have equal but opposite effects on the speed of sound, and the two contributions cancel out exactly. In a similar way, compression waves in gases depend both on compressibility and density—just as in liquids—but in gases the density contributes to the compressibility in such a way that some part of each attribute factors out, leaving only a dependence on temperature, molecular weight, and heat capacity (see derivations below). Thus, for a single given gas (where molecular weight does not change) and over a small temperature range (where heat capacity is relatively constant), the speed of sound becomes dependent on only the temperature of the gas.

In non-ideal gases, such as a van der Waals gas, the proportionality is not exact, and there is a slight dependence of sound velocity on the gas pressure.

Humidity has a small, but measurable effect on sound speed (causing it to increase by about 0.1%-0.6%), because oxygen and nitrogen molecules of the air are replaced by lighter molecules of water. This is a simple mixing effect.

Implications for atmospheric acoustics

In the Earth's atmosphere, the most important factor affecting the speed of sound is the temperature (see Details below). Since temperature and thus the speed of sound normally decrease with increasing altitude, sound is refracted upward, away from listeners on the ground, creating an acoustic shadow at some distance from the source.^[4] The decrease of the sound speed with height is referred to as a negative sound speed gradient. However, in the stratosphere, the speed of sound

increases with height due to heating within the ozone layer, producing a positive sound speed gradient.

Practical formula for dry air

The approximate speed of sound in dry (0% humidity) air, in meters per second ($\text{m}\cdot\text{s}^{-1}$), at temperatures near $0\text{ }^{\circ}\text{C}$, can be calculated from:

$$c_{\text{air}} = (331.3 + (0.606^{\circ}\text{C}^{-1} \cdot \vartheta)) \text{ m} \cdot \text{s}^{-1}$$

where ϑ is the temperature in degrees Celsius ($^{\circ}\text{C}$).

This equation is derived from the first two terms of the Taylor expansion of the following more accurate equation:

$$c_{\text{air}} = 331.3 \text{ m} \cdot \text{s}^{-1} \sqrt{1 + \frac{\vartheta}{273.15^{\circ}\text{C}}}$$

The value of 331.3 m/s , which represents the $0\text{ }^{\circ}\text{C}$ speed, is based on theoretical (and some measured) values of the heat capacity ratio, γ , as well as on the fact that at 1 atm real air is very well described by the ideal gas approximation. Commonly found values for the speed of sound at $0\text{ }^{\circ}\text{C}$ may vary from 331.2 to 331.6 due to the assumptions made when it is calculated. If ideal gas γ is assumed to be $7/5 = 1.4$ exactly, the $0\text{ }^{\circ}\text{C}$ speed is calculated (see section below) to be 331.3 m/s , the coefficient used above.

This equation is correct to a much wider temperature range, but still depends on the approximation of heat capacity ratio being independent of temperature, and will fail, particularly at higher temperatures. It gives good predictions in relatively dry, cold, low pressure conditions, such as the Earth's stratosphere. A derivation of these equations will be given in the following section.

Details

Speed in ideal gases and in air

For a gas, K (the bulk modulus in equations above, equivalent to C , the coefficient of stiffness in solids) is approximately given by

$$K = \gamma \cdot p$$

thus

$$c = \sqrt{\gamma \cdot \frac{p}{\rho}}$$

Where:

γ is the adiabatic index also known as the *isentropic expansion factor*. It is the ratio of specific heats of a gas at a constant-pressure to a gas at a constant-volume (C_p / C_v), and arises because a classical sound wave induces an adiabatic compression, in which the heat of the compression does not have enough time to escape the pressure pulse, and thus contributes to the pressure induced by the compression.

p is the pressure.

ρ is the density

Using the ideal gas law to replace p with nRT/V , and replacing ρ with nM/V , the equation for an ideal gas becomes:

$$c_{\text{ideal}} = \sqrt{\gamma \cdot \frac{p}{\rho}} = \sqrt{\frac{\gamma \cdot R \cdot T}{M}} = \sqrt{\frac{\gamma \cdot k \cdot T}{m}}$$

where

- c_{ideal} is the speed of sound in an ideal gas.
- R (approximately $8.3145 \text{ J} \cdot \text{mol}^{-1} \cdot \text{K}^{-1}$) is the molar gas constant.[1]
- k is the Boltzmann constant
- γ (gamma) is the adiabatic index (sometimes assumed $7/5 = 1.400$ for diatomic molecules from kinetic theory, assuming from quantum theory a temperature range at which thermal energy is fully partitioned into rotation (rotations are fully excited), but none into vibrational modes. Gamma is actually experimentally measured over a range from 1.3991 to 1.403 at 0 degrees Celsius, for air. Gamma is assumed from kinetic theory to be exactly $5/3 = 1.6667$ for monoatomic molecules such as noble gases).
- T is the absolute temperature in kelvins.
- M is the molar mass in kilograms per mole. The mean molar mass for dry air is about 0.0289645 kg/mol .
- m is the mass of a single molecule in kilograms.

This equation applies only when the sound wave is a small perturbation on the ambient condition, and the certain other noted conditions are fulfilled, as noted below. Calculated values for c_{air} have been found to vary slightly from experimentally determined values.^[5]

Newton famously considered the speed of sound before most of the development of thermodynamics and so incorrectly used isothermal calculations instead of adiabatic. His result was missing the factor of γ but was otherwise correct.

Numerical substitution of the above values gives the ideal gas approximation of sound velocity for gases, which is accurate at relatively low gas pressures and densities (for air, this includes standard Earth sea-level conditions). Also, for diatomic gases the use of $\gamma = 1.4000$ requires that the gas exist in a temperature range high enough that rotational heat capacity is fully excited (i.e., molecular rotation is fully used as a heat energy "partition" or reservoir); but at the same time the temperature must be low enough that molecular vibrational modes contribute no heat capacity (i.e., insignificant heat goes into vibration, as all vibrational quantum modes above the minimum-energy-mode, have energies too high to be populated by a significant number of molecules at this temperature). For air, these conditions are fulfilled at room temperature, and also temperatures considerably below room temperature (see tables below). See the section on gases in specific heat capacity for a more complete discussion of this phenomenon.

If temperatures in degrees Celsius($^{\circ}\text{C}$) are to be used to calculate air speed in the region near 273 kelvins, then Celsius temperature $\vartheta = T - 273.15$ may be used.

$$c_{\text{ideal}} = \sqrt{\gamma \cdot R \cdot T} = \sqrt{\gamma \cdot R \cdot (\vartheta + 273.15 \text{ }^{\circ}\text{C})}$$

$$c_{\text{ideal}} = \sqrt{\gamma \cdot R \cdot 273.15} \cdot \sqrt{1 + \frac{\vartheta}{273.15 \text{ }^{\circ}\text{C}}}$$

For dry air, where ϑ (theta) is the temperature in degrees Celsius($^{\circ}\text{C}$).

Making the following numerical substitutions: $R = R_*/M_{\text{air}}$, where

$R_* = 8.314510 \cdot \text{J} \cdot \text{mol}^{-1} \cdot \text{K}^{-1}$ is the molar gas constant,

$M_{\text{air}} = 0.0289645 \cdot \text{kg} \cdot \text{mol}^{-1}$, and using the ideal diatomic gas value of $\gamma = 1.4000$

Then:

$$c_{\text{air}} = 331.3 \text{ m} \cdot \text{s}^{-1} \sqrt{1 + \frac{\vartheta^{\circ}\text{C}}{273.15 \text{ }^{\circ}\text{C}}}$$

Using the first two terms of the Taylor expansion:

$$c_{\text{air}} = 331.3 \text{ m} \cdot \text{s}^{-1} \left(1 + \frac{\vartheta^{\circ}\text{C}}{2 \cdot 273.15 \text{ }^{\circ}\text{C}}\right)$$

$$c_{\text{air}} = (331.3 + 0.606 \text{ }^{\circ}\text{C}^{-1} \cdot \vartheta) \text{ m} \cdot \text{s}^{-1}$$

The derivation includes the two approximate equations which were given in the introduction.

Effects due to wind shear

The speed of sound varies with temperature. Since temperature and sound velocity normally decrease with increasing altitude, sound is refracted upward, away from listeners on the ground, creating an acoustic shadow at some distance from the source.^[6] Wind shear of $4 \text{ m} \cdot \text{s}^{-1} \cdot \text{km}^{-1}$ can produce refraction equal to a typical temperature lapse rate of $7.5 \text{ }^{\circ}\text{C}/\text{km}$.^[7] Higher values of wind gradient will refract sound downward toward the surface in the downwind direction,^[8] eliminating the acoustic shadow on the downwind side. This will increase the audibility of sounds downwind. This downwind refraction effect occurs because there is a wind gradient; the sound is not being carried along by the wind.^[9]

For sound propagation, the exponential variation of wind speed with height can be defined as follows:^[10]

$$U(h) = U(0)h^{\zeta}$$

$$\frac{dU}{dH} = \zeta \frac{U(h)}{h}$$

where:

$U(h)$ = speed of the wind at height h , and $U(0)$ is a constant

ζ = exponential coefficient based on ground surface roughness, typically between 0.08 and 0.52

$$\frac{dU}{dH} = \text{expected wind gradient at height } h$$

In the 1862 American Civil War Battle of Iuka, an acoustic shadow, believed to have been enhanced by a northeast wind, kept two divisions of Union soldiers out of the battle,^[11] because they could not hear the sounds of battle only six miles downwind.^[12]

Tables

In the standard atmosphere:

T_0 is 273.15 K (= 0 °C = 32 °F), giving a theoretical value of 331.3 m·s⁻¹ (= 1086.9 ft/s = 1193 km·h⁻¹ = 741.1 mph = 644.0 knots). Values ranging from 331.3-331.6 may be found in reference literature, however.

T_{20} is 293.15 K (= 20 °C = 68 °F), giving a value of 343.2 m·s⁻¹ (= 1126.0 ft/s = 1236 km·h⁻¹ = 767.8 mph = 667.2 knots).

T_{25} is 298.15 K (= 25 °C = 77 °F), giving a value of 346.1 m·s⁻¹ (= 1135.6 ft/s = 1246 km·h⁻¹ = 774.3 mph = 672.8 knots).

In fact, assuming an ideal gas, the speed of sound c depends on temperature only, **not on the pressure** or **density** (since these change in lockstep for a given temperature and cancel out). Air is almost an ideal gas. The temperature of the air varies with altitude, giving the following variations in the speed of sound using the standard atmosphere - *actual conditions may vary*.

Effect of temperature			
Temperature	Speed of sound	Density of air	Acoustic impedance
ϑ in °C	c in m·s ⁻¹	ρ in kg·m ⁻³	Z in N·s·m ⁻³
-25	315.8	1.423	449.4
-20	318.9	1.395	444.9
-15	322.1	1.368	440.6
-10	325.2	1.342	436.1
-5	328.3	1.317	432.0
0	331.3	1.292	428.4
+5	334.3	1.269	424.3
+10	337.3	1.247	420.6
+15	340.3	1.225	416.8
+20	343.2	1.204	413.2
+25	346.1	1.184	409.8
+30	349.0	1.164	406.2
+35	351.9	1.146	403.3

Given normal atmospheric conditions, the temperature, and thus speed of sound, varies with altitude:

Altitude	Temperature	m·s ⁻¹	km·h ⁻¹	mph	knots
Sea level	15 °C (59 °F)	340	1225	761	661
11 000 m–20 000 m (Cruising altitude of commercial jets, and first supersonic flight)	-57 °C (-70 °F)	295	1062	660	573
29 000 m (Flight of X-43A)	-48 °C (-53 °F)	301	1083	673	585

Effect of frequency and gas composition

The medium in which a sound wave is traveling does not always respond adiabatically, and as a result the speed of sound can vary with frequency.^[13]

The limitations of the concept of speed of sound due to extreme attenuation are also of concern. The attenuation which exists at sea level for high frequencies applies to successively lower frequencies as atmospheric pressure decreases, or as the mean free path increases. For this reason, the concept of speed of sound (except for frequencies approaching zero) progressively loses its range of applicability at high altitudes.^[5]

The molecular composition of the gas contributes both as the mass (M) of the molecules, and their heat capacities, and so both have an influence on speed of sound. In general, at the same molecular mass, monatomic gases have slightly higher sound speeds (over 9% higher) because they have a higher γ ($5/3 = 1.66\dots$) than diatomics do ($7/5 = 1.4$). Thus, at the same molecular mass, the sound speed of a monatomic gas goes up by a factor of

$$\frac{c_{\text{gas:monatomic}}}{c_{\text{gas:diatomic}}} = \sqrt{\frac{5/3}{7/5}} = \sqrt{\frac{25}{21}} = 1.091\dots$$

This gives the 9 % difference, and would be a typical ratio for sound speeds at room temperature in helium vs. deuterium, each with a molecular weight of 4. Sound travels faster in helium than deuterium because adiabatic compression heats helium more, since the helium molecules can store heat energy from compression only in translation, but not rotation. Thus helium molecules (monatomic molecules) travel faster in a sound wave and transmit sound faster. (Sound generally travels at about 70% of the mean molecular speed in gases).

Note that in this example we have assumed that temperature is low enough that heat capacities are not influenced by molecular vibration (see heat capacity). However, vibrational modes simply cause gammas which decrease toward 1, since vibration modes in a polyatomic gas gives the gas additional ways to store heat which do not affect temperature, and thus do not affect molecular velocity and sound velocity. Thus, the effect of higher temperatures and vibrational heat capacity acts to increase the difference between sound speed in monatomic vs. polyatomic molecules, with the speed remaining greater in monatomics.

Mach number

Mach number, a useful quantity in aerodynamics, is the ratio of an object's speed to the speed of sound in the medium through which it is passing (again, usually air). At altitude, for reasons explained, Mach number is a function of temperature.

Aircraft flight instruments, however, operate using pressure differential to compute Mach number; not temperature. The assumption is that a particular pressure represents a particular altitude and, therefore, a standard temperature. Aircraft flight instruments need to operate this way because the impact pressure sensed by a Pitot tube is dependent on altitude as well as speed.

Assuming air to be an ideal gas, the formula to compute Mach number in a subsonic compressible flow is derived from Bernoulli's equation for $M < 1$.^[14]

$$M = \sqrt{5 \left[\left(\frac{q_c}{P} + 1 \right)^{\frac{2}{7}} - 1 \right]}$$

where

M is Mach number

q_c is impact pressure and

P is static pressure.

The formula to compute Mach number in a supersonic compressible flow is derived from the Rayleigh Supersonic Pitot equation:

$$M = 0.88128485 \sqrt{\left[\left(\frac{q_c}{P} + 1 \right) \left(1 - \frac{1}{7M^2} \right)^{2.5} \right]}$$

where

M is Mach number

q_c is impact pressure measured behind a normal shock

P is static pressure.

As can be seen, M appears on both sides of the equation. The easiest method to solve the supersonic M calculation is to enter both the subsonic and supersonic equations into a computer spreadsheet such as Microsoft Excel, OpenOffice.org Calc, or some equivalent program. First determine if M is indeed greater than 1.0 by calculating M from the subsonic equation. If M is greater than 1.0 at that point, then use the value of M from the subsonic equation as the initial condition in the supersonic equation. Then perform a simple iteration of the supersonic equation, each time using the last computed value of M , until M converges to a value--usually in just a few iterations.^[14]

Experimental methods

A range of different methods exist for the measurement of sound in air.

The first man to successfully measure the speed of Sound was William Derham

Single-shot timing methods

The simplest concept is the measurement made using two microphones and a fast recording device such as a digital storage scope. This method uses the following idea.

If a sound source and two microphones are arranged in a straight line, with the sound source at one end, then the following can be measured:

1. The distance between the microphones (x), called microphone basis.
2. The time of arrival between the signals (delay) reaching the different microphones (t)

Then $v = x / t$

An older method is to create a sound at one end of a field with an object that can be seen to move when it creates the sound. When the observer sees the sound-creating device act they start a stopwatch and when the observer hears the sound they stop their stopwatch. Again using $v = x / t$ you can calculate the speed of sound. A separation of at least 200 m between the two experimental parties is required for good results with this method.

Other methods

In these methods the time measurement has been replaced by a measurement of the inverse of time (frequency).

Kundt's tube is an example of an experiment which can be used to measure the speed of sound in a small volume. It has the advantage of being able to measure the speed of sound in any gas. This method uses a powder to make the nodes and antinodes visible to the human eye. This is an example of a compact experimental setup.

A tuning fork can be held near the mouth of a long pipe which is dipping into a barrel of water. In this system it is the case that the pipe can be brought to resonance if the length of the air column in the pipe is equal to $(\{1+2n\}\lambda/4)$ where n is an integer. As the antinodal point for the pipe at the open end is slightly outside the mouth of the pipe it is best to find two or more points of resonance and then measure half a wavelength between these.

Here it is the case that $v = f\lambda$

Non-gaseous media

Speed of sound in solids

In a solid, there is a non-zero stiffness both for volumetric and shear deformations. Hence, it is possible to generate sound waves with different velocities dependent on the deformation mode. Sound waves generating volumetric deformations and shear deformations are called longitudinal waves and shear waves, respectively. The sound velocities of such waves are respectively given by^[15]:

$$c_l = \sqrt{\frac{K}{\rho}} = \sqrt{\frac{E}{3\rho(1-2\nu)}}$$

$$c_s = \sqrt{\frac{G}{\rho}},$$

where K and G are the bulk modulus and shear modulus of the elastic materials, respectively, E is the Young's modulus, and ν is Poisson's ratio.

For example, for steel, $K = 17 \times 10^{10}$ [Pa], and $\rho = 7700$ [kg/m³], yielding a c_l of 4699 m/s.^[16] Notice, however, that a more commonly accepted value of c_l seems to be 5930 m/s.^[17]

Speed of sound in liquids

In a fluid the only non-zero stiffness is to volumetric deformation (a fluid does not sustain shear forces).

Hence the speed of sound in a fluid is given by

$$c_{\text{fluid}} = \sqrt{\frac{K}{\rho}}$$

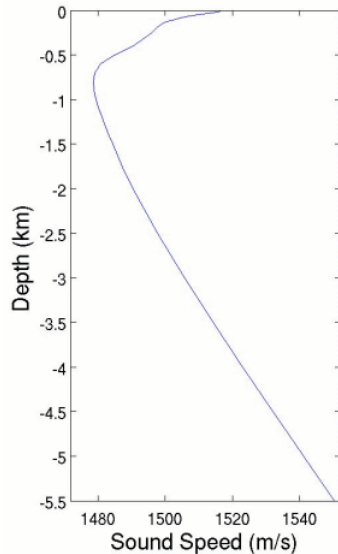
where

K is the bulk modulus of the fluid

Water

The speed of sound in water is of interest to anyone using underwater sound as a tool, whether in a laboratory, a lake or the ocean. Examples are sonar, acoustic communication and acoustical oceanography. See *Discovery of Sound in the Sea* for other examples of the uses of sound in the ocean (by both man and other animals). In fresh water, sound travels at about 1497 m/s at 25 °C. See *Technical Guides - Speed of Sound in Pure Water* for an online calculator.

Seawater



Sound speed as a function of depth at a position north of Hawaii in the Pacific Ocean derived from the 2005 World Ocean Atlas. The SOFAR channel is centered on the minimum in sound speed at ca. 750-m depth.

In salt water that is free of air bubbles or suspended sediment, sound travels at about 1560 m/s. The speed of sound in seawater depends on pressure (hence depth), temperature (a change of 1 °C ~ 4 m/s), and salinity (a change of 1‰ ~ 1 m/s), and empirical equations have been derived to accurately calculate sound speed from these variables.^[18] Other factors affecting sound speed are minor. For more information see Dushaw et al.^[19]

A simple empirical equation for the speed of sound in sea water with reasonable accuracy for the world's oceans is due to Mackenzie:^[20]

$$c(T, S, z) = a_1 + a_2T + a_3T^2 + a_4T^3 + a_5(S - 35) + a_6z + a_7z^2 + a_8T(S - 35) + a_9Tz^3$$

where T , S , and z are temperature in degrees Celsius, salinity in parts per thousand and depth in metres, respectively. The constants a_1, a_2, \dots, a_9 are:

$$a_1 = 1448.96, a_2 = 4.591, a_3 = -5.304 \times 10^{-2}, a_4 = 2.374 \times 10^{-4}, a_5 = 1.340, a_6 = 1.630 \times 10^{-2}, \\ a_7 = 1.675 \times 10^{-7}, a_8 = -1.025 \times 10^{-2}, a_9 = -7.139 \times 10^{-13}$$

with check value 1550.744 m/s for $T=25\text{ }^{\circ}\text{C}$, $S=35\text{‰}$, $z=1000\text{ m}$. This equation has a standard error of 0.070 m/s for salinities between 25 and 40 ppt. See Technical Guides - Speed of Sound in Sea-Water for an online calculator.

Other equations for sound speed in sea water are accurate over a wide range of conditions, but are far more complicated, e.g., that by V. A. Del Grosso^[21] and the Chen-Millero-Li Equation.^{[22][19]}

Speed in plasma

The speed of sound in a plasma for the common case that the electrons are hotter than the ions (but not too much hotter) is given by the formula (see here)

$$c_s = (\gamma Z k T_e / m_i)^{1/2} = 9.79 \times 10^3 (\gamma Z T_e / \mu)^{1/2} \text{ m/s}$$

In contrast to a gas, the pressure and the density are provided by separate species, the pressure by the electrons and the density by the ions. The two are coupled through a fluctuating electric field.

Gradients

When sound spreads out evenly in all directions, the intensity drops in proportion to the inverse square of the distance. However, in the ocean there is a layer called the 'deep sound channel' or SOFAR channel which can confine sound waves at a particular depth, allowing them to travel much further. In the SOFAR channel, the speed of sound is lower than that in the layers above and below. Just as light waves will refract towards a region of higher index, sound waves will refract towards a region where their speed is reduced. The result is that sound gets confined in the layer, much the way light can be confined in a sheet of glass or optical fiber.

A similar effect occurs in the atmosphere. Project Mogul successfully used this effect to detect a nuclear explosion at a considerable distance.

References

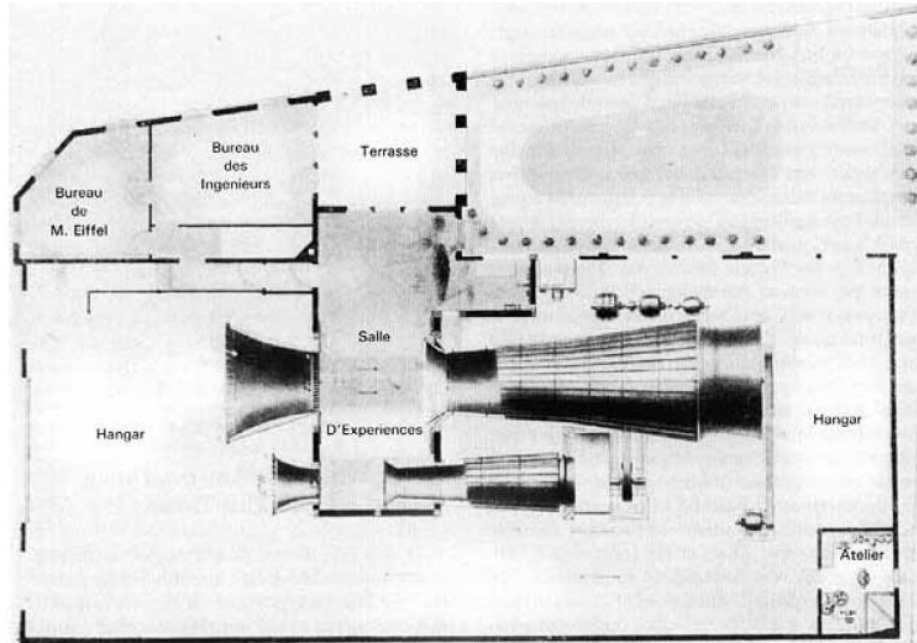
1. ^ APOD: 19 August 2007- A Sonic Boom
2. ^ <http://www.eng.vt.edu/fluids/msc/gallery/conden/mpegf14.htm>
3. ^ Dean, E. A. (August 1979). Atmospheric Effects on the Speed of Sound, Technical report of Defense Technical Information Center
4. ^ Everest, F. (2001). *The Master Handbook of Acoustics*. New York: McGraw-Hill. pp. 262–263. ISBN 0071360972.
5. ^ ^a ^b U.S. Standard Atmosphere, 1976, U.S. Government Printing Office, Washington, D.C., 1976.
6. ^ Everest, F. (2001). *The Master Handbook of Acoustics*. New York: McGraw-Hill. pp. 262–263. ISBN 0071360972.
7. ^ Uman, Martin (1984). *Lightning*. New York: Dover Publications. ISBN 0486645754.
8. ^ Volland, Hans (1995). *Handbook of Atmospheric Electrodynamics*. Boca Raton: CRC Press. pp. 22. ISBN 0849386470.

9. ^ Singal, S. (2005). *Noise Pollution and Control Strategy*. Alpha Science International, Ltd. pp. 7. ISBN 1842652370. "It may be seen that refraction effects occur only because there is a wind gradient and it is not due to the result of sound being convected along by the wind."
10. ^ Bies, David (2003). *Engineering Noise Control; Theory and Practice*. London: Spon Press. pp. 235. ISBN 0415267137. "As wind speed generally increases with altitude, wind blowing towards the listener from the source will refract sound waves downwards, resulting in increased noise levels."
11. ^ Cornwall, Sir (1996). *Grant as Military Commander*. Barnes & Noble Inc. ISBN 1566199131 pages = p. 92.
12. ^ Cozzens, Peter (2006). *The Darkest Days of the War: the Battles of Iuka and Corinth*. Chapel Hill: The University of North Carolina Press. ISBN 0807857831.
13. ^ A B Wood, A Textbook of Sound (Bell, London, 1946)
14. ^ ^{a b} Olson, Wayne M. (2002). "AFFTC-TIH-99-02, *Aircraft Performance Flight Testing*." (PDF). Air Force Flight Test Center, Edwards AFB, CA, United States Air Force.
15. ^ L. E. Kinsler et al. (2000), *Fundamentals of acoustics*, 4th Ed., John Wiley and sons Inc., New York, USA
16. ^ L. E. Kinsler et al. (2000), *Fundamentals of acoustics*, 4th Ed., John Wiley and sons Inc., New York, USA
17. ^ J. Krautkrämer and H. Krautkrämer (1990), *Ultrasonic testing of materials*, 4th fully revised edition, Springer-Verlag, Berlin, Germany, p. 497
18. ^ APL-UW TR 9407 High-Frequency Ocean Environmental Acoustic Models Handbook, pp. I1-I2.
19. ^ ^{a b} Dushaw, Brian D.; Worcester, P.F.; Cornuelle, B.D.; and Howe, B.M. (1993). "On equations for the speed of sound in seawater". *Journal of the Acoustical Society of America* **93** (1): 255-275. doi:10.1121/1.405660.
20. ^ Mackenzie, Kenneth V. (1981). "Discussion of sea-water sound-speed determinations". *Journal of the Acoustical Society of America* **70** (3): 801-806. doi:10.1121/1.386919.
21. ^ Del Grosso, V. A. (1974). "New equation for speed of sound in natural waters (with comparisons to other equations)". *Journal of the Acoustical Society of America* **56** (4): 1084-1091. doi:10.1121/1.1903388.
22. ^ Meinen, Christopher S.; Watts, D. Randolph (1997). "Further evidence that the sound-speed algorithm of Del Grosso is more accurate than that of Chen and Millero". *Journal of the Acoustical Society of America* **102** (4): 2058-2062. doi:10.1121/1.419655.

- Applied Physics Laboratory – University of Washington, 1994

Subsonic and Transonic Wind Tunnel

From Wikipedia, the free encyclopedia

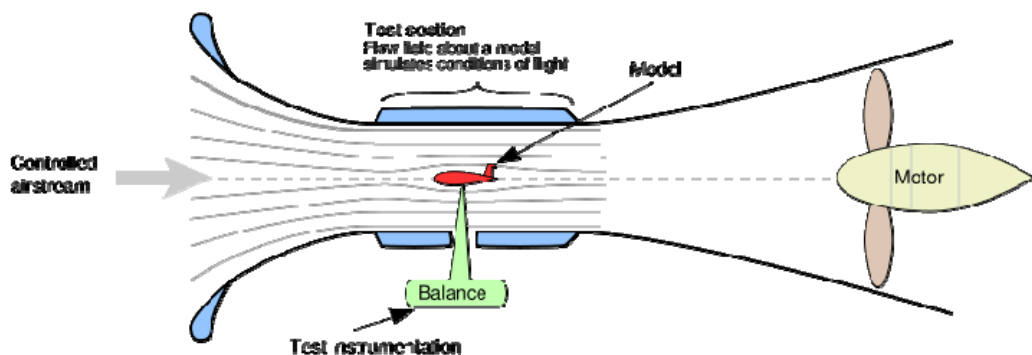


Eiffel wind tunnel

Subsonic tunnel

Low speed wind tunnels are used for operations at very low mach number, with speeds in the test section up to 400 km/h (~ 100 m/s, $M = 0.3$). They are of open-return type (see figure below), or return flow (see figure below). The air is moved with a propulsion system made of a large axial fan that increases the dynamic pressure to overcome the viscous losses.

Open wind tunnel



Schematic of Eiffel type open wind tunnel.

The working principle is based on the continuity and Bernoulli's equation:

The continuity equation is given by:

$$AV = \text{constant} \Rightarrow \frac{dA}{A} = -\frac{dV}{V}$$

The Bernoulli equation states:

$$P_{\text{total}} = P_{\text{static}} + P_{\text{dynamic}} = P_s + \frac{1}{2}\rho V^2$$

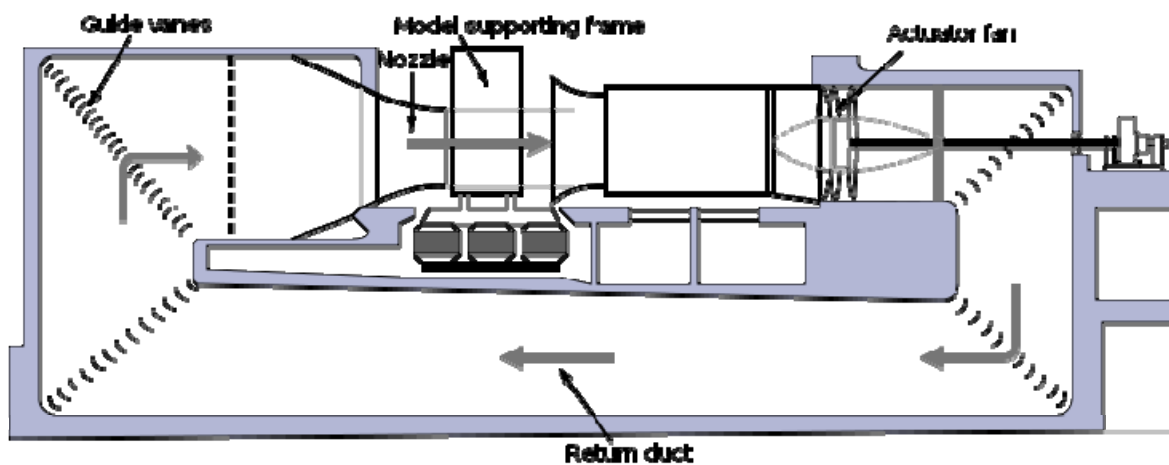
Putting Bernoulli into the continuity equation gives:

$$V_m^2 = 2 \frac{C^2}{C^2 - 1} \frac{P_{\text{settl}} - p_m}{\rho} \approx 2 \frac{\Delta p}{\rho}$$

The contraction ratio of a wind tunnel can now be calculated by:

$$C = \frac{A_{\text{settl}}}{A_m}$$

Closed wind tunnel



Closed circuit or return flow low speed wind tunnel.

In a return-flow wind tunnel the return duct must be properly designed to reduce the pressure losses and to ensure smooth flow in the test section. The compressible flow regime: Again with the continuity law, but now for isentropic flow gives:

$$-\frac{d\rho}{\rho} = -\frac{1}{a^2} \frac{dp}{\rho} = -\frac{1}{a^2} \frac{-\rho V dV}{\rho} = \frac{V}{a^2} dV$$

The 1-D area-velocity is known as:

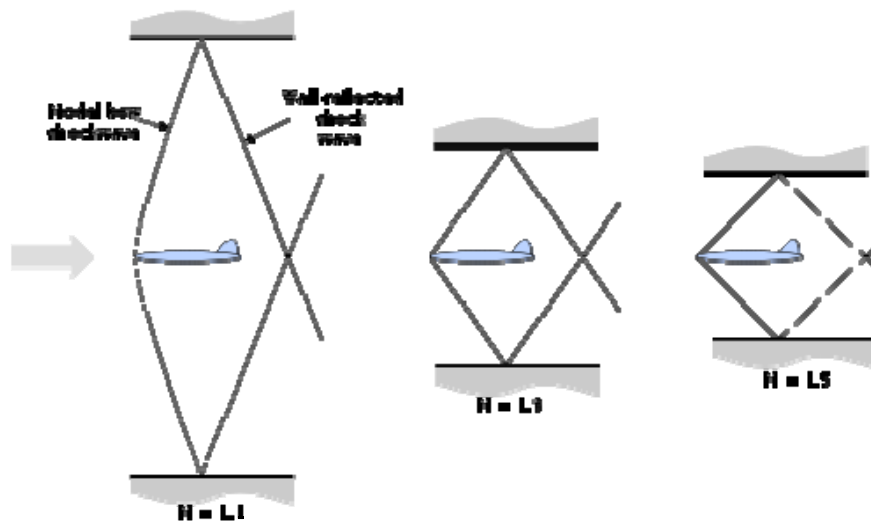
$$\frac{dA}{A} = (M^2 - 1) \frac{dV}{V}$$

The minimal area A where $M=1$, also known as the *sonic throat* area is then given for a perfect gas:

$$\left(\frac{A}{A_{throat}}\right)^2 = \frac{1}{M^2} \left(\frac{2}{\gamma + 1} \left(1 + \frac{\gamma - 1}{2} M^2 \right) \right)^{\frac{\gamma + 1}{\gamma - 1}}$$

Transonic tunnel

High subsonic wind tunnels ($0.4 < M < 0.75$) or transonic wind tunnels ($0.75 < M < 1.2$) are designed on the same principles as the subsonic wind tunnels. Transonic wind tunnels are able to achieve speeds close to the speeds of sound. The highest speed is reached in the test section. The Mach number is approximately one with combined subsonic and supersonic flow regions. Testing at transonic speeds presents additional problems, mainly due to the reflection of the shock waves from the walls of the test section (see figure below or enlarge the thumb picture at the right). Therefore, perforated or slotted walls are required to reduce shock reflection from the walls. Since important viscous or inviscid interactions occur (such as shock waves or boundary layer interaction) both Mach and Reynolds number are important and must be properly simulated. Large scale facilities and/or pressurized or cryogenic wind tunnels are used.



de Laval nozzle

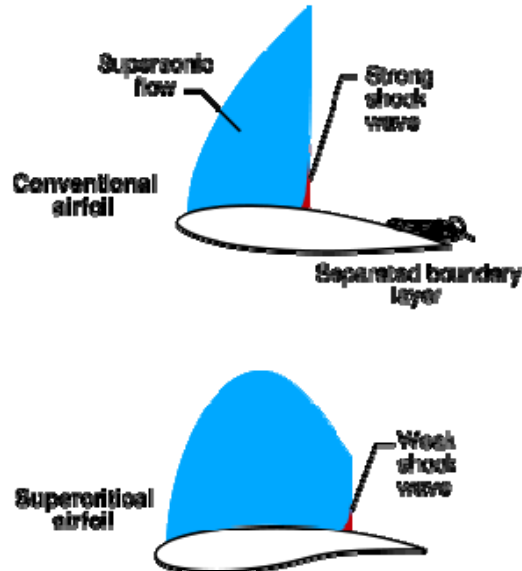
With a sonic throat, the flow can be accelerated or slowed down. This follows from the 1-D area-Velocity equation. If an acceleration to supersonic flow is required, a convergent-divergent nozzle is required. Otherwise:

- Subsonic ($M < 1$) then $\frac{dA}{dx} < 0 \Rightarrow$ converging
- Sonic throat ($M = 1$) where $\frac{dA}{dx} = 0$
- Supersonic ($M > 1$) then $\frac{dA}{dx} > 0 \Rightarrow$ diverging

Conclusion: The Mach number is controlled by the expansion ratio $\frac{A}{A_{throat}}$

Supercritical Airfoil

From Wikipedia, the free encyclopedia



The supercritical airfoil, below, maintains a lower Mach number over its upper surface than the conventional airfoil, above, which induces a weaker shock.

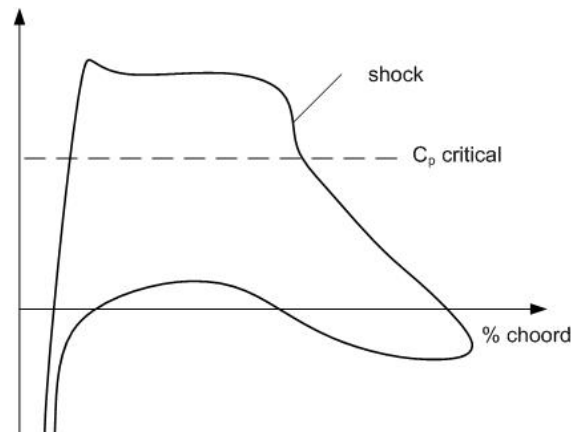
A **supercritical airfoil** is an airfoil designed, primarily, to delay the onset of wave drag in the transonic speed range. Supercritical airfoils are characterized by their flattened upper surface, highly cambered (curved) aft section, and greater leading edge radius as compared to traditional airfoil shapes. The supercritical airfoils were designed in the 1960s, by then NASA scientist Richard Whitcomb, and were first tested on the TF-8A Crusader. While the design was initially developed as part of the supersonic transport (SST) project at NASA, it has since been mainly applied to increase the fuel efficiency of many high subsonic aircraft. Research in 1940 by DVL's K. A. Kawalki led to subsonic profiles very similar to the supercritical profiles, which was the basis for the objection in 1984 against the US-patent specification for the supercritical airfoil.^[1] The supercritical airfoil shape is incorporated into the design of a supercritical wing.

Research aircraft of the 1950s and 60s found it difficult to break the sound barrier, or even reach Mach 0.9, with conventional airfoils. Supersonic airflow over the upper surface of the traditional airfoil induced excessive wave drag and a form of stability loss called Mach tuck. Due to the airfoil shape used, supercritical wings experience these problems less severely and at much higher speeds, thus allowing the wing to maintain high performance at speeds closer to Mach 1. Techniques learned from studies of the original supercritical airfoil sections are used to design airfoils for high-speed subsonic and transonic aircraft from the Boeing 777 to the McDonnell Douglas AV-8B Harrier II.



NASA TF-8A in 1973

Supercritical airfoils have four main benefits: they have a higher drag divergence Mach number,^[2] they develop shock waves farther aft than traditional airfoils,^[3] they greatly reduce shock-induced boundary layer separation, and their geometry allows for more efficient wing design (e.g., a thicker wing and/or reduced wing sweep, each of which may allow for a lighter wing). At a particular speed for a given airfoil section, the critical Mach number, flow over the upper surface of an airfoil can become locally supersonic, but slow down to match the pressure at the trailing edge of the lower surface without a shock. However, at a certain higher speed, the drag divergence Mach number, a shock is required to recover enough pressure to match the pressures at the trailing edge. This shock causes transonic wave drag, and induces flow separation behind it; both have negative effects on the airfoil's performance.



Supercritical airfoil Mach Number/pressure coefficient diagram. The sudden increase in pressure coefficient at midchord is due to the shock. (y-axis: Mach number (or pressure coefficient, negative up); x-axis: position along chord, leading edge left)

At a certain point along the airfoil, a shock is generated, which increases the pressure coefficient to the critical value C_{p-crit} , where the local flow velocity will be Mach 1. The position of this shockwave is determined by the geometry of the airfoil; a supercritical foil is more efficient because the shockwave is minimized and is created as far aft as possible thus reducing drag. Compared to a typical airfoil section, the supercritical airfoil creates more of its lift at the aft end, due to its more even pressure distribution over the upper surface.

In addition to improved transonic performance, a supercritical wing's enlarged leading edge gives it excellent high-lift characteristics. As a result, aircraft utilizing a supercritical wing have superior

takeoff and landing performance. This makes the supercritical wing a favorite for designers of cargo transport aircraft. A notable example of one such heavy-lift aircraft that uses a supercritical wing is the C-17 Globemaster III.

Notes

1. ^ Hans-Ulrich Meier, Die Pfeilflügelentwicklung in Deutschland bis 1945, ISBN 3763761306 Einspruch (1984) gegen US-Patentschrift NASA über »superkritische Profile«, basierend auf den Berechnungsmethoden von K. H. Kawalki (1940) p.107 german
2. ^ Anderson, J: *Fundamentals of Aerodynamics*, p. 622. McGraw-Hill, 2001.
3. ^ *ibid.*: p. 623.

Supersonic

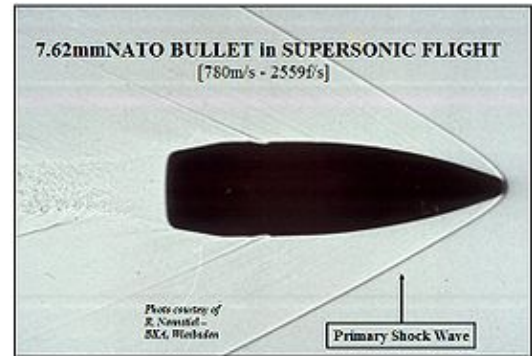
From Wikipedia, the free encyclopedia



A United States Navy F/A-18E/F Super Hornet in transonic flight.



U.S. Navy F/A-18 approaching the sound barrier. The white halo is formed by condensed water droplets which result from a drop in air pressure around the aircraft (see Prandtl-Glauert Singularity).
[1][2]



Shadowgraph of a 7,62 x 51 NATO bullet in supersonic flight at Mach 2.4. Notice the shockwave (Mach cone) from the bullet's tip, a secondary shockwave coining from the cannellure and the turbulence in the air behind the bullet

The term **supersonic** is used to define a speed that is over the speed of sound (Mach 1). At a typical temperature like 21 °C (70 °F), the threshold value required for an object to be traveling at a supersonic speed is approximately 344 m/s, (1,129 ft/s, 761 mph or 1,238 km/h). Speeds greater than 5 times the speed of sound are often referred to as hypersonic. Speeds where only some parts of the air around an object (such as the ends of rotor blades) reach supersonic speeds are labeled transonic (typically somewhere between Mach 0.8 and Mach 1.2).

Sounds are travelling vibrations (pressure waves) in an elastic medium. In gases sound travels longitudinally at different speeds, mostly depending on the molecular mass and temperature of the gas; (pressure has little effect). Since air temperature and composition varies significantly with altitude, Mach numbers for aircraft can change without airspeed varying. In water at room temperature supersonic can be considered as any speed greater than 1,440 m/s (4,724 ft/s). In solids, sound waves can be longitudinal or transverse and have even higher velocities. Supersonic fracture is crack motion faster than the speed of sound in a brittle material.

Supersonic objects

Most modern fighter aircraft are supersonic, but Concorde and the Tupolev Tu-144 were the only supersonic passenger aircraft. An aircraft that can still sustain supersonic flight without using an afterburner is called a supercruise aircraft. Due to its ability to supercruise for several hours and the relatively high frequency of flight over several decades, Concorde spent more time flying supersonically than all other aircraft put together by a considerable margin. Since Concorde's final retirement flight on November 26, 2003, there are no supersonic passenger aircraft left in service.

Some large bombers, such as the Tupolev Tu-160 and Rockwell/Boeing B-1B are also supersonic-capable.

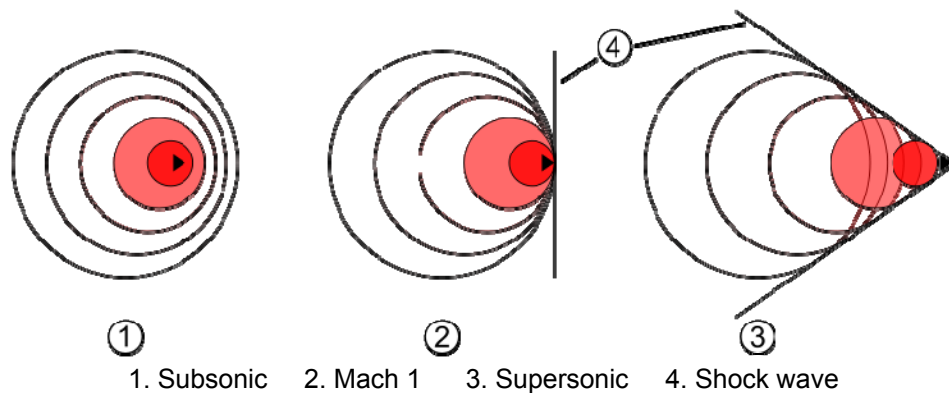
Most modern firearm bullets are supersonic, with rifle projectiles often travelling at speeds approaching and in some cases largely exceeding Mach 3.

Most spacecraft, most notably the Space Shuttle are supersonic at least during portions of their reentry, though the effects on the spacecraft are reduced by low air pressures. During ascent, launch vehicles generally avoid going supersonic below 30 km (~98,400 feet) to reduce air drag.

Note that the speed of sound decreases somewhat with altitude, due to lower temperatures found there (typically up to 25 km). At even higher altitudes the temperature starts increasing, with the corresponding increase in the speed of sound.^[3]

A wave traveling through a bull whip is also capable of achieving supersonic speeds.^[4]

Breaking the sound barrier



In aerodynamics, the **sound barrier** usually refers to the point at which an aircraft moves from transonic to **supersonic** speed. The term came into use during World War II when a number of aircraft started to encounter the effects of compressibility, a grab-bag of unrelated aerodynamic effects. The term fell out of use in the 1950s when aircraft started to routinely "break" the sound barrier. Refer to the speed of sound for the science behind the velocity referred to as the **sound barrier**, and to sonic boom for information on the sound associated with supersonic flight. Captain Charles E. Yeager was the first man to reach supersonic speed in controlled level flight.

Supersonic flight

Supersonic aerodynamics are simpler than subsonic because the airsheets at different points along the plane often can't affect each other. Supersonic jets and rocket vehicles require several times greater thrust to push through the extra drag experienced within the transonic region (around Mach 0.85-1.2). At these speeds Aerospace engineers can gently guide air around the fuselage of the aircraft without producing new shock waves but any change in cross sectional area further down the vehicle leads to shock waves along the body. Designers use the Supersonic area rule and the Whitcomb area rule to minimize sudden changes in size.

It should be kept in mind, however, that the aerodynamic principles behind a supersonic aircraft are often more complex than described above because such an aircraft must be efficient and stable at supersonic, transonic *and* subsonic flight.

One problem with sustained supersonic flight is the generation of heat in flight. At high speeds aerodynamic heating can occur, so an aircraft must be designed to operate and function under very high temperatures. Duralumin, the traditional aircraft material, starts to lose strength and go plastic at relatively low temperatures, and is unsuitable for continuous use at speeds above Mach 2.2 to 2.4. Materials such as titanium and stainless steel allow operations at much higher temperatures. For example, the SR-71 Blackbird jet could fly continuously at Mach 3.1 while some parts were above 315°C (600°F).

Another area of concern for continued high-speed operation is the engines. Jet engines create thrust by increasing the temperature of the air they ingest, and as the aircraft speeds up, friction and compression heats this air before it reaches the engines. The maximum temperature of the exhaust is determined by the materials in the turbine at the rear of the engine, so as the aircraft speeds up the difference in intake and exhaust temperature the engine can extract decreases, and the thrust along with it. Air cooling the turbine area to allow operations at higher temperatures was a key solution, one that continued to improve through the 1950s and on to this day.

Intake design was also a major issue. Normal jet engines can only ingest subsonic air, so for supersonic operation the air has to be slowed down. Ramps or cones in the intake are used to create shock waves that slows the airflow before it reaches the engine. Doing so removes energy from the airflow, causing drag. The key to reducing this drag is to use multiple small oblique shock waves, but this was difficult because the angle they make inside the intake changes with Mach number. In order to efficiently operate across a range of speeds, the shock waves have to be "tuned."

An aircraft able to operate for extended periods at supersonic speeds has a potential range advantage over a similar design operating subsonically. Most of the drag an aircraft sees while speeding up to supersonic speeds occurs just below the speed of sound, due to an aerodynamic effect known as wave drag. An aircraft that can accelerate past this speed sees a significant drag decrease, and can fly supersonically with improved fuel economy. However, due to the way lift is generated supersonically, the lift-to-drag ratio of the aircraft as a whole drops, leading to lower range, offsetting or overturning this advantage.

The key to having low supersonic drag is to properly shape the overall aircraft to be long and skinny, as close as possible to a "perfect" shape, the von Karman ogive or Sears-Haack body. This has led to almost every supersonic cruising aircraft looking very similar to every other, with a very long and skinny fuselage and large delta wings, cf. SR-71, Concorde, etc. Although not ideal for passenger aircraft, this shaping is quite adaptable for bomber use.

History

The Hungarian-American scientist Theodore Kármán was the inventor of the mathematical tools to study fluid flow, the mathematical background of supersonic flight, and the swept-back wing. He is often called as "the father of Supersonic Flight" stability of laminar flow, turbulence, airfoils in steady and unsteady flow, boundary layers, and supersonic aerodynamics. He made additional

contributions in other fields, including elasticity, vibration, heat transfer, and crystallography. His name appears in at least the following concepts: Foppl-von Kármán equations (large deflection of elastic plates) Born-von Kármán lattice model (crystallography) Chaplygin-Kármán-Tsien approximation (potential flow) Falkowich-Kármán equation (transonic flow) von Kármán constant (wall turbulence) Kármán line (aerodynamics/astronautics) Kármán-Howarth equation (turbulence) Kármán-Nikuradse correlation (viscous flow; coauthored by Johann Nikuradse) Kármán-Pohlhausen parameter (boundary layers) Kármán-Trefftz transformation (airfoil theory) Prandtl-von Kármán law (velocity in open channel flow) von Kármán integral equation (boundary layers) von Kármán ogive (supersonic aerodynamics) von Kármán vortex street (flow past cylinder) von Kármán-Tsien compressibility correction

References

1. ^ APOD: 2007 August 19 - A Sonic Boom
2. ^ <http://www.eng.vt.edu/fluids/msc/gallery/conden/mpegf14.htm>
3. ^ eXtreme High Altitude Conditions Calculator
4. ^ Hypography - Science for everyone - Whip Cracking Mystery Explained

Supersonic Transport Aircraft

From Wikipedia, the free encyclopedia



The Concorde supersonic transport had an ogival delta wing, a slender fuselage and four underslung Rolls-Royce/Snecma Olympus 593 engines.

A **supersonic transport (SST)** is a civil supersonic aircraft designed to transport passengers at speeds greater than the speed of sound. The only SST to see regular international service was Concorde, and the only other design built in quantity was the Tupolev Tu-144. The last passenger flight of the Tu-144 was in June 1978, and Concorde's last flight was on November 26, 2003. Following the permanent cessation of flying by all Concorde, there are no SSTs in commercial service.

Challenges of supersonic passenger flight

Aerodynamics

For all aircraft the power lost to drag is proportional to the cube of airspeed and proportional to the density of the air. Since supersonic aircraft fly faster, everything else being equal this would give much higher drag. Supersonic aircraft avoid this by simply flying higher, where the air density is much lower.

However, as speeds approach the speed of sound, the phenomenon of wave drag appears. This is a powerful form of drag that begins at about Mach 0.8, and ends at about Mach 1.2, (transonic speeds). Between these speeds, the peak coefficient of drag (C_d) can be up to four times that of subsonic drag. Above the transonic range, C_d drops dramatically again, although it remains 30 to 50% higher than at subsonic speeds. Supersonic aircraft must have considerably more power than subsonic aircraft require to overcome this wave drag, and although cruising performance above transonic speed is more efficient, it is still rather less efficient than flying subsonically.

Another issue in supersonic flight is the lift to drag ratio (L/D ratio) of the wings. At supersonic speeds, airfoils generate lift in an entirely different manner than at subsonic speeds, and are invariably less efficient. For this reason, considerable research has been put into designing planforms for sustained supersonic cruise. At about Mach 2, a typical wing design will cut its L/D ratio in half (e.g., the Concorde vehicle managed a ratio of 7.14, whereas the subsonic Boeing 747 has an L/D ratio of 17).^[1] Because an aircraft's design must provide enough lift to overcome its own weight, a reduction of its L/D ratio at supersonic speeds requires additional thrust to maintain its airspeed and altitude.

Engines

Jet engine design differs significantly between supersonic and subsonic aircraft. Jet engines, as a class, can supply *increased* fuel efficiency at supersonic speeds, even though their specific fuel consumption is greater at higher speeds. Because their speed over the ground is greater, this decrease in efficiency is less than proportional to speed until well above Mach 2, and the consumption per mile is lower.



A preserved ex-British Airways Concorde at Filton Aerodrome, Bristol, England shows the slender fuselage necessary for supersonic flight

When Concorde was being designed by Aérospatiale-BAC, high bypass jet engines had not yet been deployed on subsonic aircraft, and Concorde would have been more competitive. When these high bypass jet engines reached commercial service in the 1960s, subsonic jet engines immediately became much more efficient, closer to the efficiency of turbojets at supersonic speeds. A bypass design is more fuel efficient at subsonic speeds, as they can reduce the jet exhaust speed to better match that of the aircraft. This capability would not improve efficiency, indeed would reduce it, during supersonic cruise, where the smaller size of turbojet engines gives low drag and better net efficiency.^[2] For example the early TU-144S was fitted with a low bypass jet engine which was much less efficient than Concorde's turbojets. The later TU-144D featured a turbojet engine and was comparable.

Modern jet engines employ a high overall pressure ratio wherever possible, which, for fundamental reasons, yields better fuel efficiency and it may be that a more modern design would give even better fuel efficiency than Concorde's engines.

Structural issues

Supersonic vehicle speeds demand narrower wing and fuselage designs, and are subject to greater stresses and temperatures. This leads to aeroelasticity problems, which require heavier structures to minimize unwanted flexing. SSTs also require a much stronger (and therefore heavier) structure because their fuselage must be pressurized to a greater differential than subsonic aircraft, which do not operate at the high altitudes necessary for supersonic flight. These factors together meant that the empty weight per seat of Concorde is more than three times that of a Boeing 747.

However, Concorde and the TU-144 were both constructed of conventional aluminum (duralumin), whereas more modern materials such as carbon fibre and Kevlar are much stronger in tension for their weight (important to deal with pressurization stresses) as well as, when mixed with polymers being more rigid, so it's likely that considerable improvements could be made, far more so than with conventional aircraft.

High costs

Higher fuel costs and lower passenger capacities due to the aerodynamic requirement for a narrow fuselage make SSTs an expensive form of commercial civil transportation compared with subsonic aircraft. Both Concorde and the Boeing 747 use approximately the same amount of fuel to cover the same distance, but the 747 can carry more than four times as many passengers.

Nevertheless, fuel costs are not the bulk of the price for most subsonic aircraft passenger tickets. For the transatlantic business market that SST aircraft were utilized for, Concorde was actually very successful, and was able to sustain a higher ticket price. Now that commercial SST aircraft have stopped flying, it has become clearer that Concorde made substantial profit for British Airways.^[3]

Sonic booms

The sonic boom was not thought to be a serious issue due to the high altitudes at which the planes flew, but experiments in the mid-1960s such as the Oklahoma City sonic boom tests and studies of the USAF's North American XB-70 Valkyrie proved otherwise.^[4]

The annoyance of a sonic boom can be avoided by waiting until the aircraft is at high altitude over water before reaching supersonic speeds; this is the technique used by Concorde. However, it precludes supersonic flight over populated areas. Supersonic aircraft have poor lift/drag ratios at subsonic speeds as compared to subsonic aircraft (unless technologies such as swing wing are employed), and hence burn more fuel, which results in their use being economically disadvantageous on such flight paths.

Additionally, during the original SST efforts in the 1960s, it was suggested that careful shaping of the fuselage of the aircraft could reduce the intensity of the sonic boom's shock waves that reach the ground. One design caused the shock wave to interfere with each other, greatly reducing sonic boom. This was difficult to test at the time, but the increasing power of computer-aided design has since made this considerably easier. In 2003, Shaped Sonic Boom Demonstration aircraft was flown which proved the soundness of the design and demonstrated the capability of reducing the boom by about half. Even lengthening the vehicle (without significantly increasing the weight) would seem to reduce the boom intensity.^[4]

If the intensity of the boom can be reduced, then this may make even very large designs of supersonic aircraft acceptable for overland flight (see sonic boom).

Need to operate aircraft over a wide range of speeds

The aerodynamic design of a supersonic aircraft needs to change with its speed for optimal performance. Thus, an SST would ideally change shape during flight to maintain optimal

performance at both subsonic and supersonic speeds. Such a design would introduce complexity which increases maintenance needs, operations costs, and safety concerns.

In practice all supersonic transports have used essentially the same shape for subsonic and supersonic flight, and a compromise in performance is chosen, often to the detriment of low speed flight. For example, Concorde had very high drag (a lift to drag ratio of about 4) at slow speed, but it travelled at high speed for most of the flight. Designers of The Concorde were forced to spend a massive 5000 hours optimizing the vehicle shape in wind tunnel tests to maximise the overall performance over the entire flightplan.

Some designs of supersonic transports possessed swing wings to give higher efficiency at low speeds, but the increased space required for such a feature produced capacity problems that proved ultimately insurmountable.

North American Aviation had an unusual approach to this problem with the XB-70 Valkyrie. By lowering the outer panels of the wings at high Mach numbers, they were able to take advantage of compression lift on the underside of the aircraft. This improved the L/D ratio by about 30%.

Noise problems

One of the problems with Concorde and the Tu-144's operation was the high engine noise levels, associated with very high jet velocities used during take-off, and even more importantly flying over communities near the airport. Other supersonic planes are even noisier. SST engines need a fairly high specific thrust (net thrust/airflow) during supersonic cruise, to minimize engine cross-sectional area and, thereby, nacelle drag. Unfortunately this implies a high jet velocity, which makes the engines noisy which causes problems particularly at low speeds/altitudes and at take-off.

Therefore, a future SST might well benefit from a Variable Cycle Engine, where the specific thrust (and therefore jet velocity and noise) is low at take-off, but is forced high during Supersonic Cruise. Transition between the two modes would occur at some point during the Climb and back again during the Descent (to minimize jet noise upon Approach). The difficulty is devising a Variable Cycle Engine configuration that meets the requirement for a low cross-sectional area during Supersonic Cruise.

Skin temperature

As a supersonic aircraft flies, it adiabatically compresses the air in front of the vehicle. This heats up the air, and some of this heat transfers to the aircraft.

Normal subsonic aircraft are traditionally made of aluminium. However aluminium, while being light and strong, is not able to withstand temperatures much over 127 °C; above 127 °C the aluminium gradually loses its temper and is weakened. This corresponds to an airspeed of about Mach 2.2.

For aircraft that fly at Mach 3, materials such as stainless steel (XB-70 Valkyrie) or titanium (SR-71) have been used, at considerable increase in expense, as the properties of these materials make the aircraft much more difficult to manufacture.

Poor range

The range of supersonic aircraft can be estimated with the Breguet range equation.

The high per-passenger takeoff weight makes it difficult to obtain a good fuel fraction. This, together with the relatively poor supersonic lift/drag ratios, supersonic aircraft have historically had relatively poor range. This meant that a lot of routes were non viable, and this in turn helped mean that they sold poorly with airlines.

Airline desirability of SSTs

Airlines buy aircraft as a means of making money, and wish to make as much return on investment as possible from their assets.

Airlines potentially value very fast aircraft, because it permits the aircraft to make more flights per day, which allows for higher return on investment. However, Concorde's high noise levels around airports, time zone issues and insufficient speed meant that only a single return trip could be made per day, so the extra speed was not an advantage to the airline other than as a selling feature to its customers.^[5]

Since SSTs emit sonic booms at supersonic speeds, and are not usually particularly efficient at subsonic speeds, this reduces the routes that the aircraft can be used on, and this massively reduces the desirability of such aircraft for most airlines.

Supersonic aircraft have higher per-passenger fuel costs than subsonic aircraft.

The American SSTs were intended to fly at Mach 3, partly for this reason. However, allowing for acceleration and deceleration time, this only would have cut 20 minutes off a transatlantic trip which would probably not have been enough to perform an extra roundtrip, and the aircraft would have been much more expensive for the airlines to purchase.

History

Throughout the 1950s an SST looked possible from a technical standpoint, but it was not clear if it could be made economically viable. There was a good argument for supersonic speeds on medium- and long-range flights at least, where the increased speed and potential good economy once supersonic would offset the tremendous amount of fuel needed to overcome the wave drag. The main advantage appeared to be practical; these designs would be flying at least three times as fast as existing subsonic transports, and would be able to replace three planes in service, and thereby lower costs in terms of manpower and maintenance.



A Concorde landing

Serious work on SST designs started in the mid-1950s, when the first generation of supersonic fighter aircraft were entering service. In Europe, government-subsidized SST programs quickly settled on the delta wing in most studies, including the Sud Aviation Super-Caravelle and Bristol 223, although Armstrong-Whitworth proposed a more radical design, the Mach 1.2 M-Wing. By the early 1960s, the designs had progressed to the point where the go-ahead for production was given, but costs were so high that Bristol and Sud eventually merged their efforts in 1962 to produce Concorde.

This development set off panic in the US industry, where it was thought that Concorde would soon replace all other long range designs. Congress was soon funding an SST design effort, selecting the existing Lockheed L-2000 and Boeing 2707 designs, to produce an even more advanced, larger, faster and longer ranged design. The Boeing design was eventually selected for continued work. The Soviet Union set out to produce its own design, the Tu-144, which was nicknamed the "Concordski."

In the 1960s environmental concerns came to the fore for the first time. The SST was seen as particularly offensive due to its sonic boom and the potential for its engine exhaust to damage the ozone layer. Both problems impacted the thinking of lawmakers, and eventually Congress dropped funding for the US SST program in 1971, and all overland commercial supersonic flight was banned.



Tupolev Tu-144LL

Concorde was now ready for service. The US political outcry was so high that New York banned the plane outright. This destroyed the aircraft's economic prospects — it had been built with the London-New York route in mind. However, the plane was allowed into Washington, DC, and the service was so popular that New Yorkers were soon complaining because they did not have it. It was not long before Concorde was flying into JFK after all.

Along with shifting political considerations, the flying public continued to show interest in high-speed ocean crossings. This started a second round of design studies in the US, under the name **AST**, for **Advanced Supersonic Transport**. Lockheed's **SCV** was a new design for this category, while Boeing continued studies with the 2707 as a baseline.

However by this time the economics of past SST concepts no longer made sense. When first designed, the SSTs were envisioned to compete with long-range aircraft seating 80 to 100

passengers such as the Boeing 707, but with newer aircraft such as the Boeing 747 carrying four times that, the speed and fuel advantages of the SST concept were washed away by sheer size.

Another problem was that the wide range of speeds over which an SST operates makes it difficult to improve engines. While subsonic engines had made great strides in increasing efficiencies through the 1960s with the introduction of the turbofan engine with ever-increasing bypass ratios, the fan concept is difficult to use at supersonic speeds where the "proper" bypass is about 0.45^[6], as opposed to 2.0 or higher for subsonic designs. For both of these reasons the SST designs were doomed to higher operational costs, and the AST programs faded away by the early 1980s.

Concorde only sold to British Airways and Air France, with subsidized purchases that were to return 80% of the profits to the government. In practice for almost all of the length of the arrangement, there was no profit to be shared. After Concorde was privatised, cost reduction measures (notably the closing of the metallurgical wing testing site which had done enough temperature cycles to validate the aircraft through to 2010) and ticket price raises led to substantial profits.

Since Concorde stopped flying it has been revealed that over the life of Concorde, the plane did prove profitable, at least to British Airways. Concorde operating costs over nearly 28 years of operation were approximately £1 billion, with revenues of £1.75 billion.^[3]

Aircraft histories

Concorde

In total, 20 Concordees were built, six for development and 14 for commercial service.

These were:

- Two prototypes
- Two pre-production aircraft
- more than 200 production of aircraft
 - The first two of these did not enter commercial service
 - Of the 10 that flew commercially, but 2 crashed in 2000,2001 and 4 went out of service before the crash. 5 of them were still in service in April 2003

All but two of these aircraft, a remarkably high percentage for any commercial fleet, are preserved; the two that are not preserved are F-BVFD (cn 211), parked as a spare-parts source in 1982 and scrapped in 1994, and F-BTSC (cn 203), which crashed in Paris on July 25, 2000.

Tupolev 144

A total of 16 airworthy Tu-144s were built: the prototype Tu-144 reg 68001, a pre-production Tu-144S reg 77101, nine production Tu-144S reg 77102 – 110, and five Tu-144D reg 77111 – 115. A seventeenth Tu-144 (reg 77116) was never completed. There was also at least one ground test airframe for static testing in parallel with the prototype 68001 development.

Hypersonic transports

While conventional turbo and ramjet engines are able to remain reasonably efficient up to Mach 5.5, some ideas for very high speed flight above Mach 6 are also sometimes discussed; with the aim of reducing travel times down to one or two hours anywhere in the world.

These vehicle proposals very typically either use rocket or scramjet engines; pulse detonation engines have also been proposed.

There are many difficulties with such flight, both technical and economic.

Rocket engined vehicles while technically practical (either as ballistic transports or as semiballistic transports using wings) would use a very large amount of propellant and operate best at speeds between about Mach 8 and orbital speeds. Rockets compete best with air breathing jet engines on cost at very long range, however even for antipodal travel, costs would be only somewhat lower than orbital launch costs.

Scramjets currently are not practical for passenger carrying vehicles.

Current research and development

In April 1994, Aerospatiale, British Aerospace and Deutsche Aerospace AG (DASA) created the European Supersonic Research Program (ESRP) with plans for a second-generation Concorde to enter service in 2010. The plane was to be called the Avion de Transport Supersonique Futur. In parallel, SNECMA, Rolls-Royce, MTU München and Fiat started working together in 1991 on the development of a new engine. Investing no more than US\$12 million per year, mainly company funded, the research program covers materials, aerodynamics, systems and engine integration for a reference configuration. The ESRP exploratory study is based on a Mach 2, 250-seat, 5,500 nautical mile-range (10,186 km) aircraft, with the baseline design looking very much like an enlarged Concorde with canards.

Meanwhile NASA started a series of projects to study advances in the state of SST design. As part of the High Speed Civil Transport program a Tu-144 aircraft was re-engined in order to carry out supersonic experiments in Russia in the mid-1990s, but development was ended in 1999.

Japan has a supersonic transport research program. In 2005, it was announced that a Japanese-French joint venture would continue research into a design the plane would be called Next Generation Supersonic Transport, JAXA hopes the Next Generation Supersonic Transport would be flying by 2015.^[7] An 11.5-meter model was successfully flight-tested in October 2005.^[8]

Another area that has seen research interest is the supersonic business jet (SSBJ). Some business jet customers are prepared to pay heavily for decreased travel times and the noise issues are less serious in a smaller craft. Sukhoi and Gulfstream co-investigated such a craft in the mid-1990s, as did Dassault Aviation in the early 2000s. Aerion Corporation's Aerion SBJ, the SAI Quiet Supersonic Transport and Tupolev's Tu-444 are current SSBJ projects.^[9]

Another development in the field of engines is the pulse detonation engine. These engines, often referred to as PDEs, offer even greater efficiencies than current turbofan engines, while allowing for high speed use. NASA maintains a PDE research effort, with the baseline being a Mach 5 airliner. A PDE was recently test flown successfully ^[10].

At the most exotic, high supersonic designs like Reaction Engines Skylon would seem to be capable of reaching Mach 5.5 within the atmosphere, before activating a rocket engine and entering orbit. The design can later reenter the atmosphere and land back on the runway it took off from.

There is also a very long distance supersonic/hypersonic transport version of Skylon, the A2, being evaluated by the European Union as part of the LAPCAT project, which would travel at Mach 5 and would be capable of travelling Brussels to Sydney in 4.6 hours.^[11]

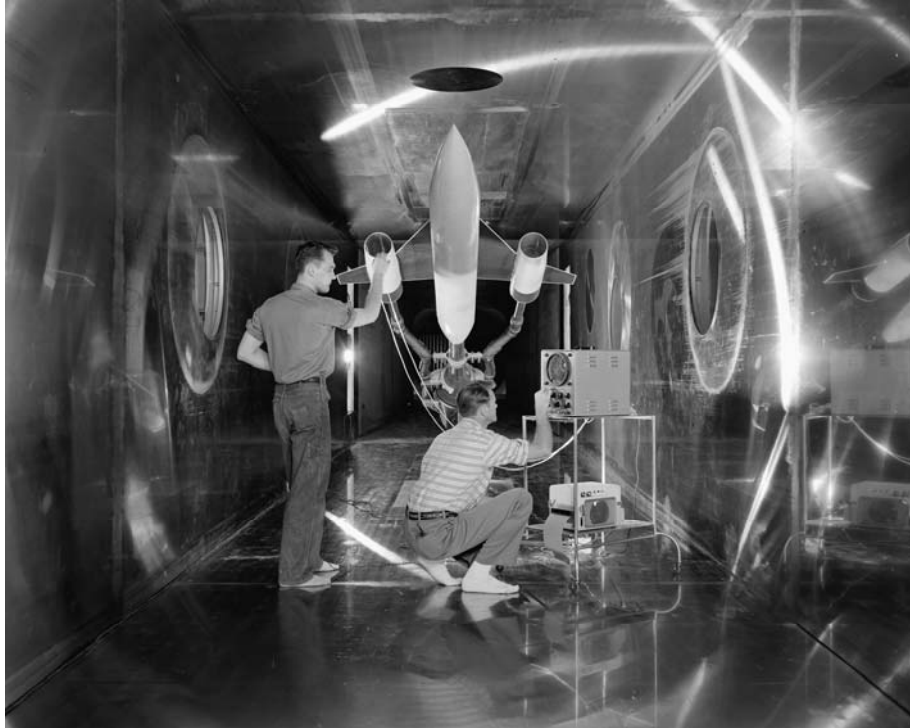
Also Tupolev plans to build the Tupolev Tu-244 although this SST may be canceled because of budget problems.

References

1. ^ Aerodynamic Database, Lift-to-Drag Ratios
2. ^ NASA SP 472-Supersonic Cruise Technology F.Edward McLean
3. ^ ^{a b} 'Did Concorde make a profit for British Airways?'
4. ^ ^{a b} Sonic boom Abatement
5. ^ BBC News | In Pictures
6. ^ http://ntrs.nasa.gov/archive/nasa/casi.ntrs.nasa.gov/19940022103_1994022103.pdf
7. ^ "Japan, France working on new supersonic jet", MSNBC, June 15, 2005.
8. ^ "Supersonic jet launch 'successful'", TheAge.com.au, October 10, 2005.
9. ^ "Supersonic travel may return, minus boom", by A. Pawlowski, June 18, 2009, CNN
10. ^ <http://www.af.mil/news/story.asp?id=123099095>
11. ^ Reaction Engines Limited: LAPCAT

Supersonic Wind Tunnel

From Wikipedia, the free encyclopedia



Engineers check an aircraft model before a test run in the Supersonic Wind Tunnel at Lewis Flight Propulsion Laboratory.

A **supersonic wind tunnel** is a wind tunnel that produces supersonic speeds ($1.2 < M < 5$). The Mach number and flow are determined by the nozzle geometry. The Reynolds number is varied changing the density level (pressure in the settling chamber). Therefore a high pressure ratio is required (for a supersonic regime at $M=4$, this ratio is of the order of 10). Apart from that, condensation or liquefaction can occur. This means that a supersonic wind tunnel needs a drying or a pre-heating facility. A supersonic wind tunnel has a large power demand leading to only intermittent operation.

Restrictions for supersonic tunnel operation

Minimum required pressure ratio

Optimistic estimate: Pressure ratio \leq the total pressure ratio over normal shock at M in test section:

$$\frac{P_t}{P_{amb}} \leq \left(\frac{P_{t1}}{P_{t2}} \right)_{M_1=M_m}$$

Examples:

Temperature effects: condensation

Temperature in the test section:

$$\frac{T_m}{T_t} = \left(1 + \frac{\gamma - 1}{2} M_m^2\right)^{-1}$$

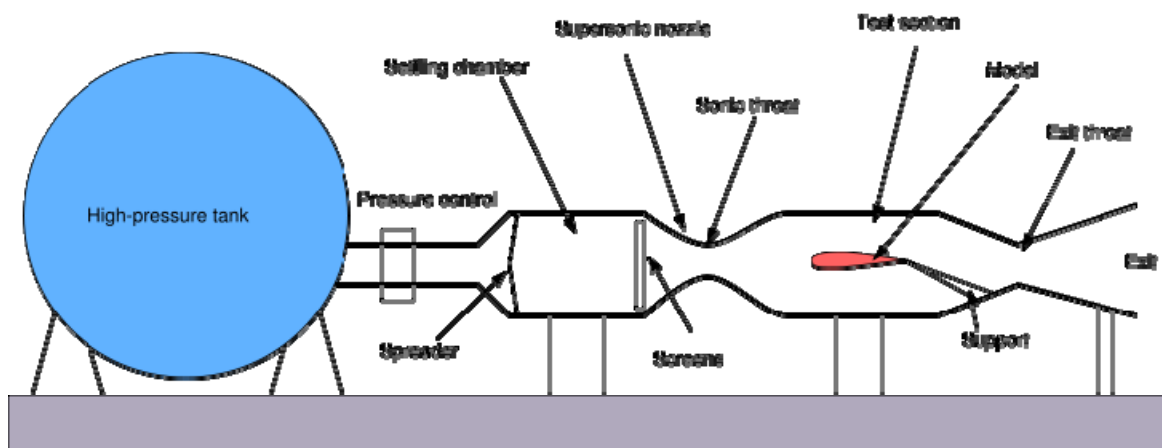
with $T_t = 330\text{K}$: $T_m = 70\text{K}$ at $M_m = 4$

The Mach range is limited by reservoir temperature

Power requirements

The power required to run a supersonic windtunnel is enormous, of the order of 50 MW per square meter of test section. For this reason most wind tunnels operate intermittently using energy stored in high-pressure tanks. These windtunnels are also called intermittent supersonic blowdown wind tunnels (of which a schematic preview is given below). Another way of achieving the huge power output is with the use of a vacuum storage tank. These tunnels are called indraft supersonic wind tunnels. Other problems operating a supersonic wind tunnel include:

- enough supply of dry air
- wall interference effects
- fast instruments needed for intermittent measurements



Tunnels such as a Ludwieg tube have short test times (usually less than one second), relatively high Reynolds number, and low power requirements.

Further reading

- Pope, A.; Goin, K. (1978). *High-speed Wind Tunnel Testing*. Krieger. ISBN 088275727X.

Transonic

From Wikipedia, the free encyclopedia



F/A-18 flying at transonic speed

Transonic is an aeronautics term referring to the condition in which a range of velocities of airflow exist surrounding and flowing past an air vehicle or an airfoil. Air flow velocities are concurrently below, at, and above the speed of sound at the pressure and temperature of the airflow of the air vehicle's local environment (about mach 0.8–1.2). It is formally defined as the range of speeds between the critical mach number, when some parts of the airflow over an air vehicle or air foil are supersonic, and a higher speed, typically near Mach 1.2, when all of the airflow is supersonic. Between these speeds some of the airflow is supersonic, and some is not.

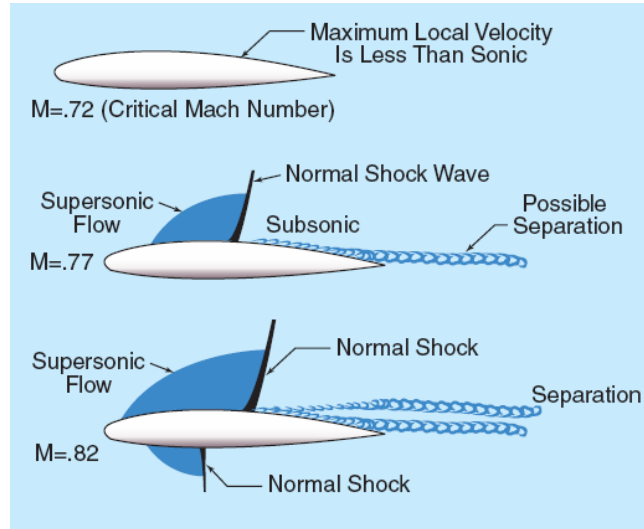
Most modern jet powered aircraft are engineered to operate with as high a transonic air speed as possible, before their air foils experience the onset of transonic wave drag, which is prevalent and really defines the beginning of the transonic speed ranges. The importance of transonic wave drag lies in the fact that it is both an unpredictable and non-linear phenomena. That is the behavior of an airfoil; or an airframe; is very difficult to predict at the onset of transonic wave drag. Also the rate of increase in drag is almost never linearly related to an increase in speed. In the transonic region an air foil's speed may increase by say 2%, but the increase in drag (in the transonic region) may be 8%. Worst of all in the transonic region for an airfoil an increase in speed that goes from a 2% to 3% increase; can yield an increase in transonic drag that rises from 8% to 16%. That is how non-linear the phenomenon is. Attempts to combat wave drag can be seen on all high-speed aircraft; most notable is the use of swept wings, but another common form is a wasp-waist fuselage as a side effect of the Whitcomb area rule.

Severe instability can occur at transonic speeds. Shock waves move through the air at the speed of sound. When an object such as an aircraft also moves at the speed of sound, these shock waves build up in front of it to form a single, very large shock wave. During transonic flight, the plane must pass through this large shock wave, as well as contending with the instability caused by air moving faster than sound over parts of the wing and slower in other parts. The difference in speed is due to Bernoulli's principle.

Transonic speeds can also occur at the tips of rotor blades of helicopters and aircraft. However, as this puts severe, unequal stresses on the rotor blade, it is avoided and may lead to dangerous accidents if it occurs. It is one of the limiting factors to the size of rotors, and also to the forward

speeds of helicopters (as this speed is added to the forward-sweeping (leading) side of the rotor, thus possibly causing localized transonics).

Interesting facts



Transonic flow patterns on an airfoil showing flow patterns at and above critical Mach number.

- At transonic speeds intense low-pressure areas form at various points around an aircraft. If conditions are right (i.e. high humidity) visible clouds will form in these low-pressure areas as shown in the illustration; these are called Prandtl-Glauert singularities. These clouds remain with the aircraft as it travels. It is not necessary for the aircraft as a whole to reach supersonic speeds for these clouds to form.



Transonic flow patterns on F-16 fighter aircraft



Transonic flow patterns on F-16 fighter aircraft

Transonic Flows in Astronomy and Astrophysics

In Astrophysics, wherever there is evidence of shocks (standing, propagating or oscillating), the flow close by must be transonic as only supersonic flows form shocks. Interestingly all the black hole accretions are transonic (S.K. Chakrabarti, ApJ, 1996, v. 471, p. 237), many of the flows also have shocks very close to the black holes.

The outflows or jets from young stellar objects or disks around black holes can also be transonic since they start subsonically and at a far distance they are invariably supersonic. Supernovae explosion is accompanied by super sonic flows and shock waves. Bow shocks formed in solar winds around the earth is a direct result of transonic wind from the sun.

Other Flow Regimes

- Subsonic flows
- Supersonic flows
- Hypersonic flows

References

Theory of transonic astrophysical flows: Sandip K. Chakrabarti, World Scientific Publishers , Singapore (1990)

Wave Drag

From Wikipedia, the free encyclopedia

Wave drag is an aerodynamics term that refers to a sudden and very powerful form of drag that appears on aircraft and blade tips moving at high-subsonic and supersonic speeds.

Overview

Wave drag is caused by the formation of shock waves around the aircraft. Shock waves radiate away a considerable amount of energy, energy that is experienced by the aircraft as drag. Although shock waves are typically associated with supersonic flow, they can form at much lower speeds at areas on the aircraft where local airflow accelerates to supersonic speeds. The effect is typically seen at transonic speeds above about Mach 0.8, but it is possible to notice the problem at any speed over that of the critical Mach of that aircraft's wing. The magnitude of the rise in drag is impressive, typically peaking at about four times the normal subsonic drag. It is so powerful that it was thought for some time that engines would not be able to provide enough power to easily overcome the effect, which led to the concept of a "sound barrier".

Research

When the problem was being studied, wave drag came to be split into two – wave drag caused by the wing as a part of generating lift, and that caused by other portions of the plane. In 1947, studies into both problems led to the development of "perfect" shapes to reduce wave drag as much as theoretically possible. For a fuselage the resulting shape was the **Sears-Haack body**, which suggested a perfect cross-sectional shape for any given internal volume. The **von Kármán ogive** was a similar shape for bodies with a blunt end, like a missile. Both were based on long narrow shapes with pointed ends, the main difference being that the ogive was pointed on only one end.

Reduction of drag

However a number of new techniques developed during and just after World War II were able to dramatically reduce the magnitude of the problem, and by the early 1950s most fighter aircraft could reach supersonic speeds without too much trouble. If the problem of wave drag is caused by the acceleration of air over curves on the aircraft, the solution is, obviously, to reduce the curves. However this is not always easy, for instance, a wing generates lift at subsonic speeds primarily due to the curvature on the leading edge of the wing. Things are somewhat better for fuselage shaping, but simple things like a cockpit canopy or smoothing off the metal around an air intake can create additional "hot spots".

These research projects were quickly put to use by aircraft designers. One common solution to the problem of wave drag due to the wings was to use a swept-wing, which had actually been developed before WWII and used on some German wartime designs such as the Me-262. Sweeping the wing to the rear makes it appear thinner and longer in the direction of the airflow, making a

"normal" wing shape closer to that of the von Kármán ogive, while still remaining useful at lower speeds where curvature and thickness are important.

The wing need not be swept as it is possible to build a wing that is extremely thin. This solution was used on a number of designs, perhaps the most obvious being the F-104 *Starfighter*. The downside to this approach is that the wing is so thin it is no longer possible to use it for fuel storage or landing gear.

Fuselage shaping was similarly changed with the introduction of the Whitcomb area rule. Whitcomb had been working on testing various airframe shapes for transonic drag when, after watching a presentation by Adolf Busemann in 1952, he realized that the Sears-Haack body had to apply to the entire aircraft. This meant that the fuselage needed to be made considerably skinnier where the wings met it, so that the cross-section of the entire aircraft matched the Sears-Haack body, not just the fuselage itself.

Application of the area rule can also be seen in the use of anti-shock bodies on subsonic aircraft, such as jet airliners. Anti-shock bodies, which are pods along the trailing edges of the wings, serve the same role as the narrow waist fuselage design of other transonic aircraft.

Other drag reduction methods

Several other attempts to reduce wave drag have been introduced over the years, but have not become common. The supercritical airfoil is a new wing design that results in reasonable low speed lift like a normal planform, but has a profile considerably closer to that of the von Kármán give. All modern civil airliners use forms of supercritical aerofoil and have substantial supersonic flow over the wing upper surface.

Busemann's Biplane avoids wave drag entirely, but is incapable of generating lift, and has never flown.